Results & Discussion

obeikandl.com

CHAPTER III

Results and Discussion

In the petroleum industry two problems arise during oil production. One of them is the corrosion of pipelines and petroleum equipment. To overcome this problem corrosion inhibitors must be added. The second problem comes from the water that accompanies the crude oil which leads to water in oil emulsion (w/o). For this reason surfactants must be added at wellheads and process areas in the petroleum field to break down the emulsion that is formed. These surfactants are named emulsion breakers or demulsifies.

For these reasons the compounds prepared in the present study were planned to be used as multifunction additives such as corrosion inhibitors and emulsion breakers. These compounds were based on polymerization of triethanolamine and its ethoxylation or esterfication. The full description of the preparations was described in the experimental section and is summarized in the **Scheme 2.**

Confirming the Chemical Structure of the Surfactants Prepared

FT-IR Spectroscopic Analysis

The structure of the prepared compounds was elucidated by FT-IR spectroscopy. The FT-IR of P_4, P_6, and P_8 are shown in **Figs 2, 3,** and **4.** From these figures, it was found that the main characteristic absorption bands appeared at 3356.8, 3385.2, and 3374.2 cm^{-1} were assigned to the primary alcohol **(-OH)** and the bands at 2951.9 and 2880.2 cm^{-1} to the asymmetric and symmetric **($-CH_2$)** respectively. A new characteristic band appeared at 1114.0 cm^{-1} due to the ethereal band **(C-O-C)**. This band indicates that the polymerization process took place. Two other bands that appeared at 1035 and 1072.8 cm^{-1} are due to the **(C-OH)** and the **(C-N)** groups respectively. The intensity of the ethereal band in **Figs. 3** and **4** increased as a result of increasing the degree of polymerization.

The FT-IR for the ethoxylated compounds $E(40)P_8$, $E(100)P_8$, and $E(120)P_8$ are shown in **Figs. 5, 6,** and **7.** By inspection of these figures it is clear that the main characteristic peaks

obeikandi.com

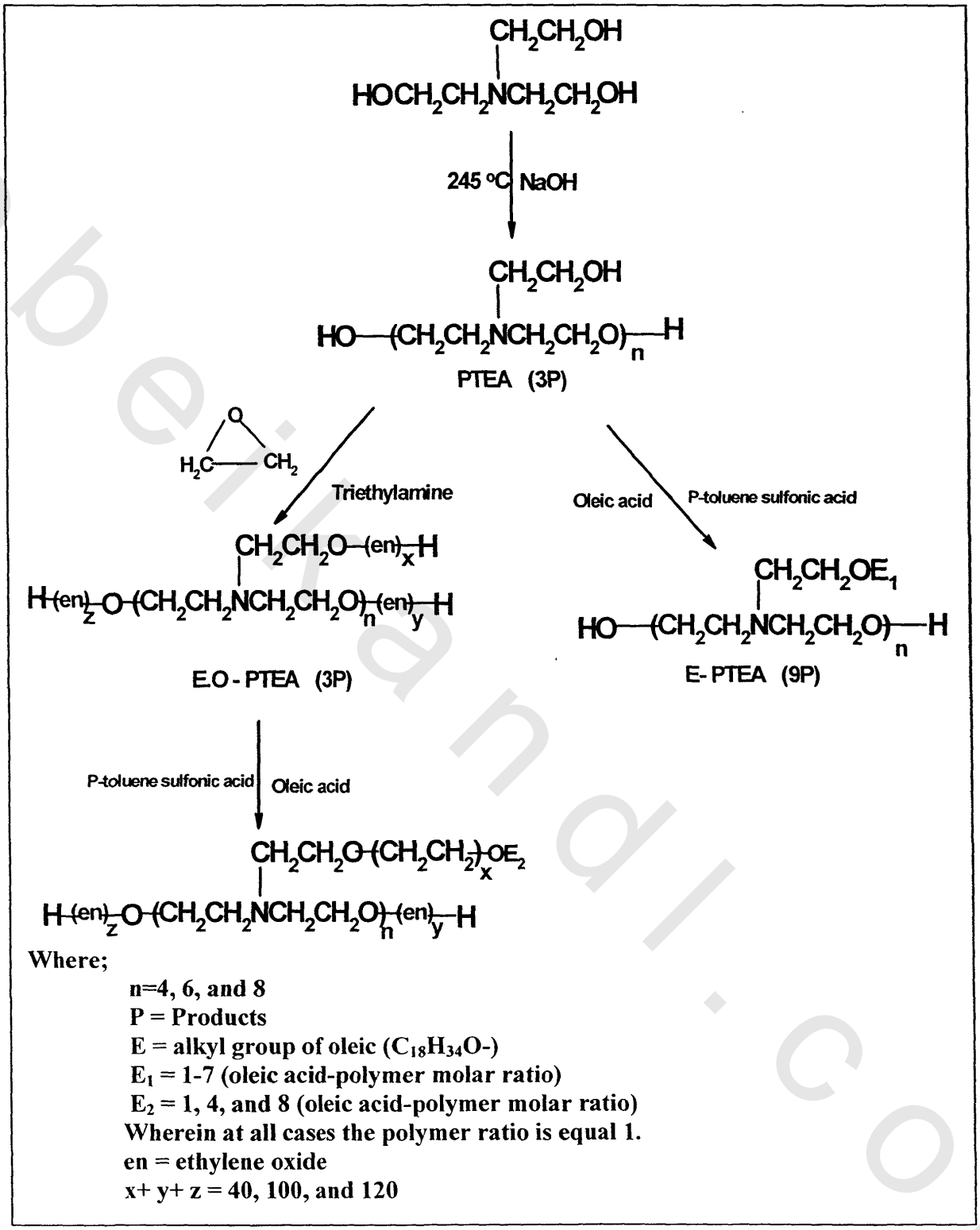

Where;

n=4, 6, and 8
P = Products
E = alkyl group of oleic ($C_{18}H_{34}O$-)
E_1 = 1-7 (oleic acid-polymer molar ratio)
E_2 = 1, 4, and 8 (oleic acid-polymer molar ratio)
Wherein at all cases the polymer ratio is equal 1.
en = ethylene oxide
x+ y+ z = 40, 100, and 120

Scheme 2: Preparation of the Polymer, the Ester of the Polymer, the Ethoxylated Polymer and the Ester of the Ethoxylated Polymer.

obeikandl.com

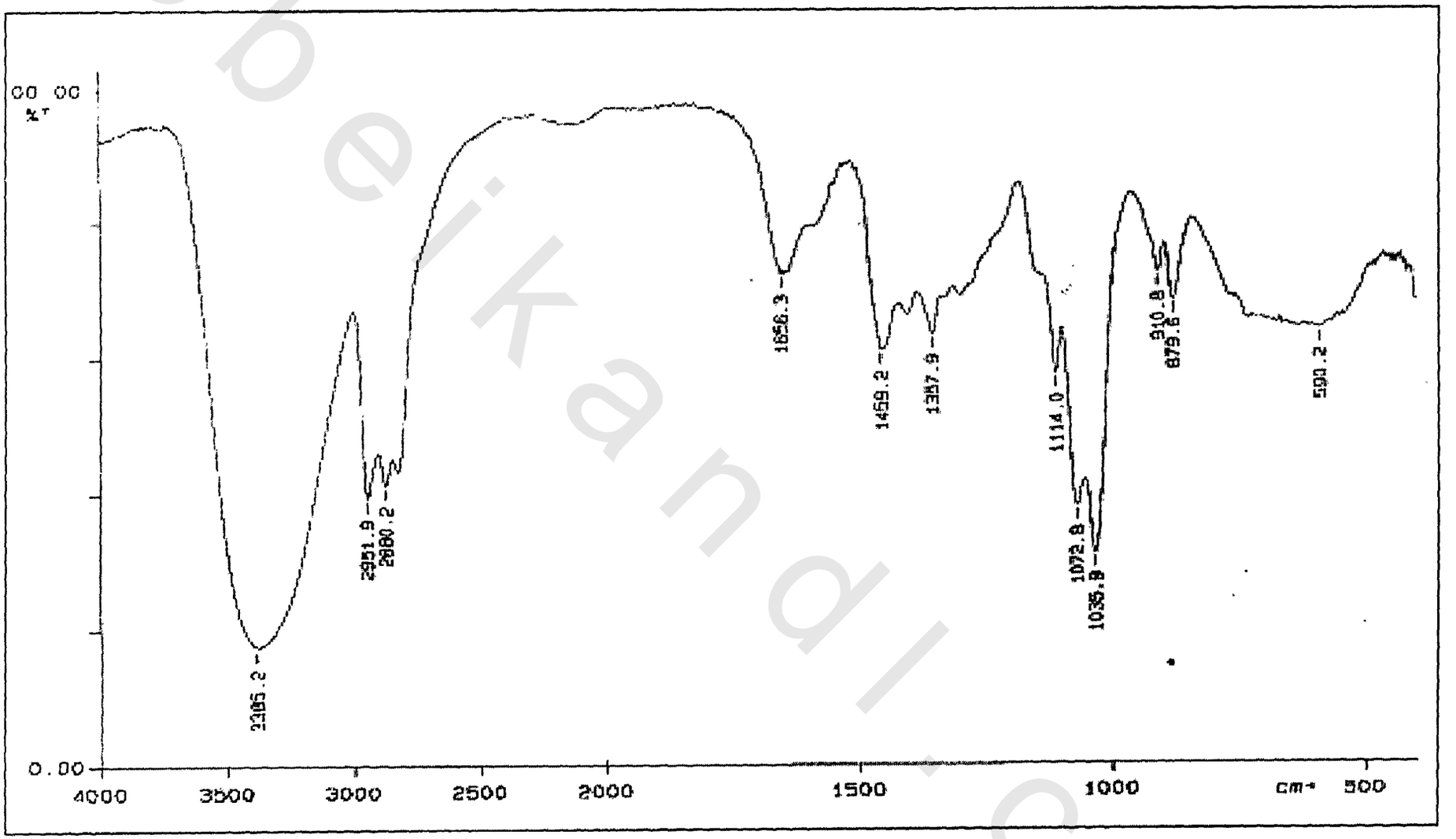

Fig. 2: FT-IR Spectrum of P_4

opelkandl.com

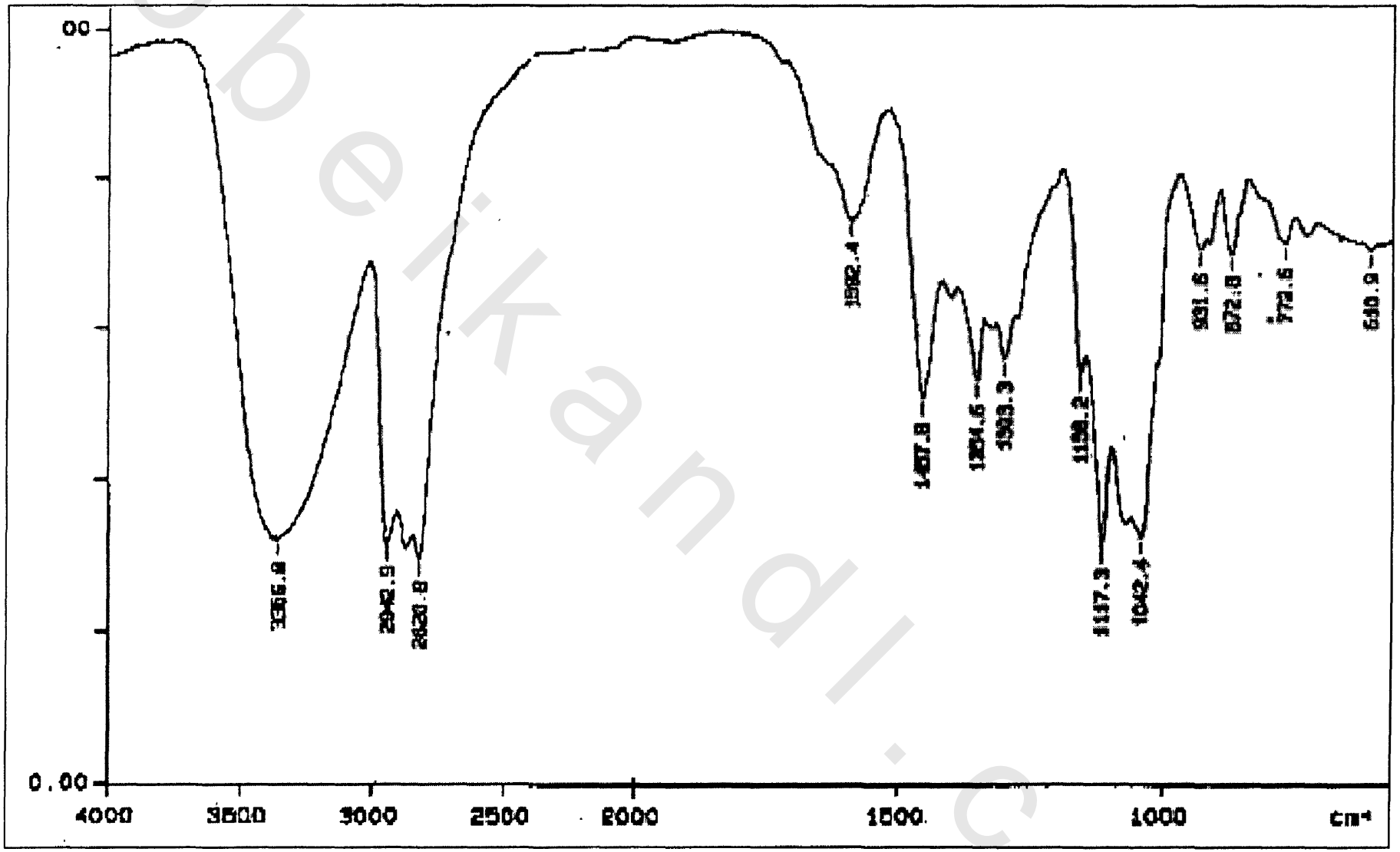

Fig. 3: FT-IR Spectrum of P_6

obeikandl.com

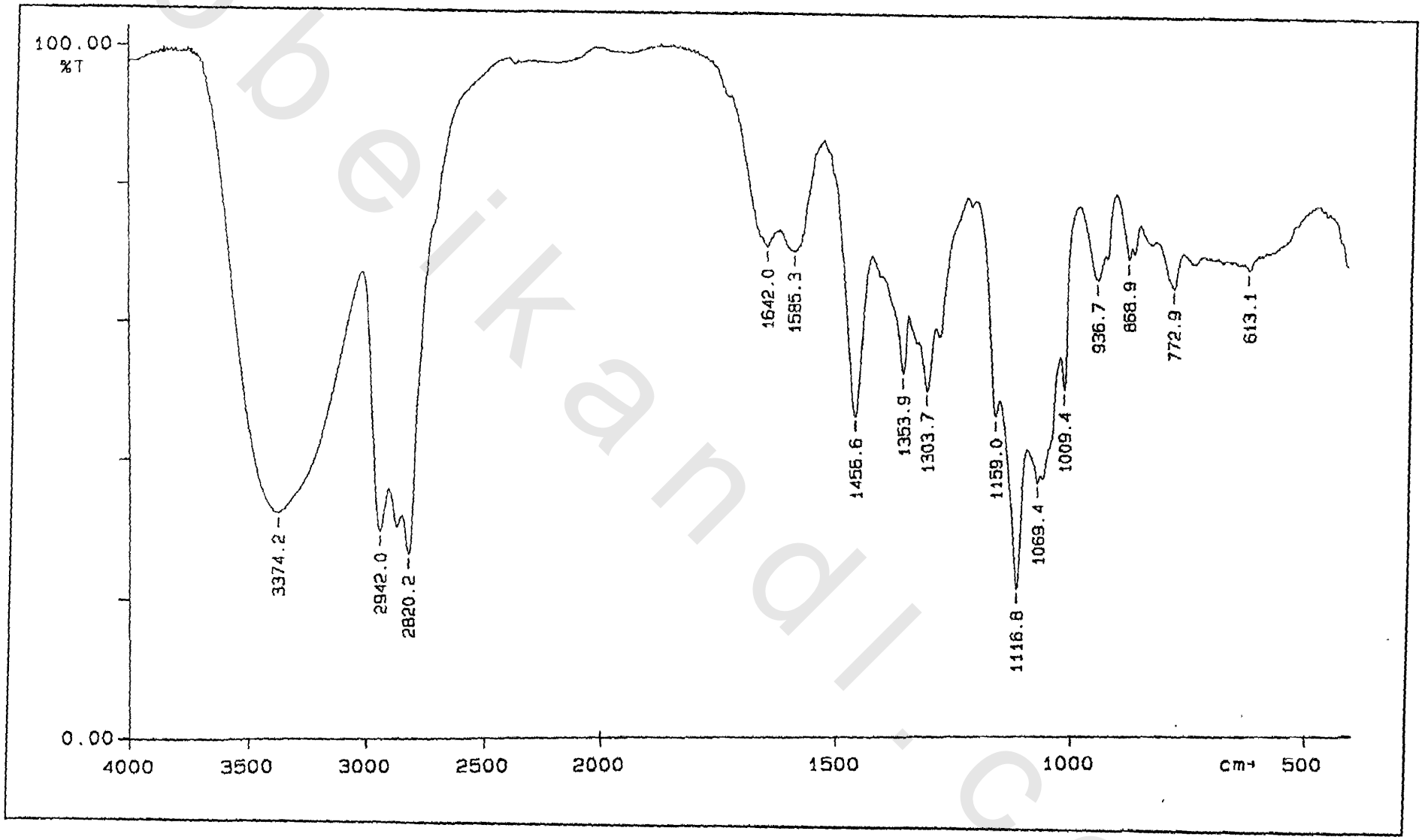

Fig. 4: FT-IR Spectrum of P_8

obeikandl.com

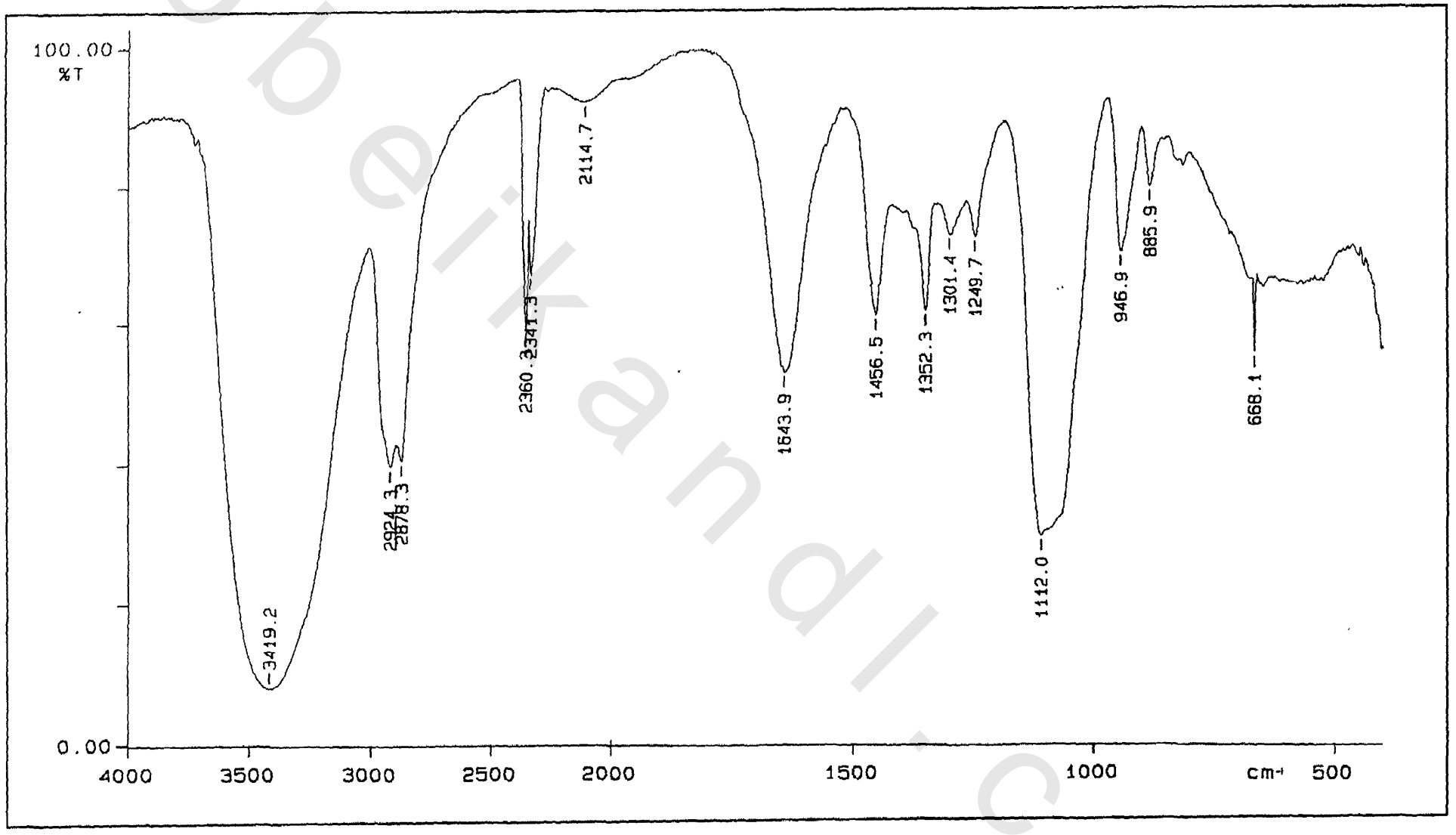

Fig. 5: FT-IR spectrum of Ethoxylated (40) P_8

obeikandl.com

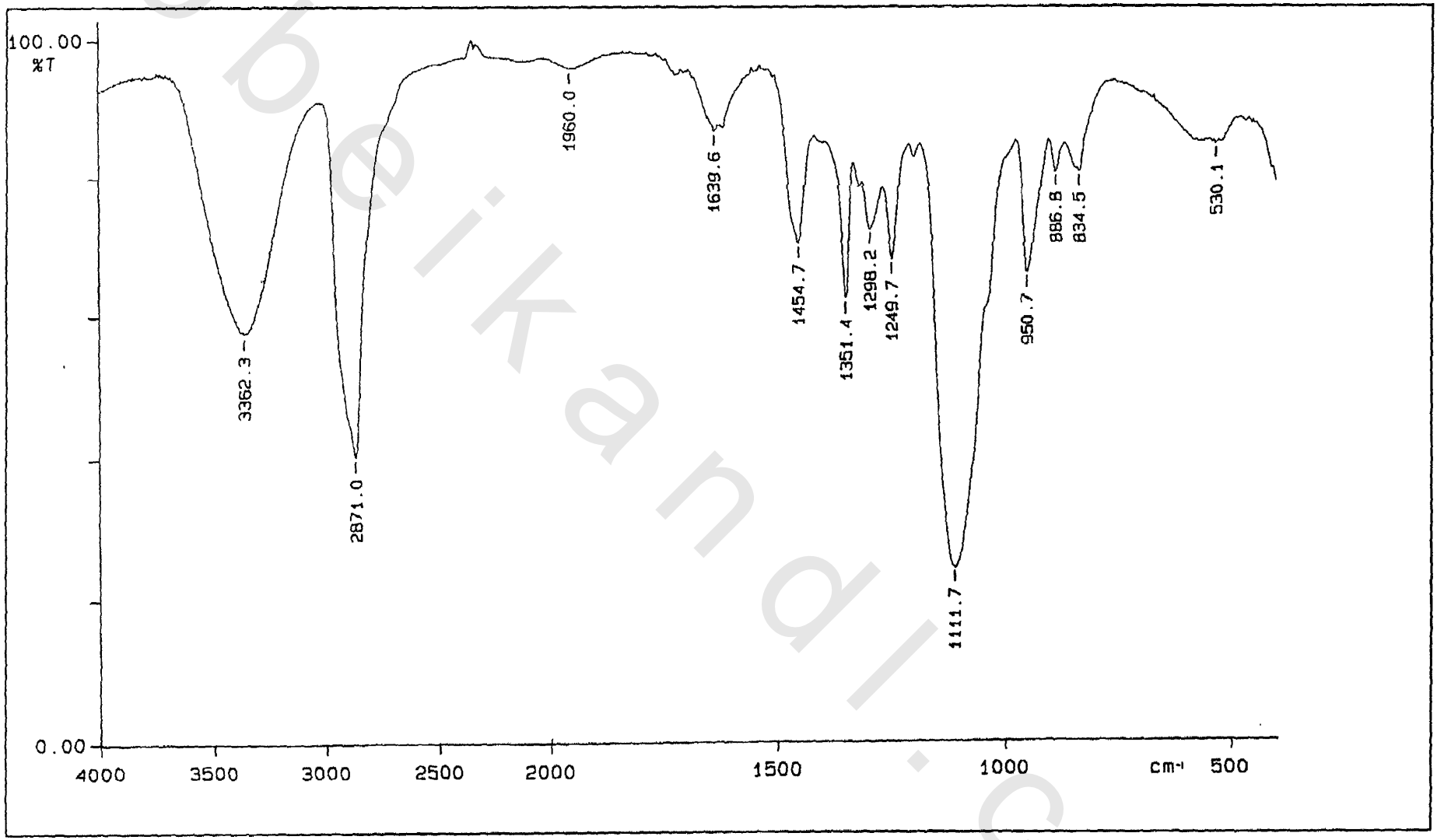

Fig. 6: FT-IR Spectrum of Ethoxylated (100) P_8

obeikandi.com

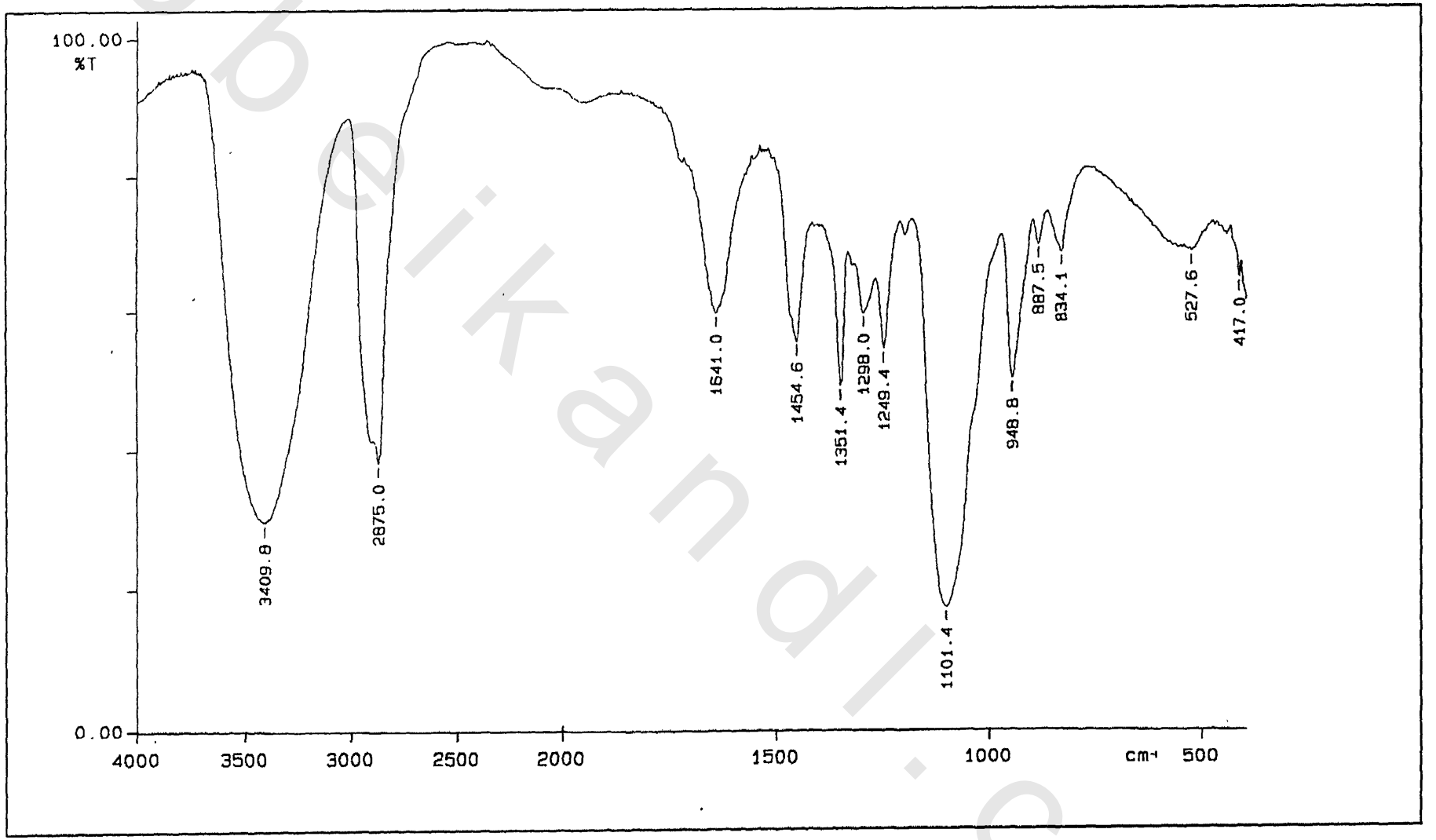

Fig. 7: FT-IR Spectrum of Ethoxylated (120) P_8

opelkandi.com

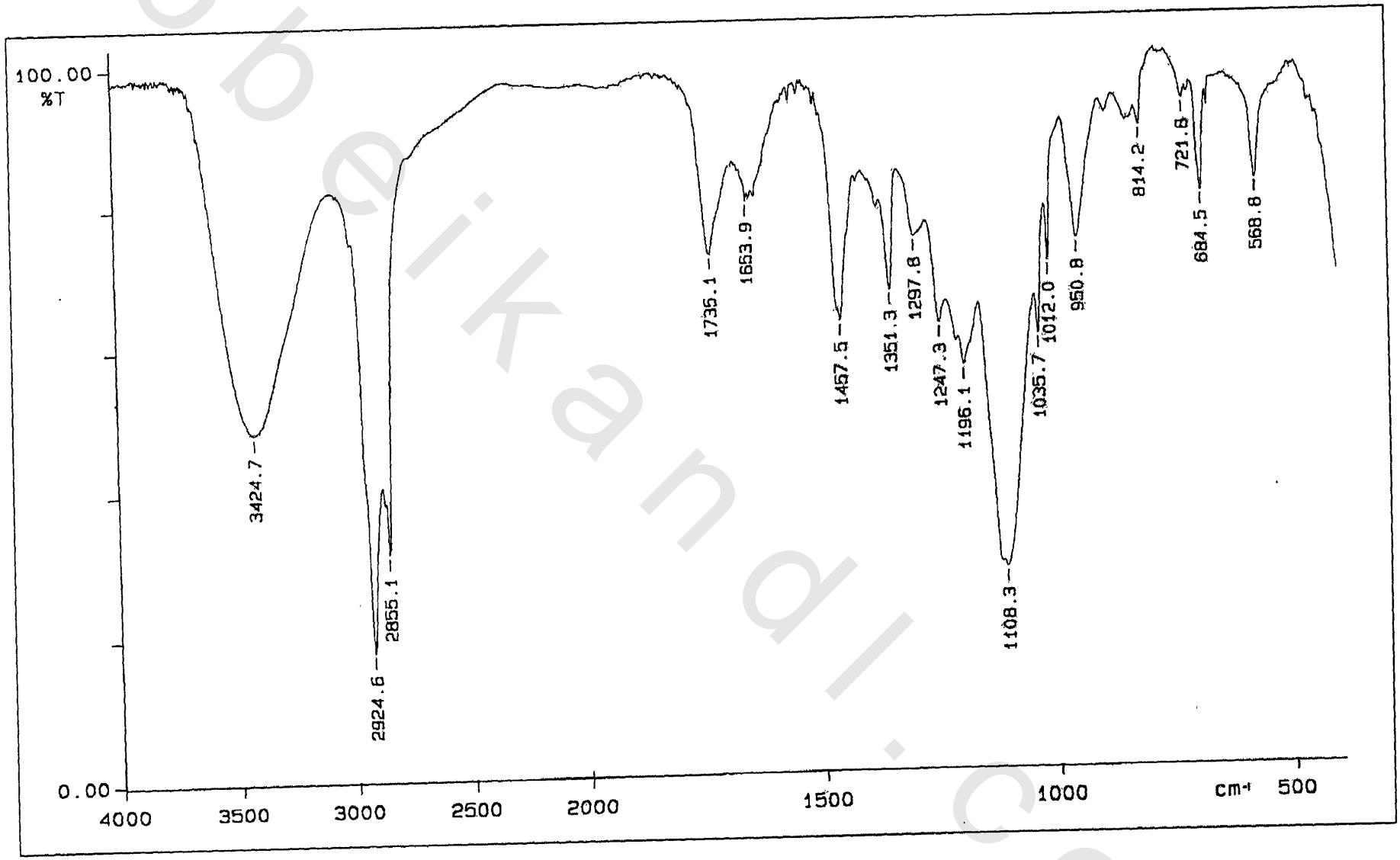

Fig. 8: FT-IR Spectrum of E(120)P_8O_1

opelkandl.com

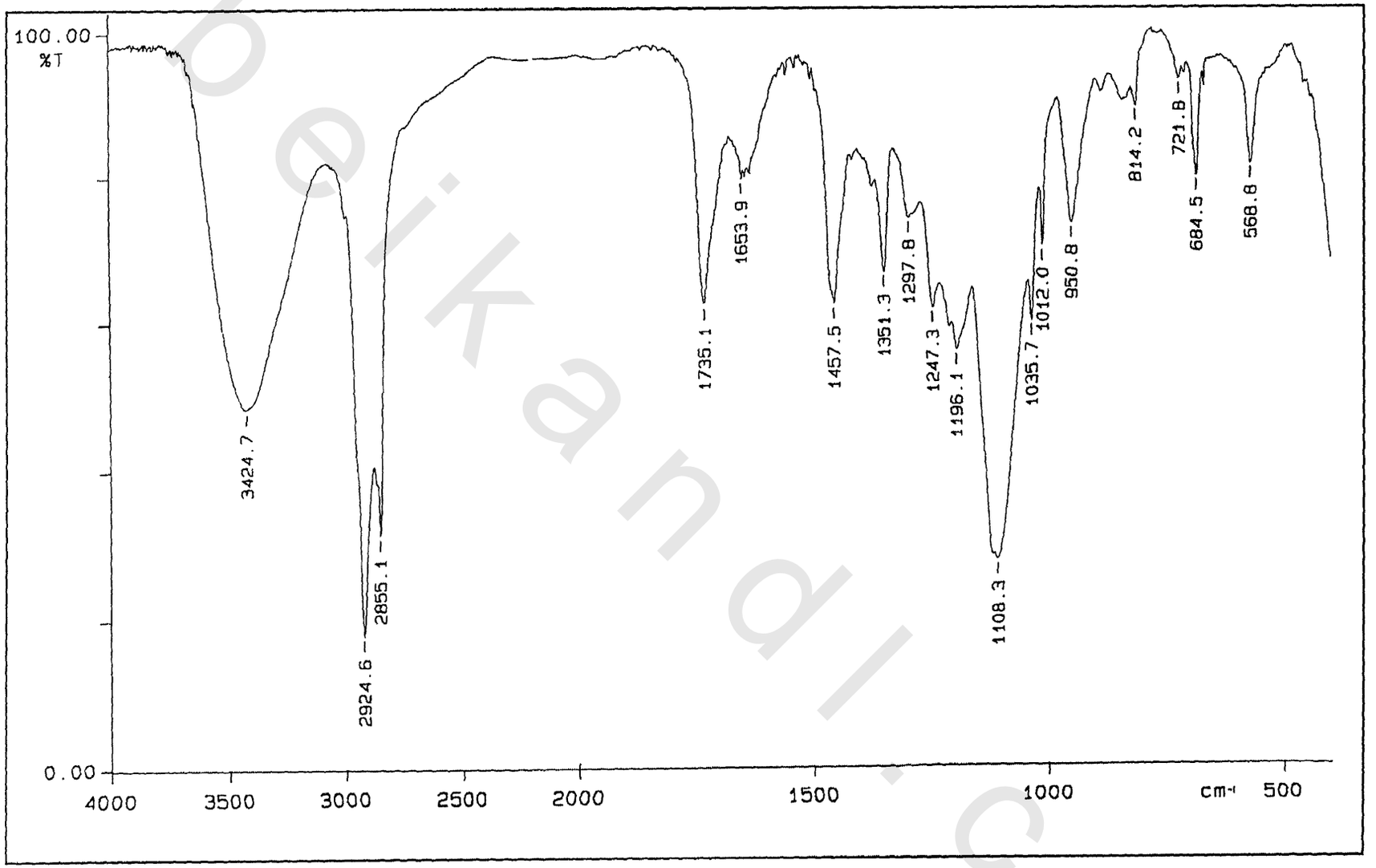

Fig. 9: FT-IR Spectrum of $E(120)P_8O_4$

opeikandi.com

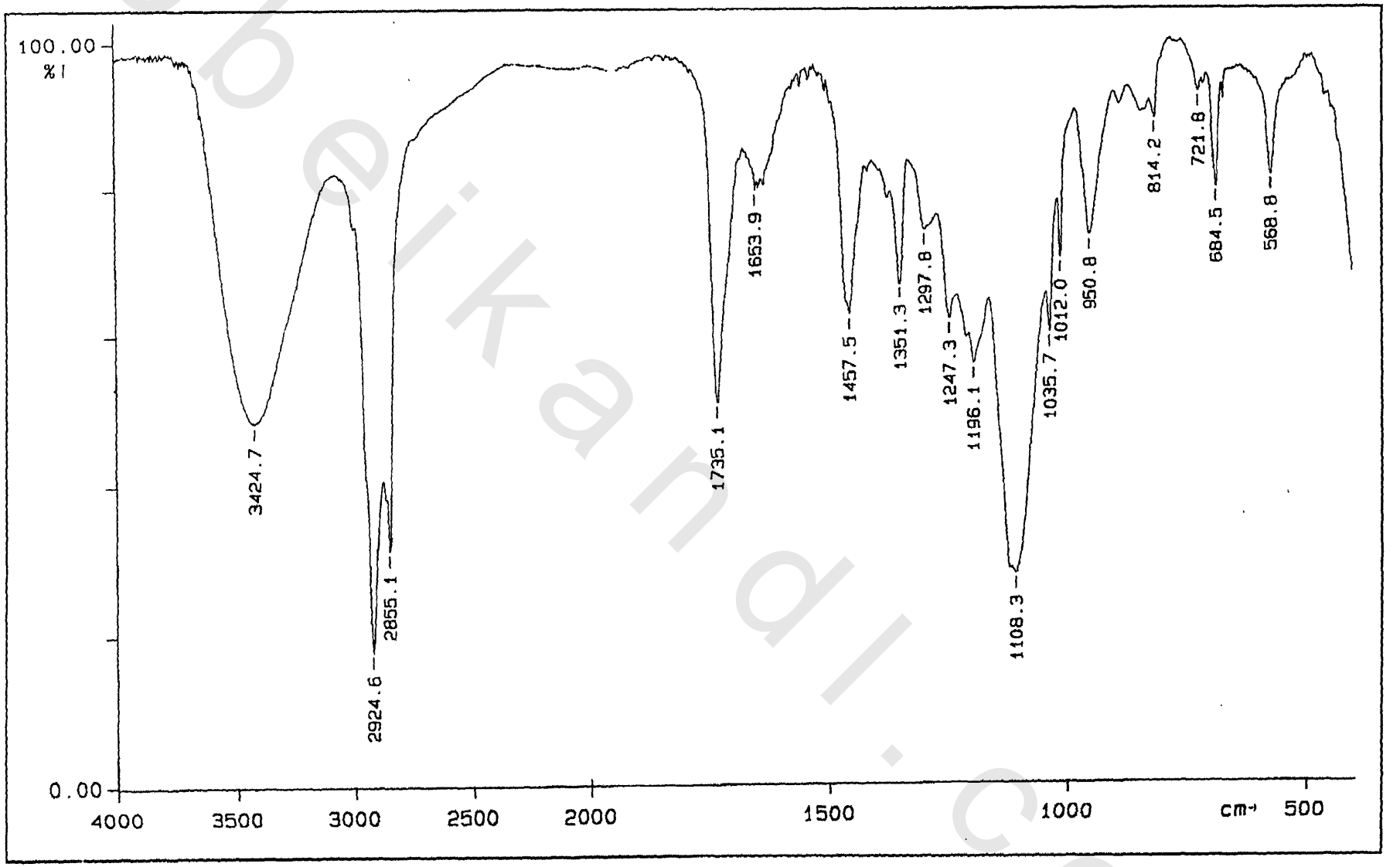

Fig. 10: FT-IR Spectrum of E(120)P_8O_8

opelkandl.com

for the ethoxylation process appeared at 1111 cm^{-1} for the ethereal band **(C-O-C)** and the broad **(-OH)** band at 3419.2 cm^{-1} for the terminal hydroxyl group of the ethoxylated chain.

The ester formation of these compounds was confirmed using FT-IR as shown in **Figs.8, 9,** and **10.** The main characteristic peak for the carbonyl ester group **(-C=O)** appeared at 1735 cm^{-1}. This indicates that the esterfication process took place. The intensity of this band increases by increasing the molar ratio of esterfication as shown in **Figs. 8, 9,** and **10** against the molar ratios 1:1, 1:4, and 1:8 respectively.

^{1}H and ^{13}C NMR Spectroscopy Analysis

The **^{1}H** and **^{13}C** NMR spectra of some of the compounds support the structural information which was provided by the FT-IR spectra. The **^{1}H** NMR spectrum of triethanolamine (TEA) shows only three main characteristic peaks. The **^{1}H** NMR spectra of the three polymer TEA (P_4, P_6, and P_8) are shown in **Figs 11, 12,** and **13** respectively. The new peak observed for **^{1}H** (d) of CH_2 at δ (3.4) indicates the formation of the ethereal bonds. This peak increases by increasing the degree of polymerization as shown in **Figs. 12** and **13** (for P_6 and P_8 respectively). The same result was observed in **Figs. 14, 15,** and **16** for the ethoxylated polytriethanolamine E(40) P_8, E(100) P_8, and E(120)P_8. The **^{1}H** NMR for the ester of ethoxylated polytriethanolamine is shown in **Fig. 17.** From this figure it can be observed that a peak appeared at δ (0.9) for **^{1}H** of the terminal CH_3, at δ (5.4) for **^{1}H** (j) of 1-ethylene (-CH=CH-).

The **^{13}C** NMR of the polymers are shown in **Figs. 18, 19,** and **20** for the polytriethanolamine. In these figures four peaks appeared for **^{13}C** a, b, c, and d at δ (60), δ (58). δ (56), and δ (63). The last peak d of the ethereal bond increases with increasing the degree of polymerization as shown in **Figs. 19**and **20** respectively.

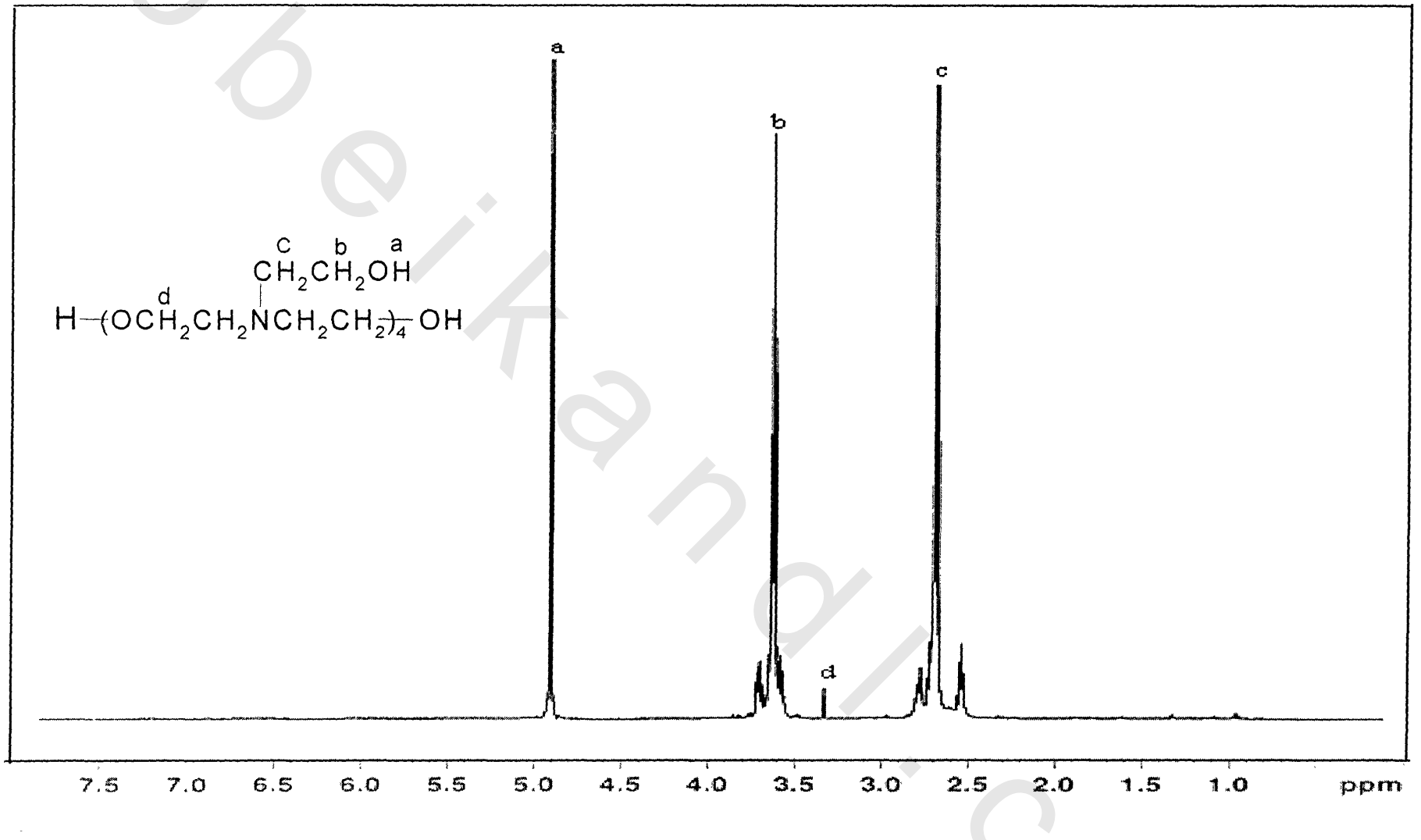

Fig. 11: ^{1}H NMR Spectrum of P_4

obeikandi.com

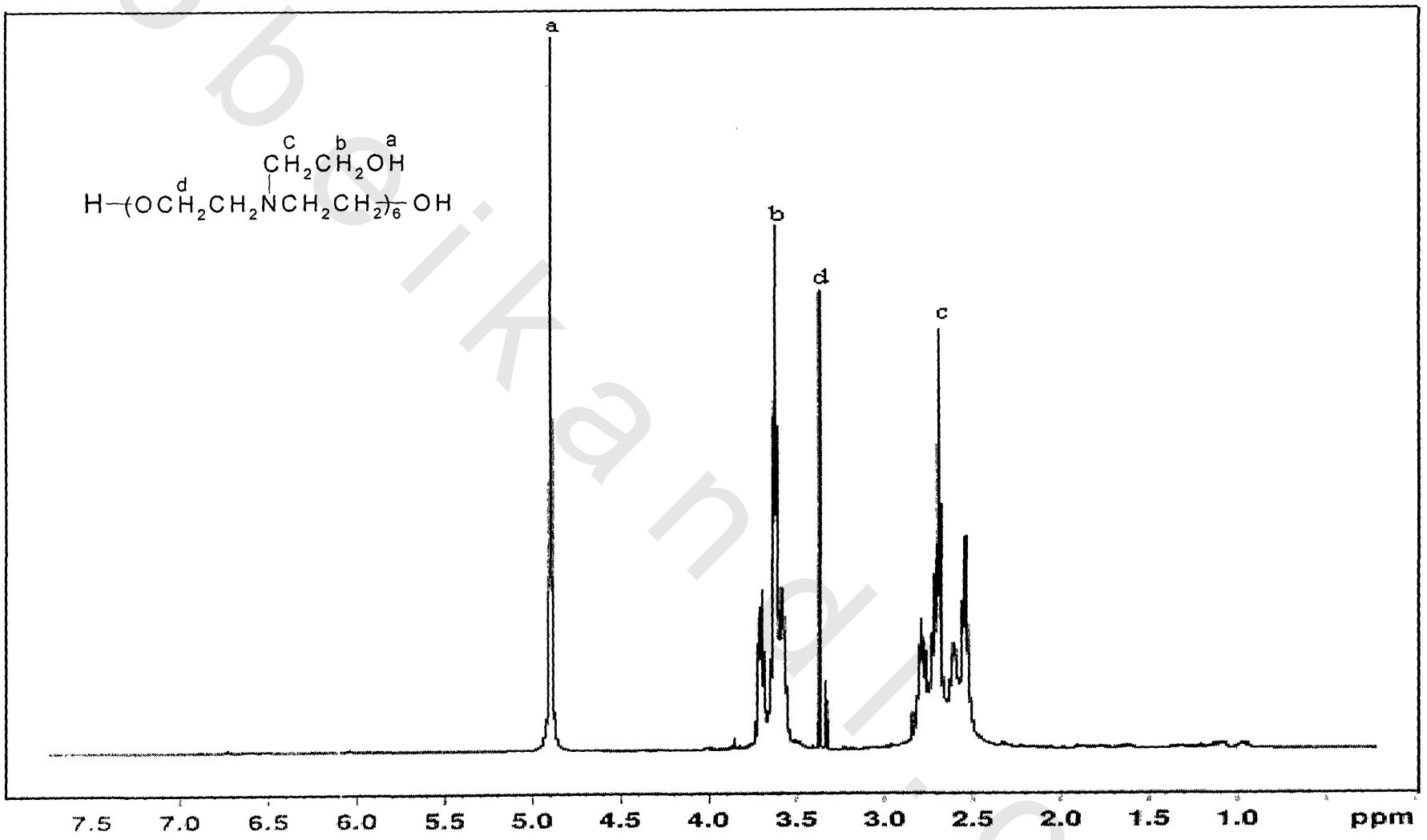

Fig. 12: ^{1}H NMR Spectrum of P_6

obeikandl.com

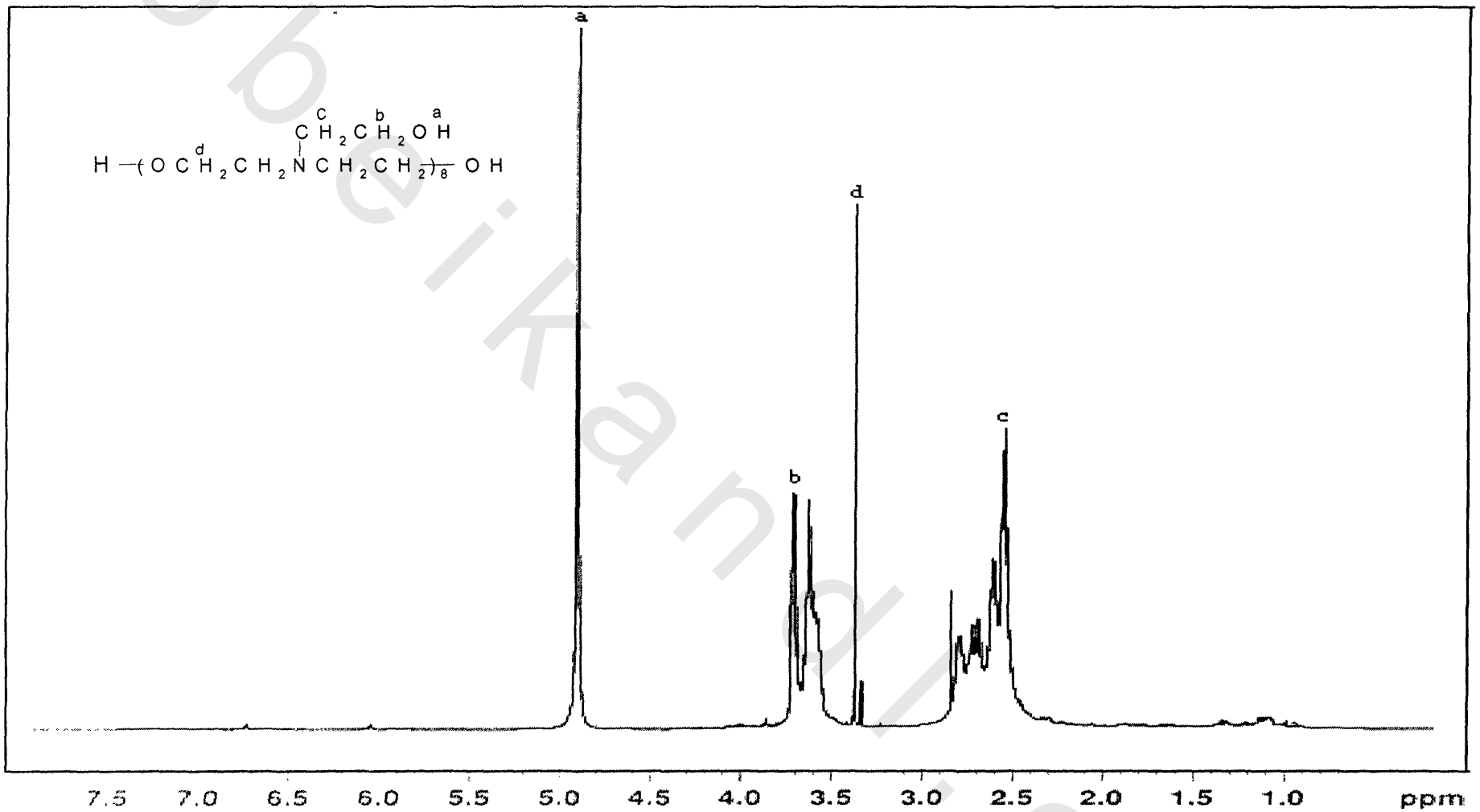

Fig. 13: ^{1}H NMR Spectrum of P_8

obeikandl.com

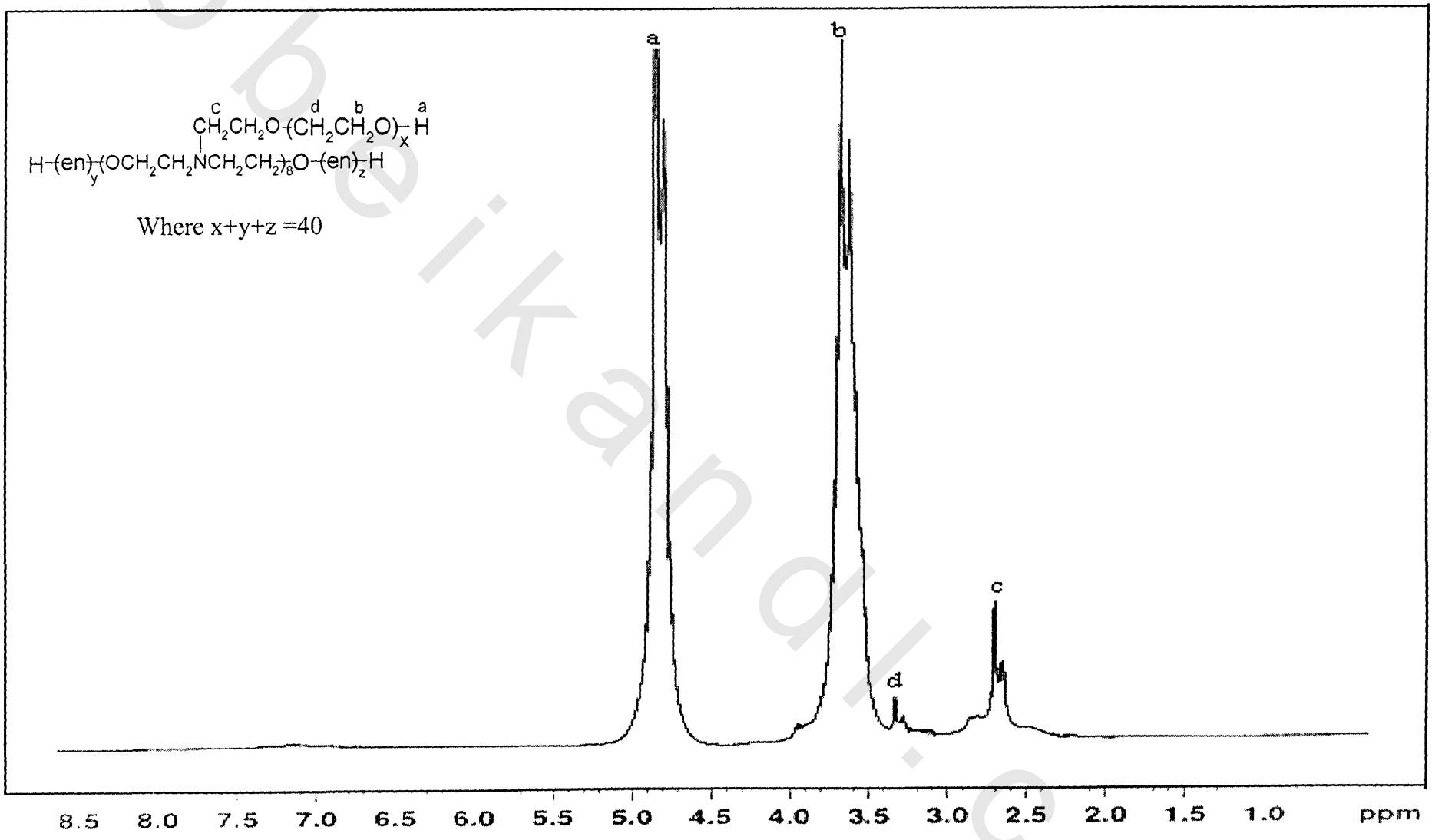

Fig. 14: ^{1}H NMR Spectrum of E(40)P$_8$

obeikandl.com

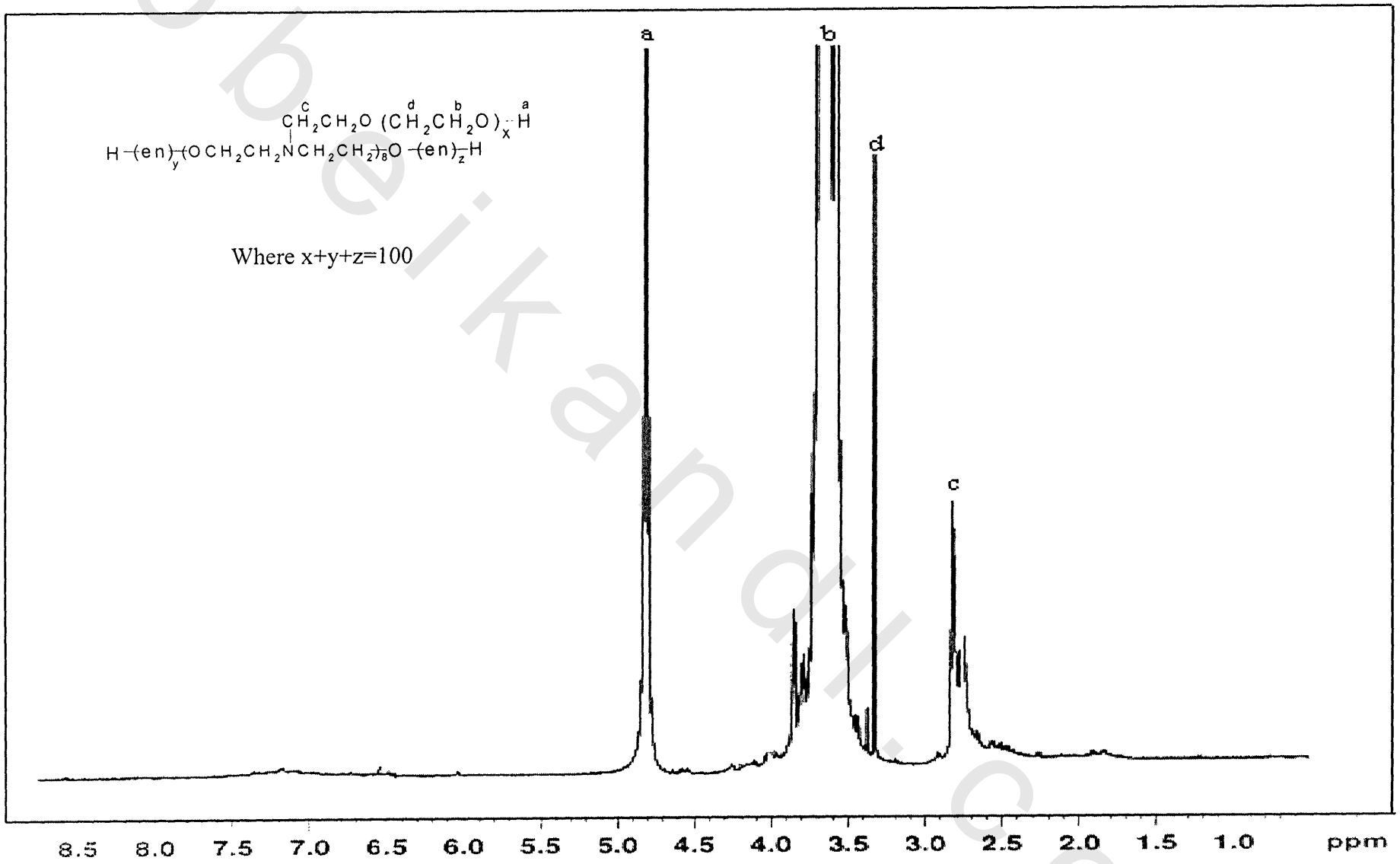

Fig. 15: ^{1}H NMR Spectrum of E(100)P$_8$

obeikandi.com

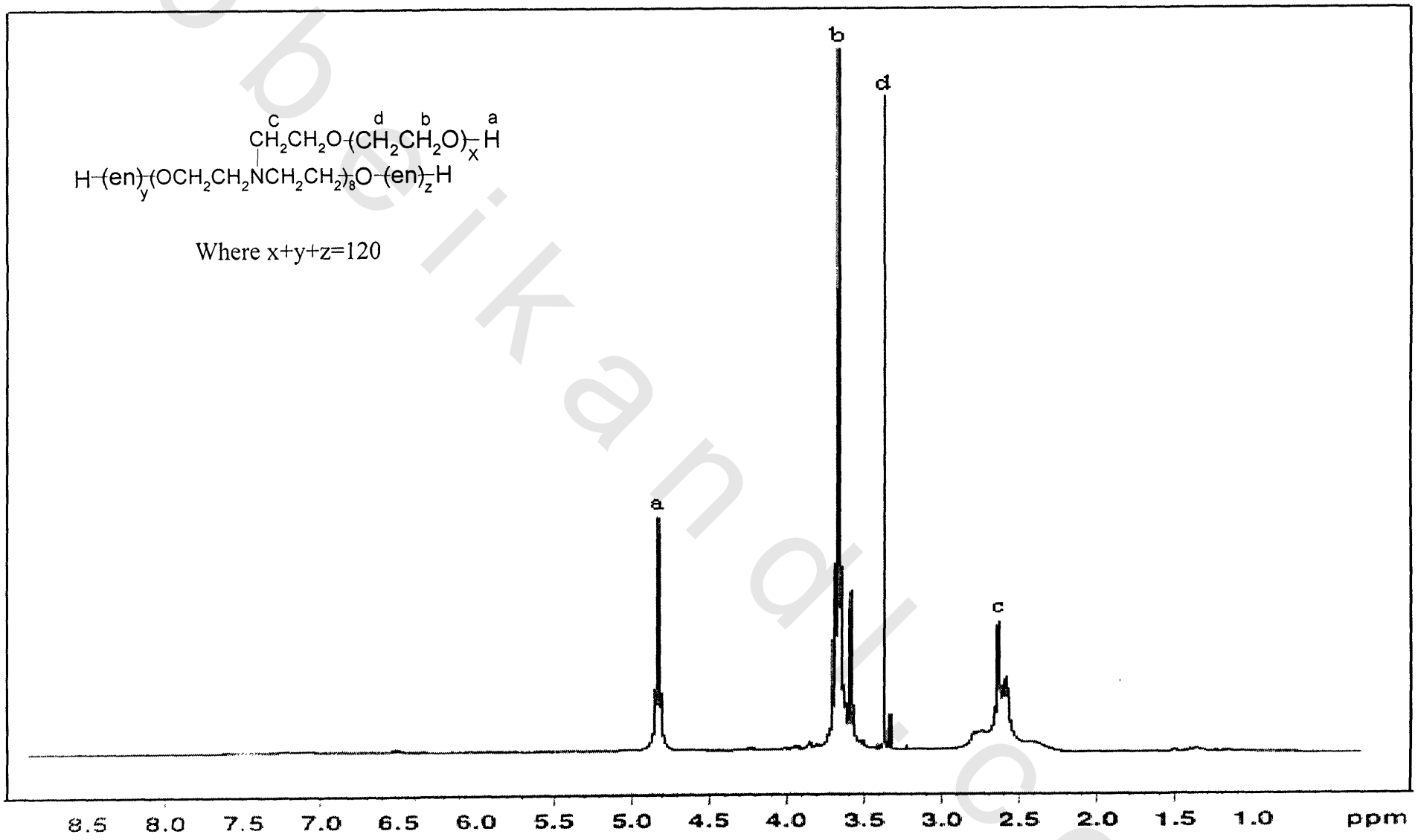

Fig. 16: ^{1}H NMR Spectrum of E(120)P$_8$

obeikandl.com

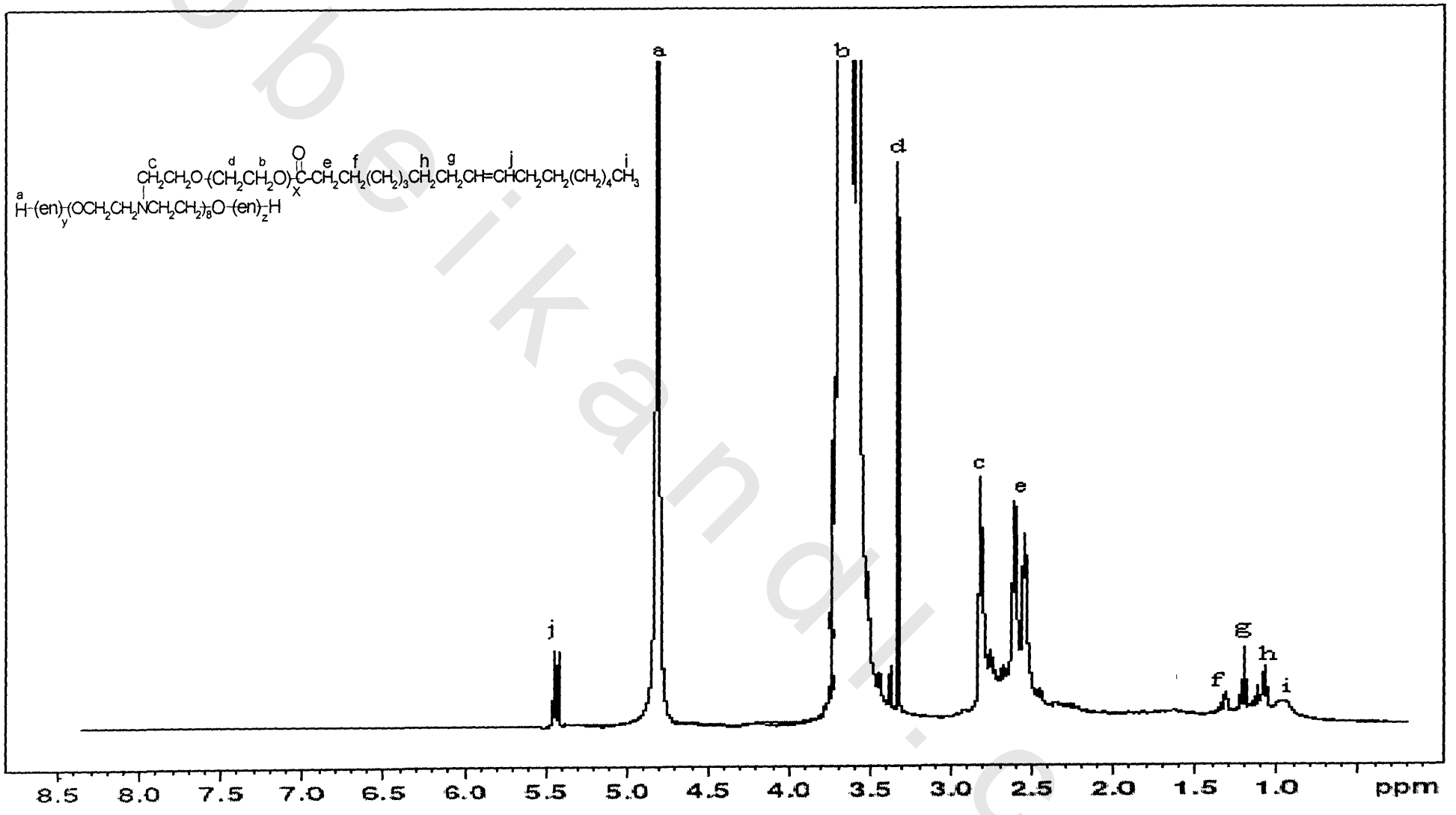

Fig. 17: ^{1}H NMR Spectrum of E(120)P_8O_8

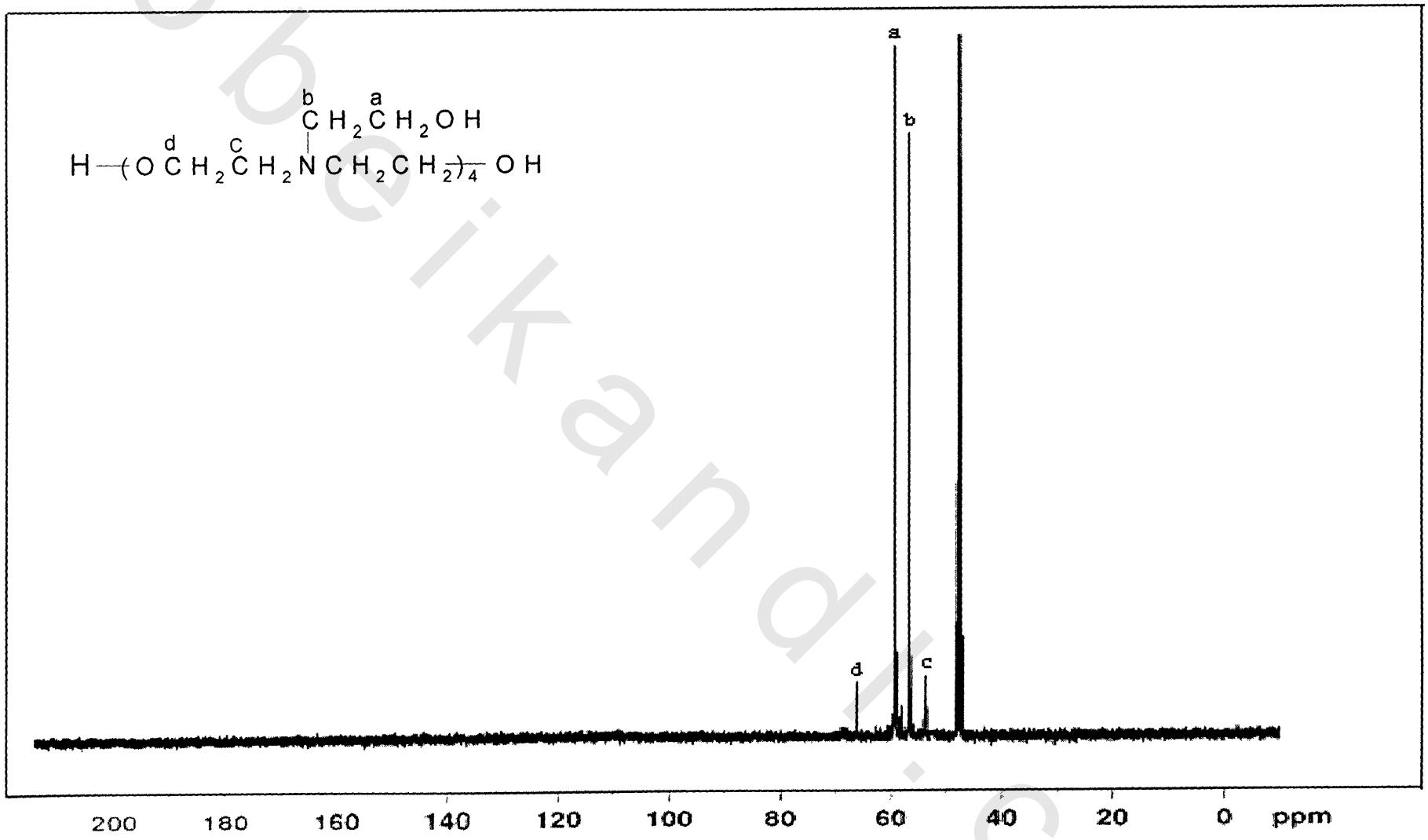

Fig. 18 : ^{13}C NMR Spectrum of P_4

obeikandi.com

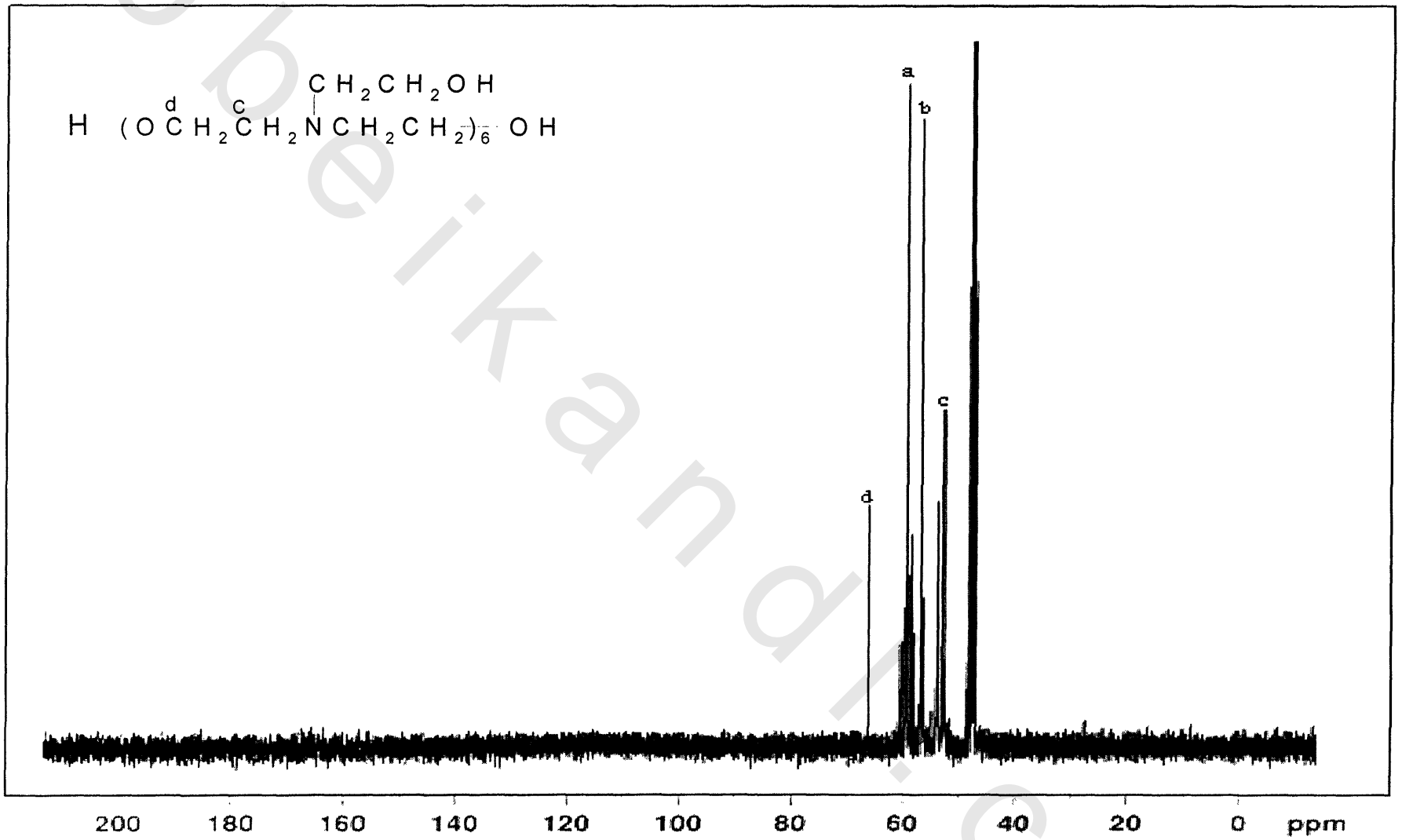

Fig. 19: ^{13}C NMR Spectrum of P_6

obeikandi.com

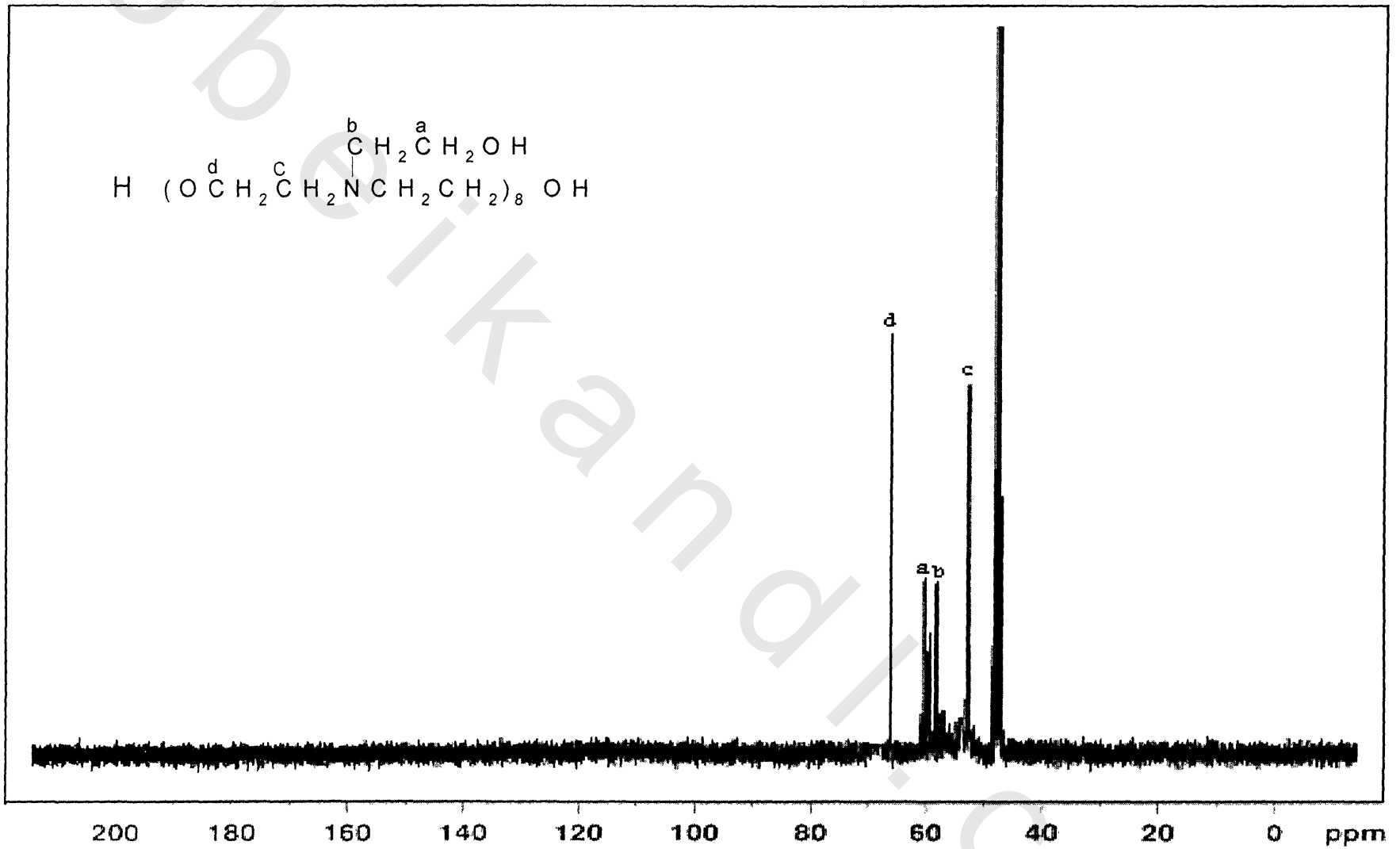

Fig. 20 : ^{13}C NMR Spectrum of P_8

obeikandi.com

Preparation Parameters and Molecular Weights Determination.

The polymerization of triethanolamine (TEA) was followed by increasing the time of the reaction as outlined in **Table 5** and illustrated in **Fig. 21** and **22**. From the data and plots, it was found that by increasing the reaction time, the water produced, the degree of polymerization and the molecular weights increased. On the other hand the weight of products decreased.

The molecular weight of the prepared polymers was calculated according to the amount of water collected during the polymerization process and nitrogen content.

The nitrogen content of the polymers was measured experimentally and calculated theoretically as the result of the produced water. By inspection of the data in **Table 6** it can conclude that the nitrogen content increases as the degree of polymerization increases. This finding was found to comply with the water produced from the polymerization reaction. From the data obtained, it was found that the nitrogen content for the ethoxylated polytriethanolamine decreases with increasing the number of ethylene oxide units. It was also found that the nitrogen content decreases with increasing the molar ratio of esterfication.

Table 5: Preparation Kinetics of the Polytriethanolamine.

Time of Polymerization	Wt. of Reactants	Wt. of Products	Produced Water	Degree of Polymerization (n)	M.Wt
1.30	298	226	72	4	524
2.30	298	190	108	6	786
3.30	298	154	144	8	1048

Surface Active and Thermodynamic Properties of the Prepared Surfactants

For all types of surfactants, the surface tension decreases with increasing concentration until a certain concentration is reached. At this concentration the surface tension remains constant no matter how much the concentration of the surfactant was increased. This concentration is known as the critical micelle concentration (CMC) where saturation in the surface adsorbed layer is attained [90].

obeikandi.com

Table 6: Polytriethanolamines and their Oleate Esters and Ethoxylates.

Structure of the prepared compounds.	Code	M.wt	HLB	Nitrogen Contents	
				N% Calculated	N% Found
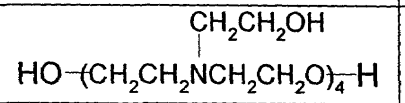	P_4	524	-	10.68	10.39
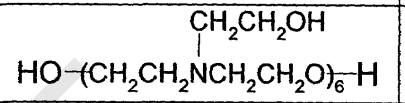	P_6	786	-	10.68	45.10
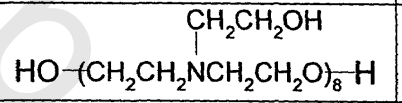	P_8	1048	-	10.69	10.72
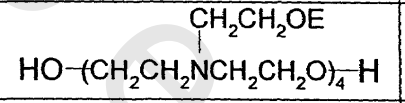	P_4O_1	788	13.0	7.10	6.95
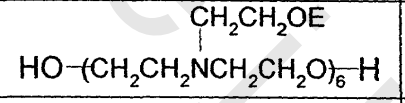	P_6O_1	1050	15.2	8.00	7.68
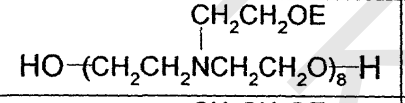	P_8O_1	1312	16.1	8.65	8.29
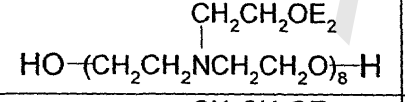	P_8O_2	1576	13.6	7.10	7.54
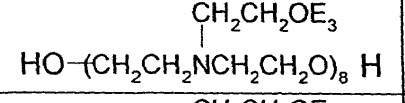	P_8O_3	1840	11.8	6.09	5.84
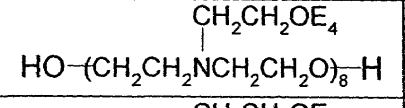	P_8O_4	2104	10.4	5.32	5.16
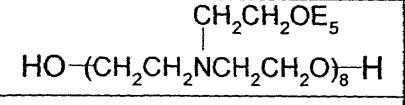	P_8O_5	2368	9.3	4.73	4.66
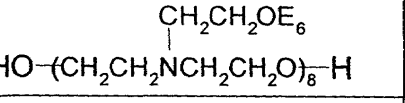	P_8O_6	2632	8.5	4.25	4.00
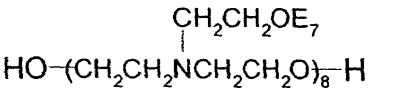	P_8O_7	2896	7.8	3.86	3.99
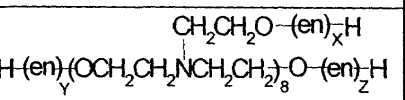 where x+y+z = 40	E(40)P_8	28028	-	3.99	3.38
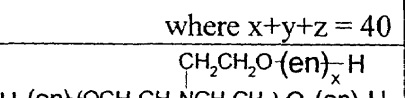 where x+y+z =100	E(100)P_8	5448	-	2.05	2.00
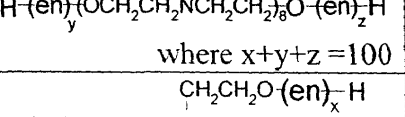 where x+y+z =120	E(120)P_8	6328	-	1.76	1.90

Opekanic.com

Continuation of Table 6: Esters of Ethoxylated Polytriethanolamine.

Structure of the prepared compounds.	Code	M.Wt	HLB	Nitrogen contents	
				N% calculated	N% found
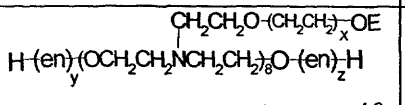 x+y+z = 40	$E(40)P_8O_1$	3072	18.4	3.64	3.42
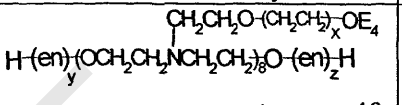 x+y+z = 40	$E(40)P_8O_4$	3864	14.8	2.89	2.79
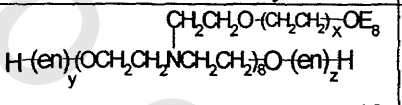 x+y+z = 40	$E(40)P_8O_8$	4920	11.8	2.27	2.01
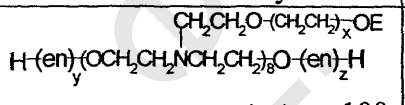 x+y+z = 100	$E(100)P_8O_1$	5712	19.1	1.96	1.56
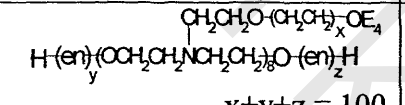 x+y+z = 100	$E(100)P_8O_4$	6504	16.9	1.72	2.01
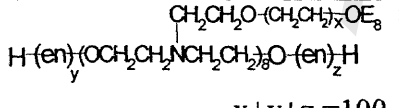 x+y+z =100	$E(100)P_8O_8$	7560	14.6	1.48	1.55
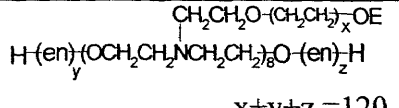 x+y+z =120	$E(120)P_8O_1$	6592	19.2	1.69	1.49
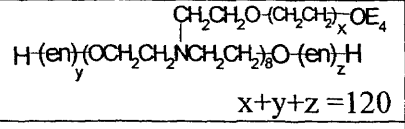 x+y+z =120	$E(120)P_8O_4$	7384	17.3	1.51	1.88
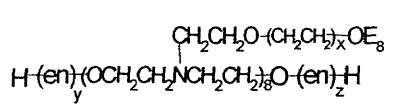 x+y+z =120	$E(120)P_8O_8$	8440	15.2	1.33	1.55

Ex = Esters from oleic acid ($C_{18}H_{34}O$-).

X = From 1 to 8 means that the degree of esterfication with regards to the oleic acid-polymer molar ratio (where in all cases the polymer ratio is equal 1).

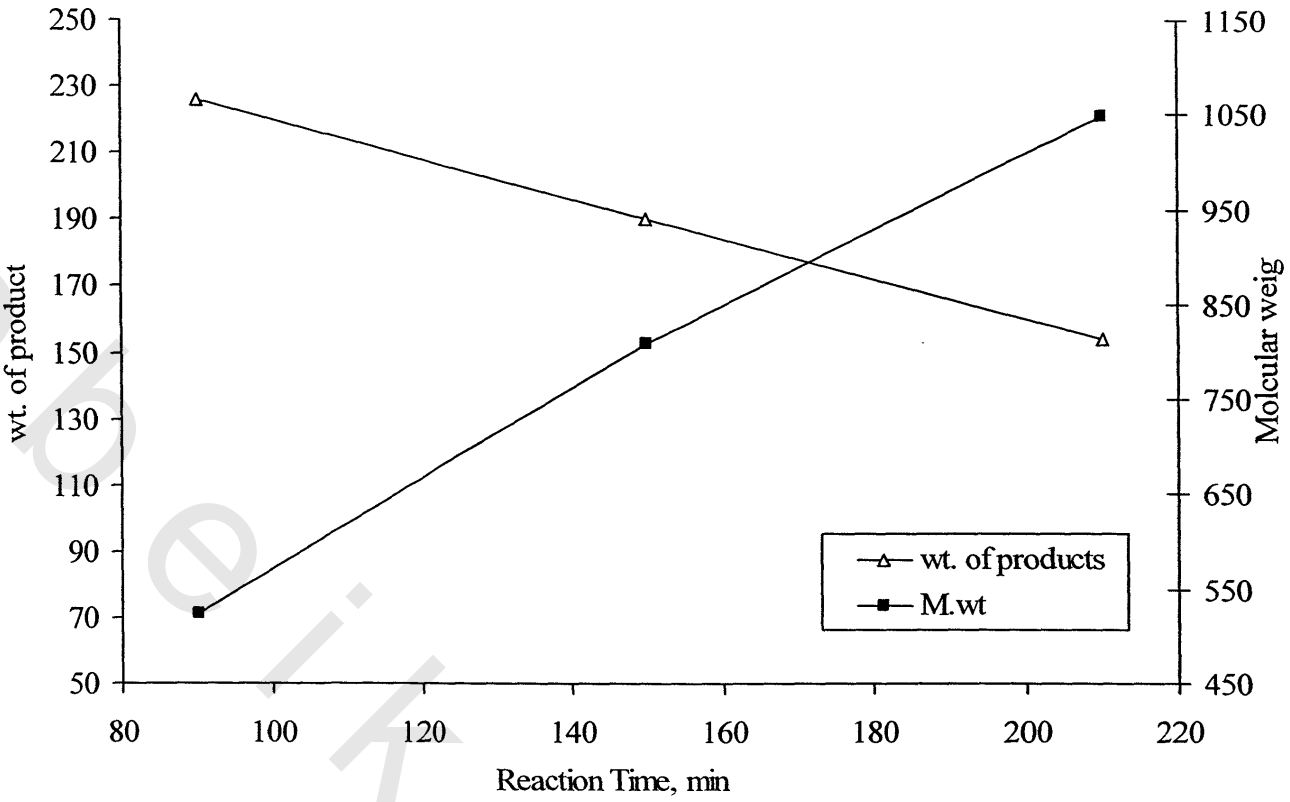

Fig. 21 : Relationship Between Reaction Time and Molecular Weight and Weights of Products.

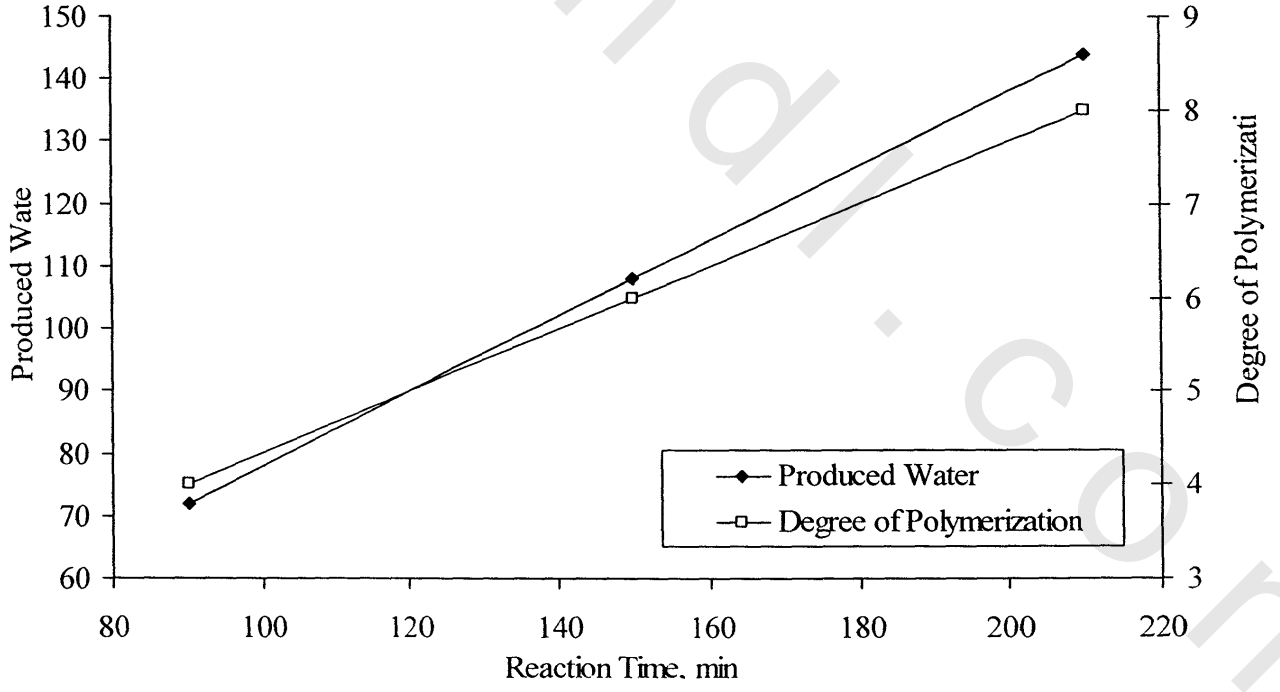

Fig. 22 : Relationship Between Reaction Time and Produced Water and Degree of Polymerization.

obeikandl.com

At this concentration the surface active molecules aggregate into clusters (micelles) with their hydrophilic groups directed towards the solvent (water). Micellization is therefore a mechanism alternative to adsorption at the interface for removing lyophobic groups from contact with the solvent, thereby reducing the free energy of the system [91]. The critical micelle concentrations (CMCs) of the compounds at 25°C were determined by plotting the surface tension γ versus ln C (solute concentration) as shown in **Figs. 23** to **28**. The CMC values were determined from the abrupt change in the slope of γ versus ln C. plot. These values are listed in **Table 7**. From **Figs. 29** and **30** it was observed that the CMC decreases with increasing the degree of polymerization and with the number of ethylene oxide units. This may be due to coiling that could be formed as a result of increasing the length of polymer and the ethylene oxide chains. This finding decreases the area covered per molecule (A_{min}) as shown in **Table 7.** From **Fig. 31** it was also found that the CMC decreases with increasing the degree of esterfication with oleic acid. The surface tensions at the CMC (γ_{CMC}) which are listed in **Table 7**. It is noticeable that the γ_{CMC} values decrease with increasing the degree of polymerization and with the number of ethylene oxide units. On the other hand the γ_{CMC} increases with increasing the degree of esterfication. The data of γ_{CMC} for the esterified ethoxylated polytriethanolamines $E(100)P_8O_1$; $E(100)P_8O_4$; $E(100)P_8O_8$, revealed γ_{CMC}; 34; 37 and 38 mNm^{-1} respectively. Thus it can be concluded that the increase of alkyl groups of esters on the polytriethanolamine ethoxylates leads to decrease their HLB and further their solubility This finding decrease the adsorption of surfactant molecules on the surface. Further the surface tension (γ_{CMC}) should be increased. This observation was also seen for the other two esterified ethoxylated groups $E(40)P_8O_1$; $E(40)P_8O_4$ (γ_{CMC} = 36 and 38 mNm_{-1}). The values for the others were $E(120)P_8O_1$; $E(120)P_8O_4$ and $E(120)P_8O_8$ (γ_{CMC} = 33, 36 and 40 mNm^{-1} respectively).

Maximum surface excess concentration (Γ_{max}) in mol/cm^2 was calculated from Gibbs equation. and the data are listed in **Table 7**. As a general trend, Γ_{max} values decrease by

increasing the degree of polymerization and the number of ethylene oxide units incorporated in the surfactant structure. The ethoxylated polymers were reacted with oleic acid to form the corresponding ester. It was observed that the Γ_{max} increases with increasing the degree of esterfication.

Decreasing A_{min} with the degree of polymerization, ethoxylation and esterification was seen as a general trend as shown in Table 7 and illustrated in **Fig. 32, 33,** and **34**. The A_{min}/molecule decreases with increasing the degree of polymerization and the total number of ethylene oxide units. This behaviour supports the idea that coiling of the molecules may occur at the interface leading to a decrease of A_{min}/molecule even with the increase in the molecular weight. The A_{min} depends mainly on the adsorption at interfaces, which in turn is affected by the total number of ethylene oxide units [92] .

The free energy of micellization data in **Table 8** indicates that the micellization process is a spontaneous ($\Delta G_{mic} < 0$). The data shows also that the negativity of ΔG_{mic} increases with an increase in the degree of polymerization and the number of e.o units incorporated. This behavior indicates that increasing the oxyethylene chain length favors the micellization process.

It is also found from **Table 8** that the negativity of ΔG_{mic} increases with increasing the esterfication degree. From the data obtained, it was found that all $\mathbf{\Delta G_{ad}}$ values are negative and they are more negative than $\mathbf{\Delta G_{mic}}$ values. This indicates that the adsorption at the interface is associated with a decrease in the free energy of the system i.e. the adsorption process is more spontaneous. Also, the more negative that the values of $\mathbf{\Delta G_{ad}}$ are indicates favorable adsorption to micellization. This may be due to steric factors inhibiting micellization that are stronger than its effect on adsorption. From **Fig. 35** and **36**, the ΔG_{ad} values increase with increasing the degree of polymerization and ethylene oxide contents.

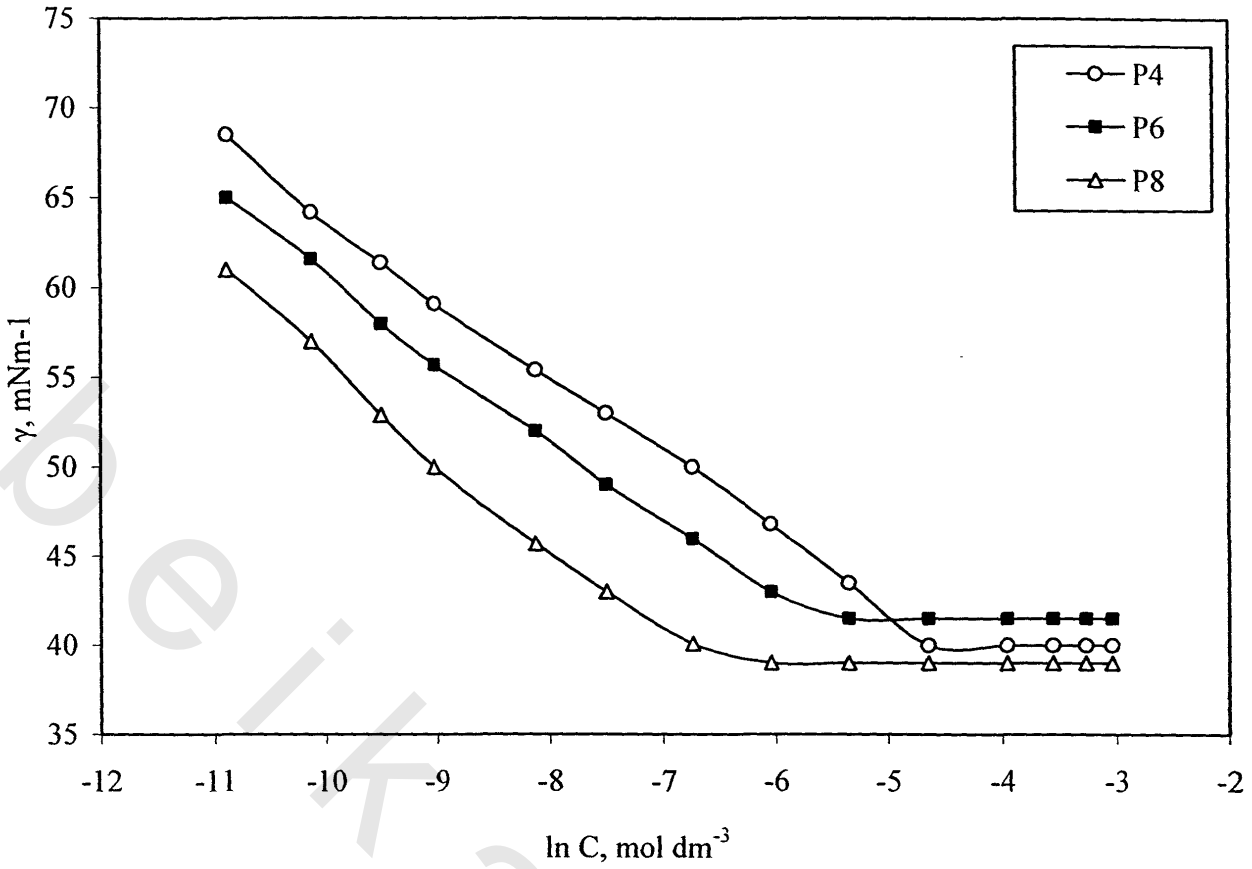

Fig. 23: γ- ln C Adsorption Isotherm for P4, P6 and P8

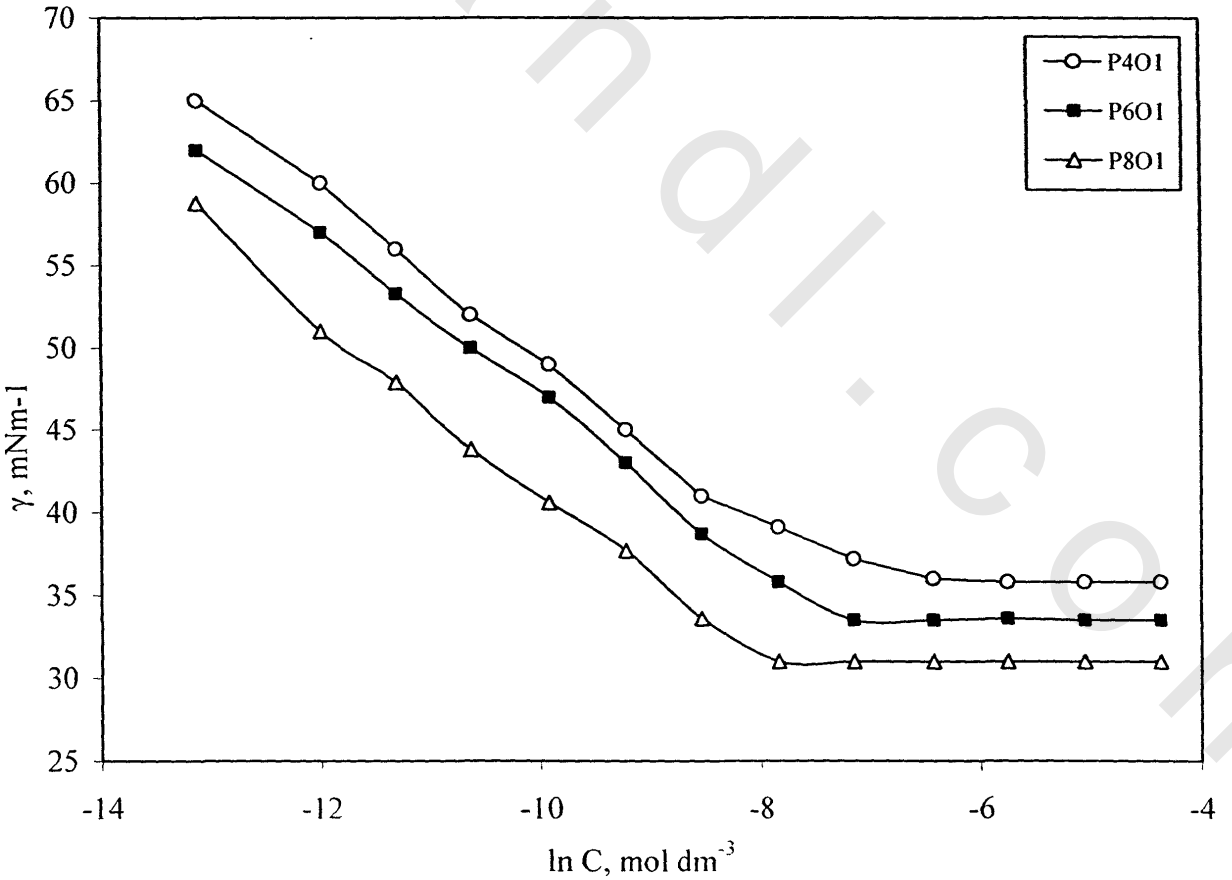

Fig. 24: γ- ln C Adsorption Isotherm for P_4O_1, P_6O_1 and P_8O_1

obeikandl.com

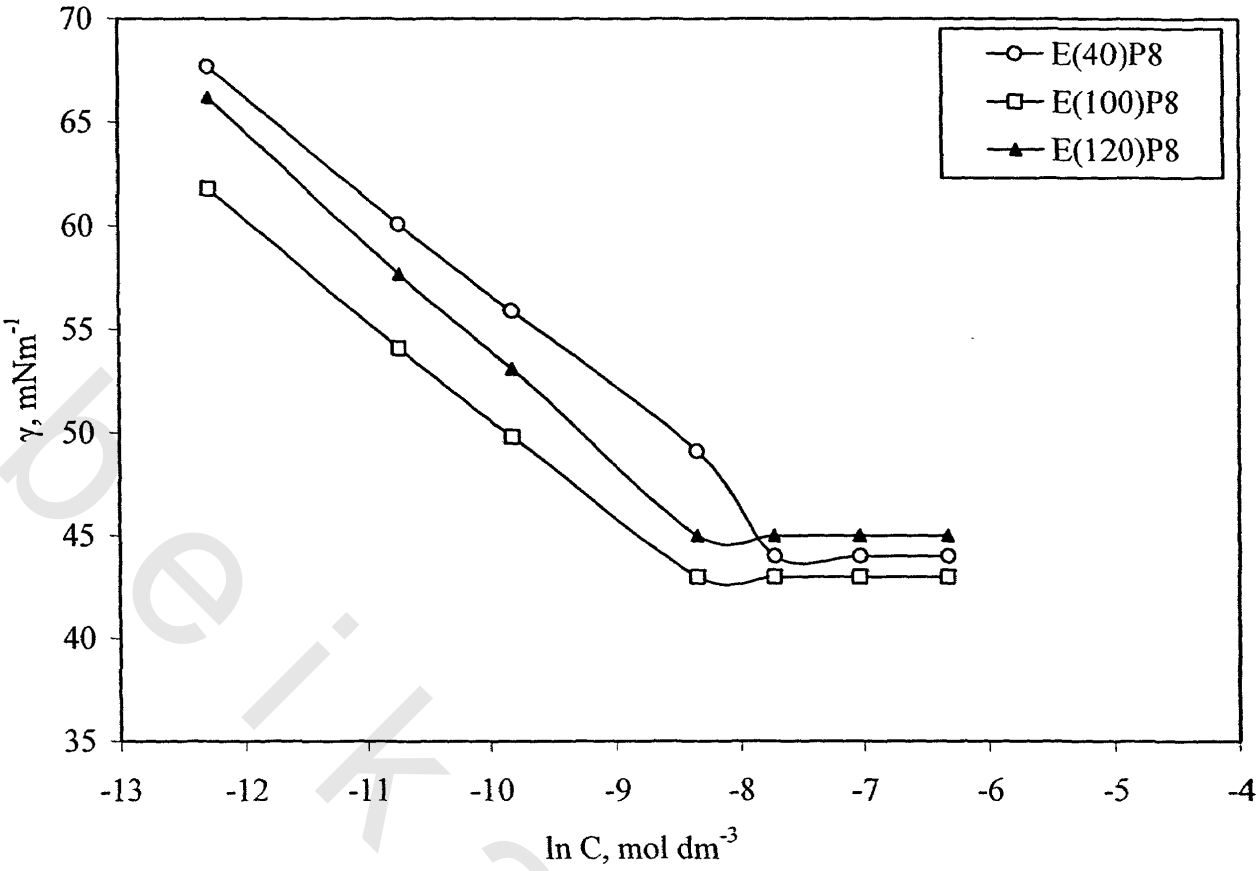

Fig. 25: γ- ln C Adsorption Isotherm for $E(40)P_8$, $E(100)P_8$ and $E(120)P_8$

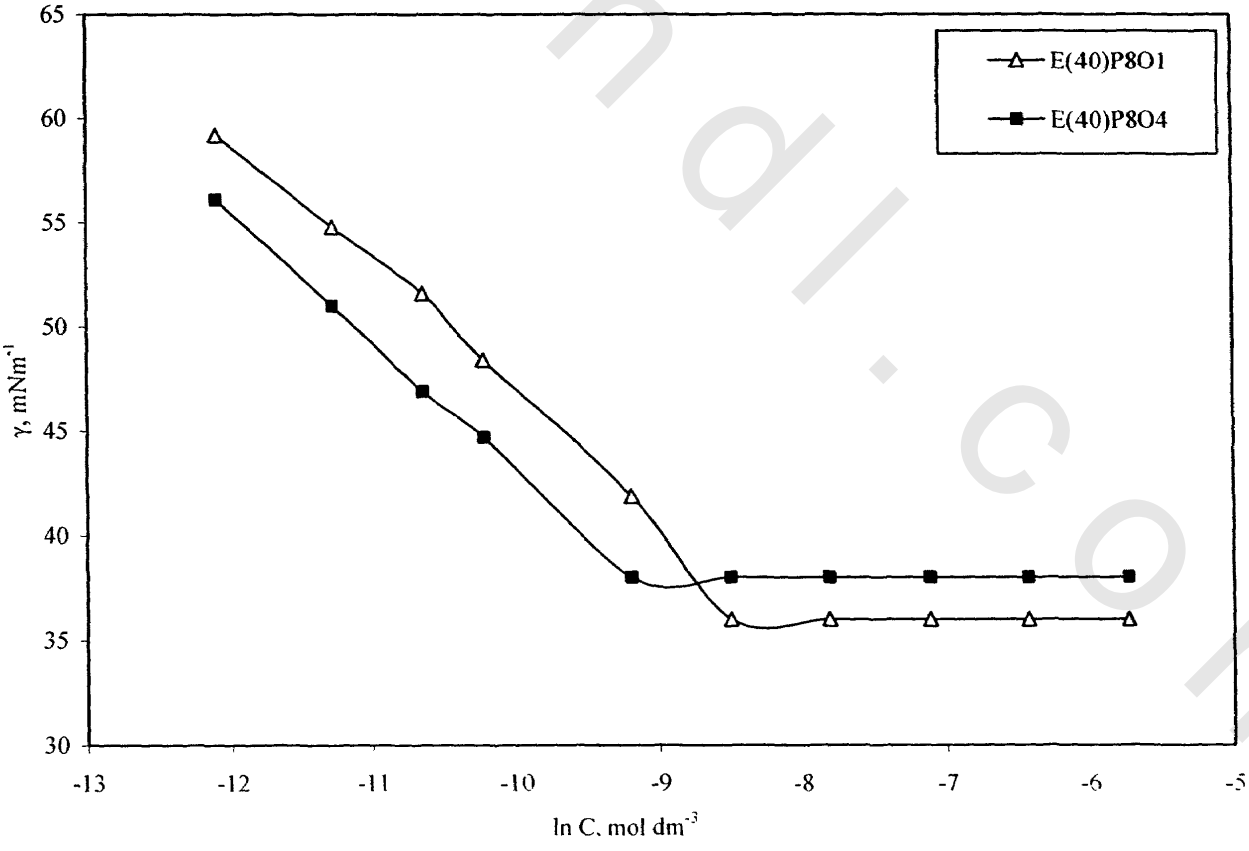

Fig. 26: γ- ln C Adsorption Isotherm for $E(40)P_8O_1$ and $E(40)P_8O_4$.

Obeikandl.com

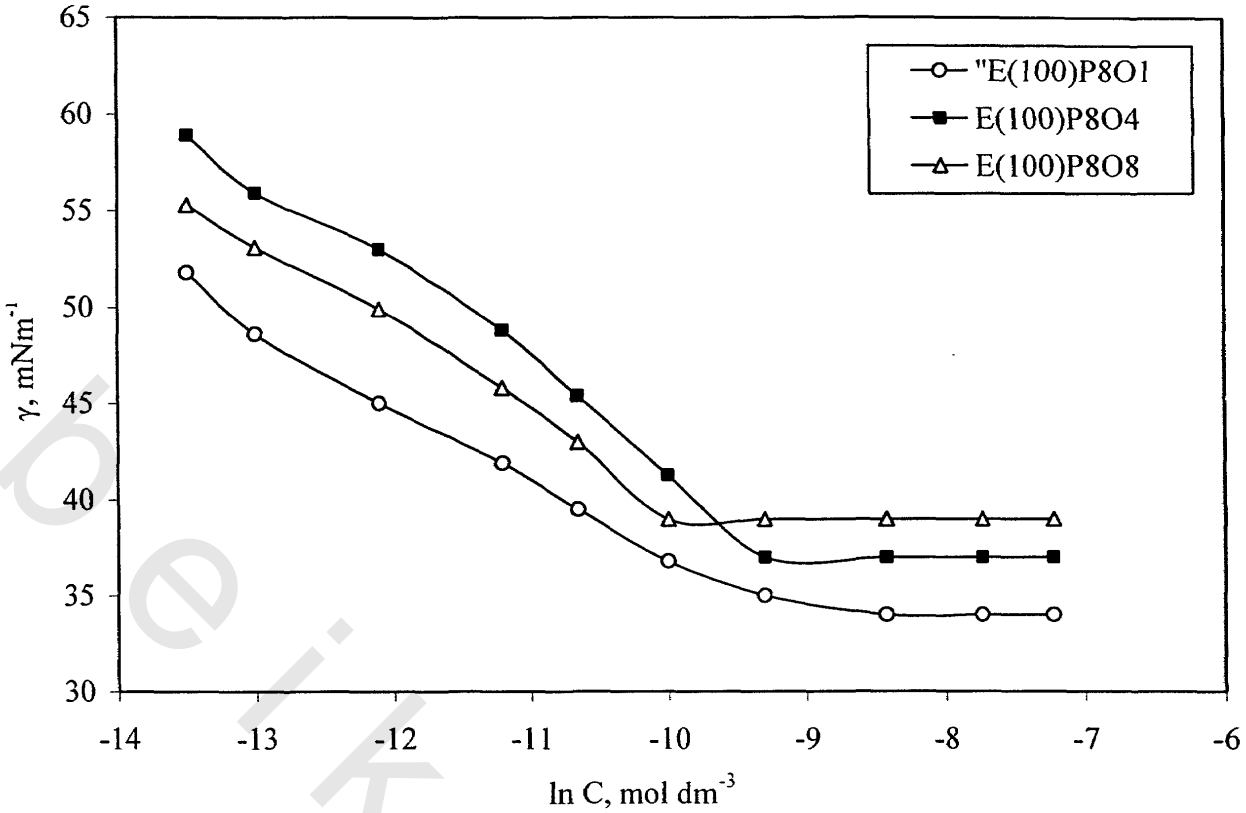

Fig. 27: γ- ln C Adsorption Isotherm for $E(100)P_8O_1$, $E(100)P_8O_4$ and $E(100)P_8O_8$

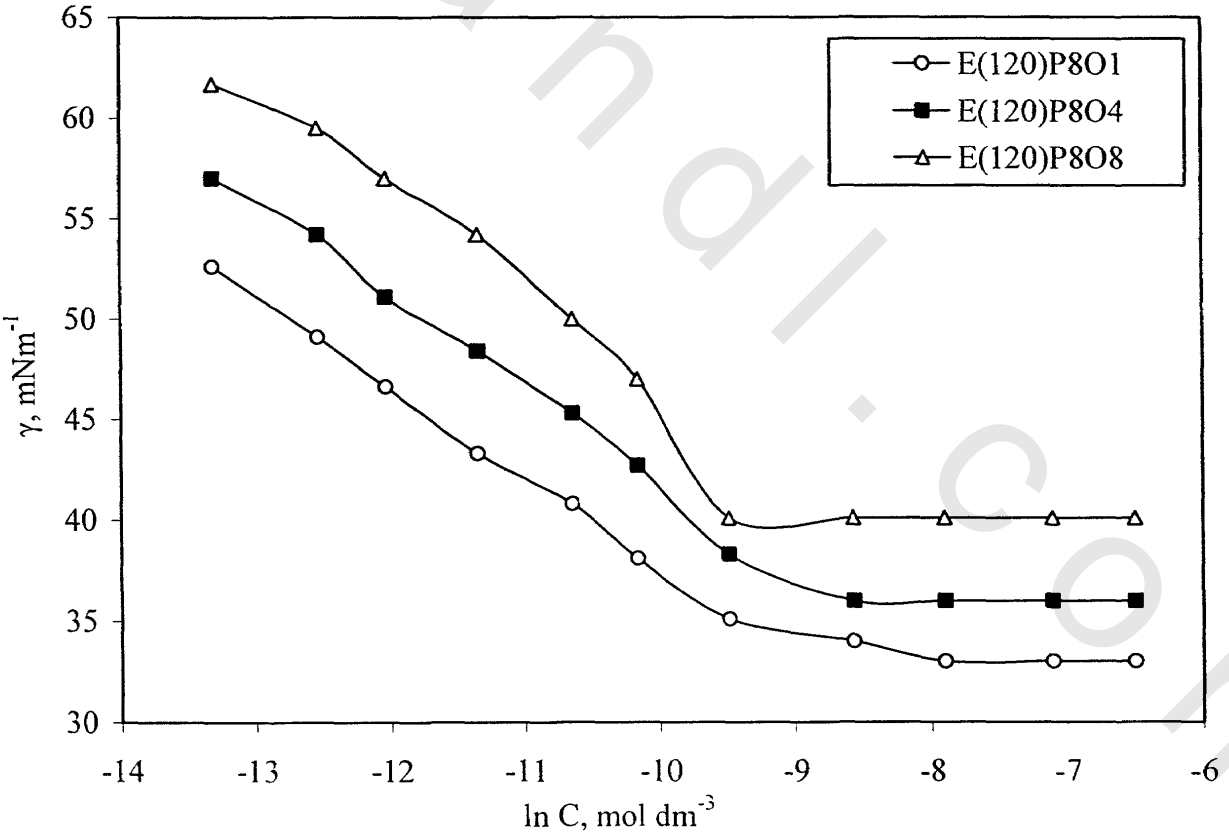

Fig. 28 : γ- ln C Adsorption Isotherm for $E(120)P_8O_1$, $E(120)P_8O_4$ and $E(120)P_8O_8$

Open Kandi.com

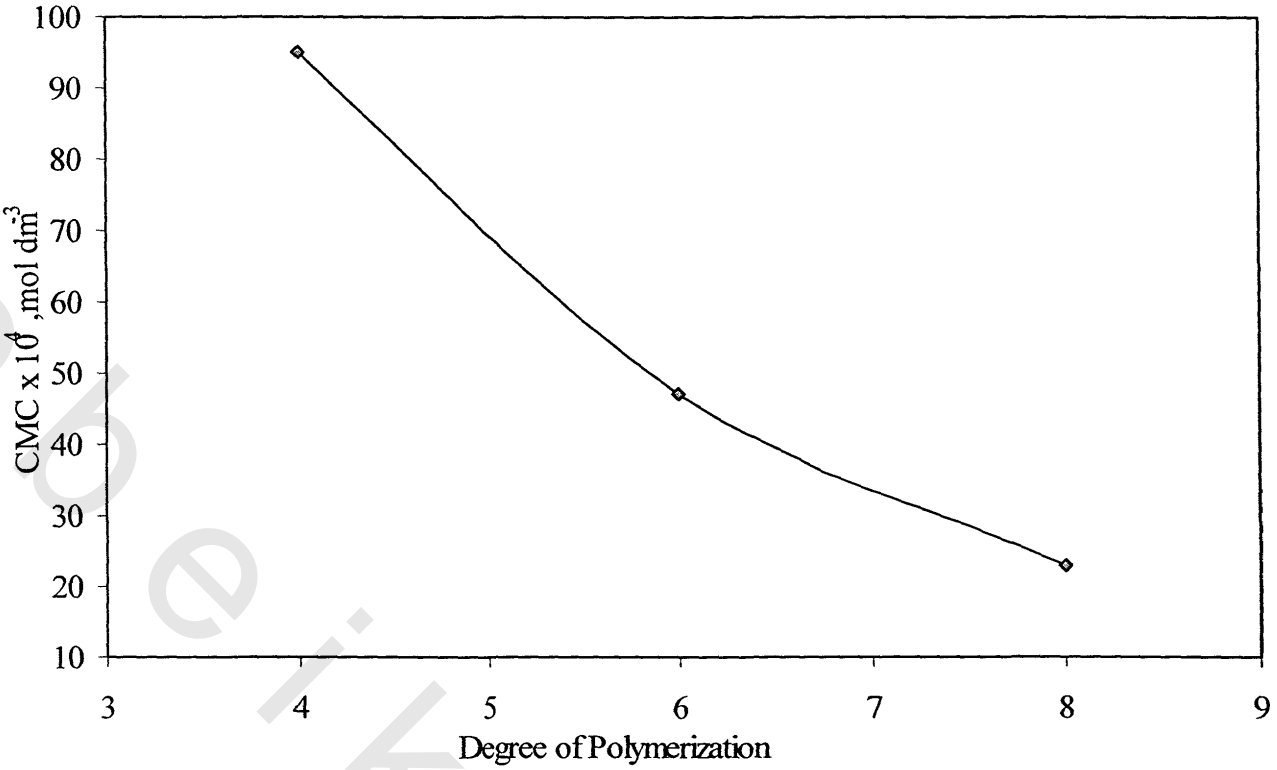

Fig. 29: Relationship Between the Degree of Polymerization and CMC.

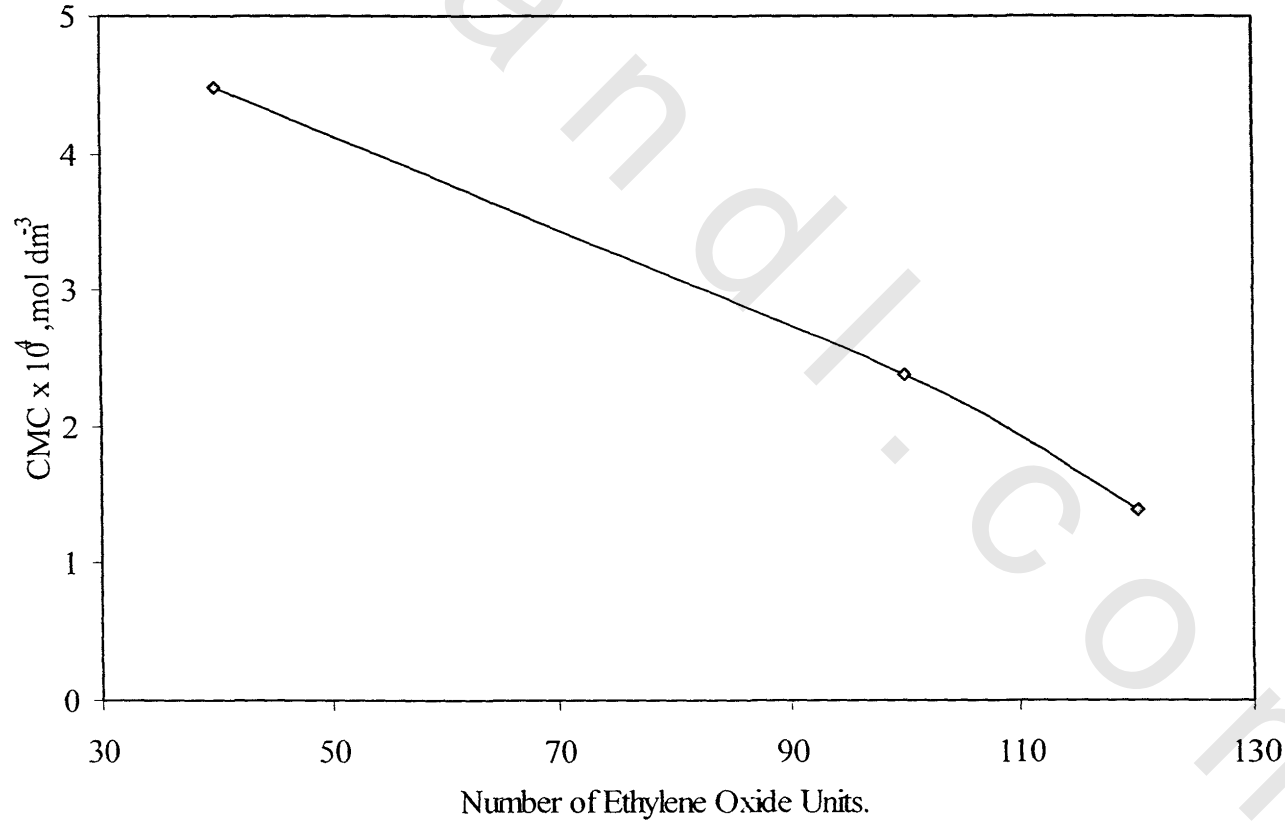

Fig. 30: Relationship Between the Number of Ethylene Oxide Units and CMC.

obeikandl.com

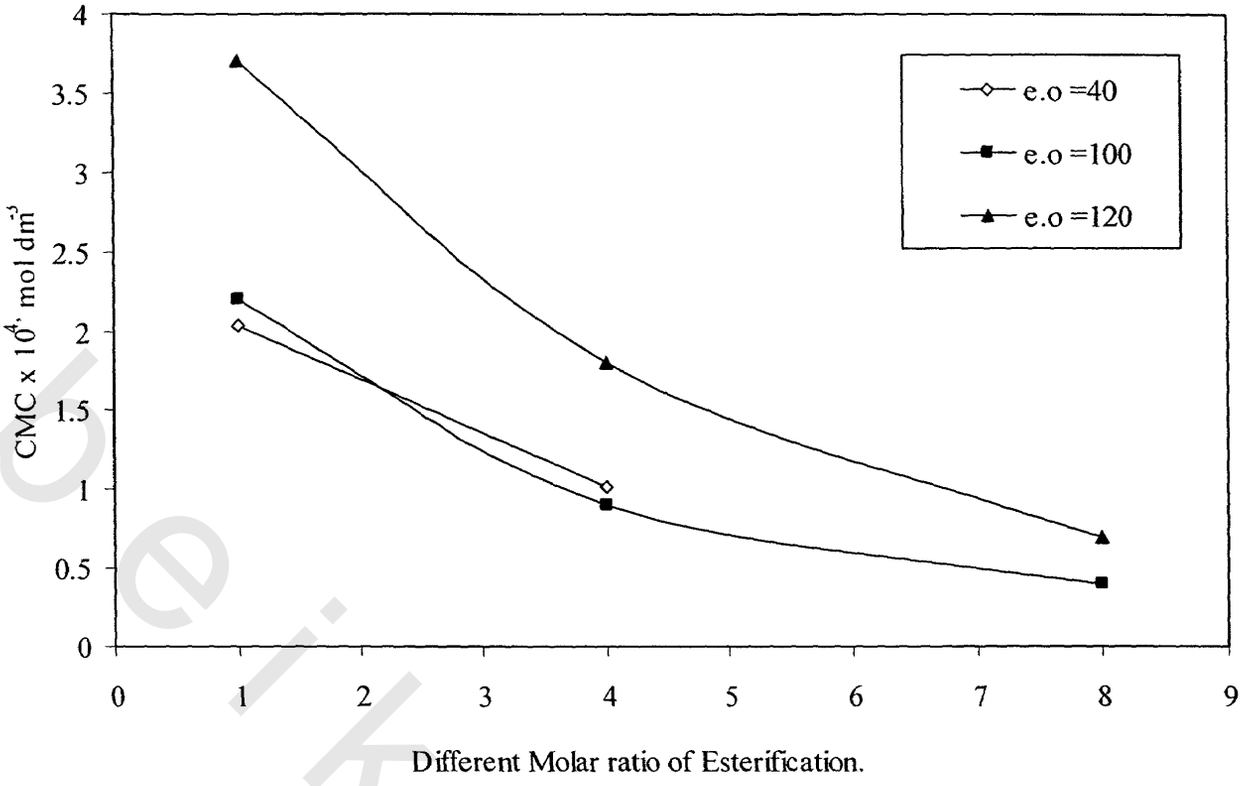

Fig. 31 : Relationship Between Different Molar Ratio of Esterification and CMC.

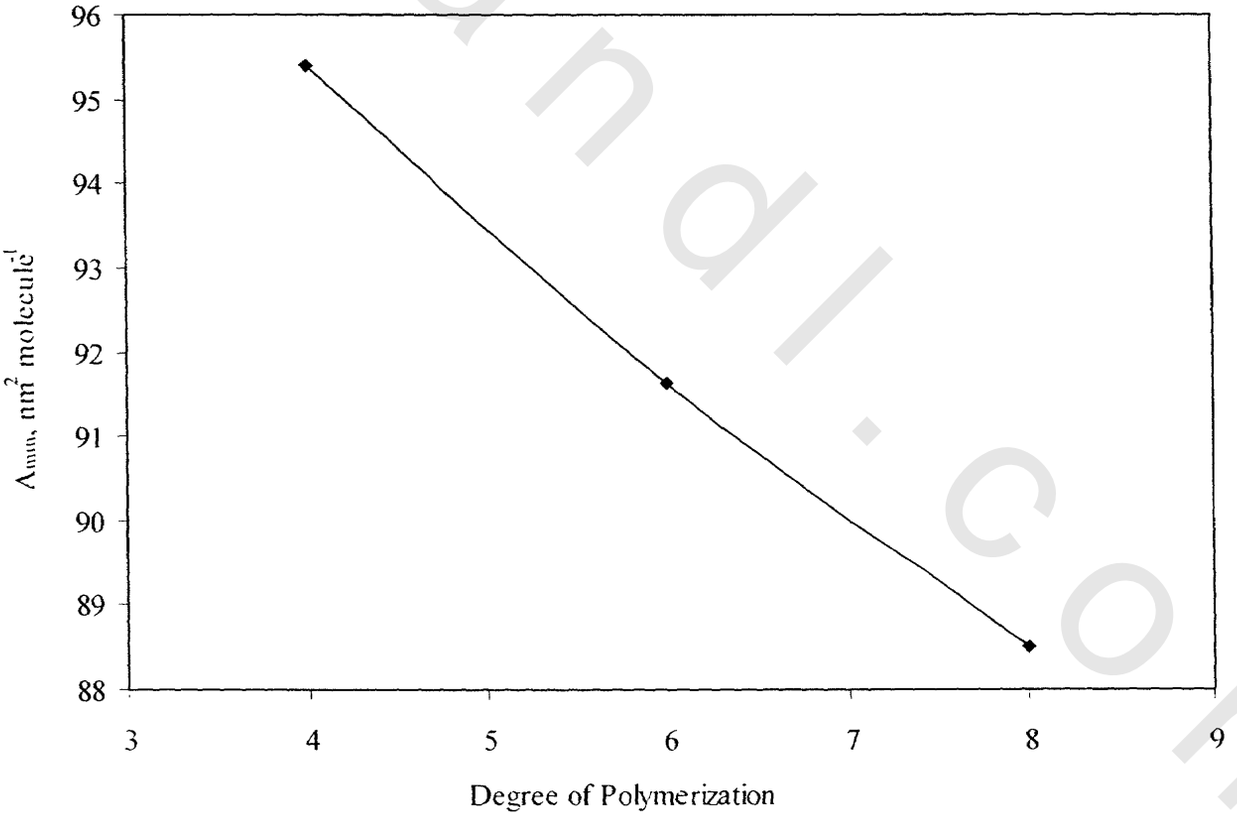

Fig. 32: Relationship Between the Degree of Polymerization and A_{min}.

obeikandl.com

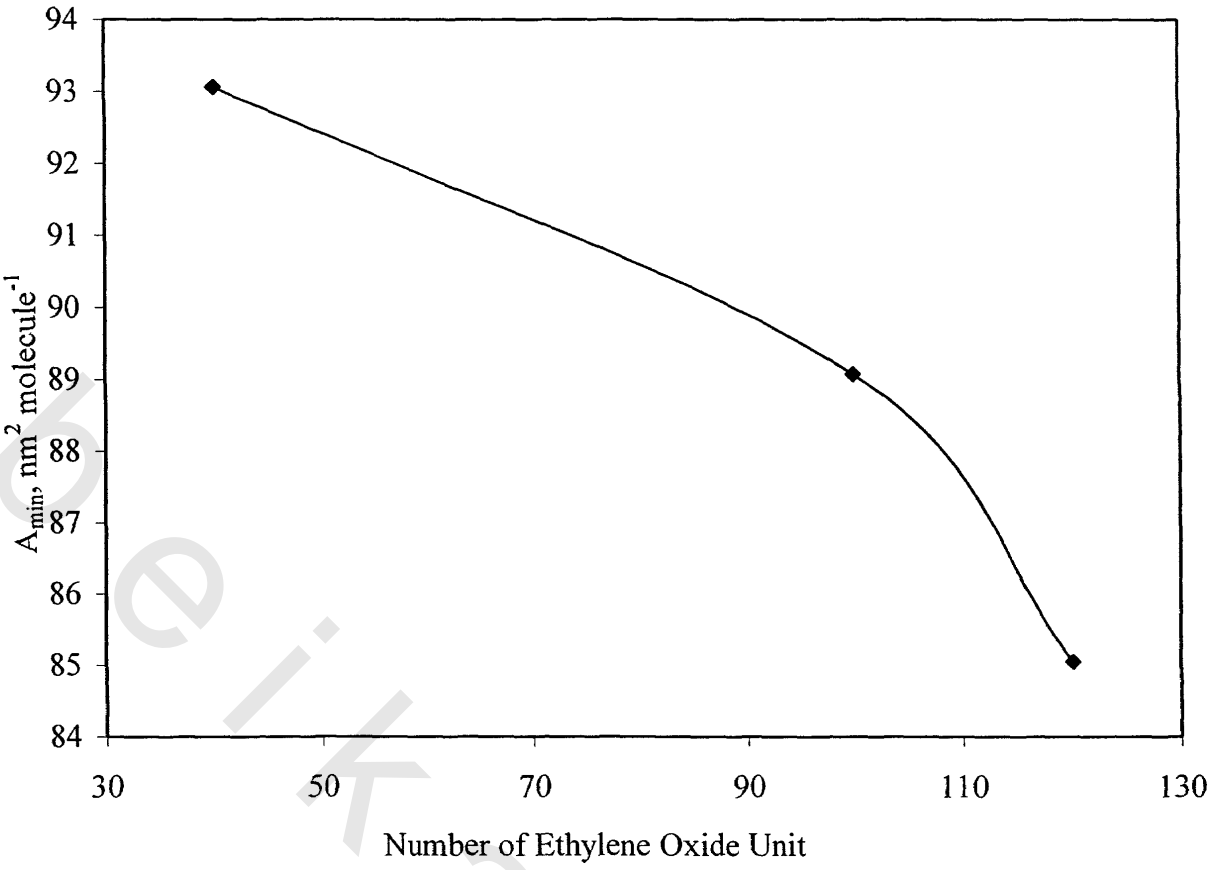

Fig. 33 : Relationship Between the Number of Ethylene Oxide Unit and A_{min}

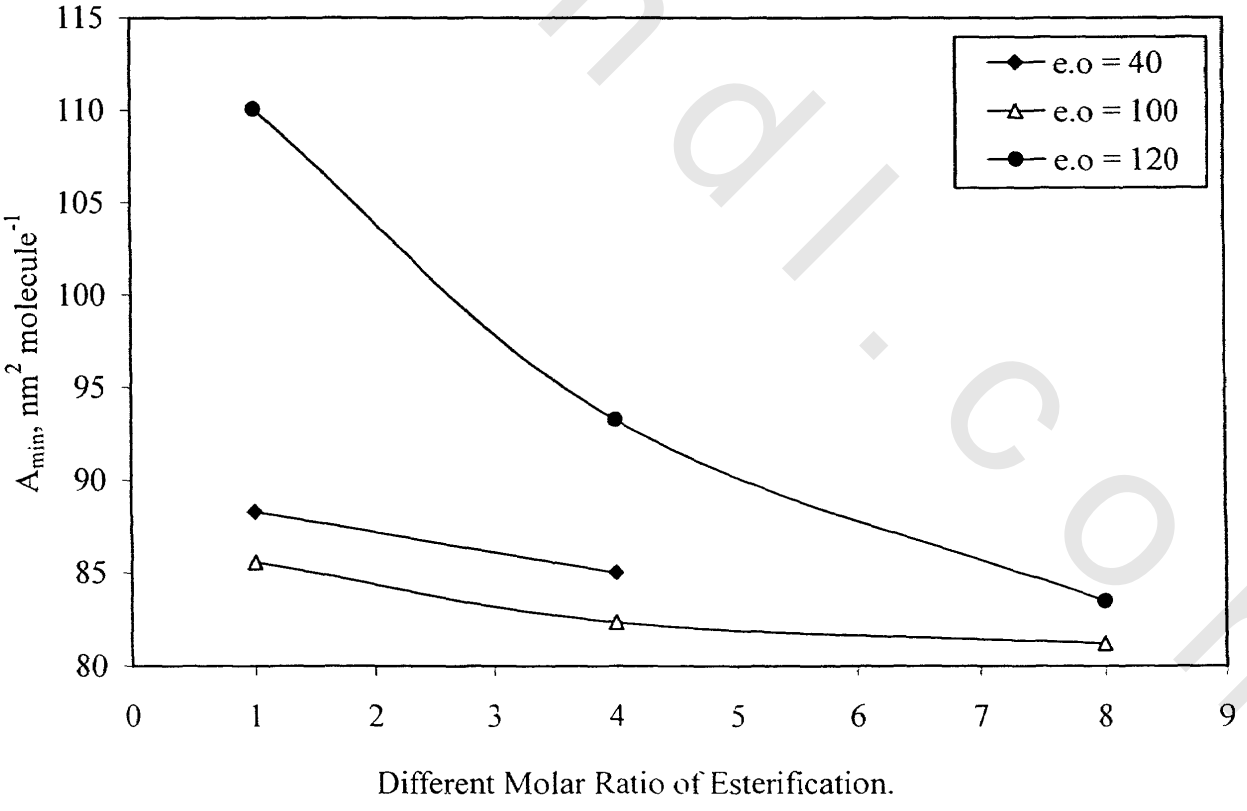

Fig. 34 : Relationship Between Different Molar Ratio of Esterification and A_{min}.

obeikandl.com

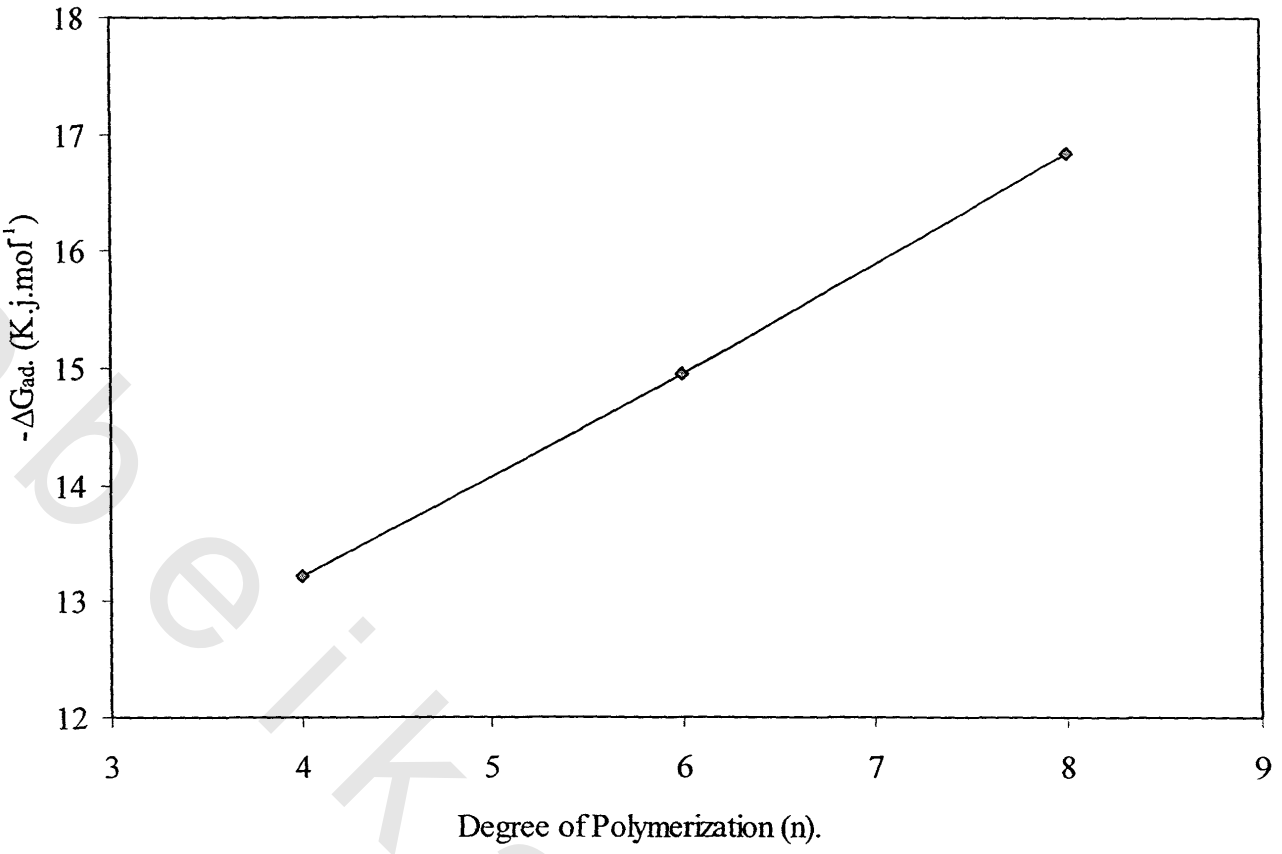

Fig. 35 : Relationship Between the Degree of Polymerization and $-\Delta G_{ad.}$

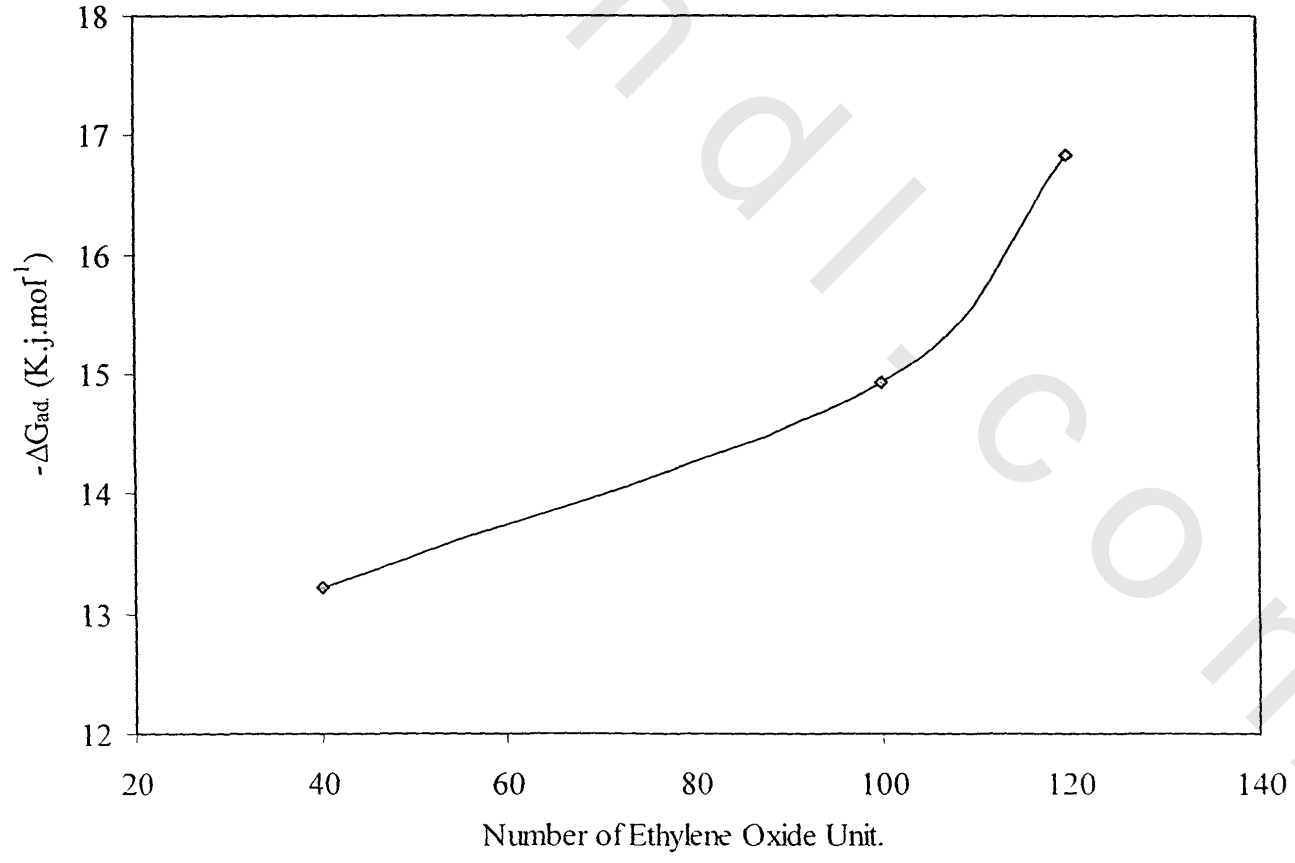

Fig. 36 : Relationship Between the Degree of Polymerization and $-\Delta G_{ad}$

obeikandi.com

The products of the structural effect $\Delta G_{mic} - \Delta G_{ad}$ used for the surfactants are also shown in **Table 8**. This positive product values reflect that these surfactants are more readily adsorbed at air/ aqueous solution interface. This in turn could account for investigating these surfactants as corrosion inhibitors.

Table 7: Surface Active Pproperties of the Polymers, Their Ethoxylates and Esters.

Inhibitor Code	γ_{CMC} (mNm^{-1})	CMC $x10^4$ ($mol\ dm^{-3}$)	Π_{CMC} (mNm^{-1})	$\Gamma_{max}\ x10^{10}$ ($mol\ cm^{-3}$)	A_{min} ($nm^2\ molecule^{-1}$)
P_4	40	95	32	1.876	95.41
P_6	41	47	31	1.812	91.62
P_8	39	23	33	1.74	88.50
$E(40)P_8$	36	4.48	36	1.95	93.06
$E(100)P_8$	33	2.38	39	1.86	89.07
$E(120)P_8$	31	2.38	41	1.78	85.05
P_4O_1	44	8.00	28	2.04	81.38
P_6O_1	43	3.97	29	1.96	84.70
P_8O_1	45	1.90	27	1.88	88.31
$E(40)P_8O_1$	36	2.03	36	1.88	88.31
$E(40)P_8O_4$	38	1.02	34	1.95	85.05
$E(100)P_8O_1$	34	2.20	38	1.94	85.58
$E(100)P_8O_4$	37	0.91	35	2.01	82.35
$E(100)P_8O_8$	36	0.45	36	2.04	81.22
$E(120)P_8O_1$	33	3.70	39	1.50	110.09
$E(120)P_8O_4$	36	1.89	36	1.78	93.27
$E(120)P_8O_8$	40	0.756	32	1.98	83.51

Open Research Library

Table 8 : Thermodynamic Parameters of Micellization, Adsorption and Structural Effect for the Prepared Surfactants.

Surfactants Code	ΔG_{mic} (Kj mol^{-1})	$\Delta G_{ad.}$ (Kj mol^{-1})	$\Delta G_{mic} - \Delta G_{ad.}$ (Kj mol^{-1})
P_4	-11.52	-13.22	1.705
P_6	-13.23	-14.94	1.71
P_8	-14.93	-16.83	1.89
$E(40)P_8$	-19.10	-20.94	1.84
$E(100)P_8$	-20.66	-22.75	2.09
$E(120)P_8$	-20.66	-22.96	2.29
P_4O_1	-17.66	-19.03	1.37
P_6O_1	-19.39	-20.87	1.47
P_8O_1	-21.10	-22.54	1.43
$E(40)P_8O_1$	-21.05	-22.97	1.91
$E(40)P_8O_4$	-22.76	-24.51	1.74
$E(100)P_8O_1$	-20.86	-22.81	1.95
$E(100)P_8O_4$	-23.04	-24.77	1.73
$E(100)P_8O_8$	-24.77	-26.53	1.76
$E(120)P_8O_1$	-19.57	-22.15	2.58
$E(120)P_8O_4$	-21.23	-23.25	2.02
$E(120)P_8O_8$	-23.51	-25.12	1.60

obeikan.com

Application of the Surfactants Prepared in this Study to the Petroleum Industry

(1). Evaluation of the prepared Surfactants as Corrosion Inhibitors

Surfactants are widely used and find a very large number of applications because of their remarkable ability to influence the properties of surfaces and interfaces. Corrosion is among the important applications of surfactants especially in the petroleum industry. Corrosion problems have received considerable attention because of strong economic losses derived from the serious damage caused by metallic corrosion on piping and plant systems.

Statistical data show that failures due to corrosion in oil and gas industry oscillate between 25 and 30 % of the total losses [93]. Although corrosion is inevitable, it can be controlled by several techniques. The use of corrosion inhibitors is one of the most practical methods for protecting the internal wall of pipelines. The corrosion inhibition of a metal involves strong adsorption of the inhibitors to the metal surface by nitrogen, sulfur, oxygen or a double bond.

The important metals in structures such as iron, aluminum, copper, etc. are inherently unstable. Their ionic solutions and their carbonates, hydroxides, oxides, sulfates and many other salts are more stable than the free metal under many conditions to which these metals are exposed. The free energy change for the conversion of these metals to a compound has a large negative value, and the thermodynamic driving force to convert the elemental metal to an oxide or salt is great. Thus to retain a required physical property of the metal, it is essential to protect the metal from the environments to which it is exposed. There are several methods that can be applied for metal protection. These methods can be divided into thermodynamic protection, kinetic protection, barrier protection, structure design, environmental control, and metallurgical design. The presence of water at the fluid/solid interface may initiate the electrochemical corrosion reaction by charge transfer coating or through cathodic and anodic areas. Thus in practice, a second line of defense is used to provide protection. The use of corrosion inhibitors is mainly applied in closed or recirculating systems. The inhibitors are chemical substances that are

obeikandi.com

added to a liquid (usually water) to prevent corrosion or to control it at an acceptable low corrosion rate. They are selected for their effectiveness in protecting the specific metal or combination of metals in a given system. Many organic compounds containing oxygen, nitrogen, sulfur, double bond or phenyl ring are used as corrosion inhibitors for carbon steel in various aggressive environments [94-96].

The consensus is that such organic compounds inhibit corrosion by adsorbing at the metal / solution interface through their functional groups [97]. Through this study, chemical (weight loss) methods are used to evaluate the corrosion inhibitors prepared in this study.

Weight Loss Measurements

Weight loss is the most common method to evaluate corrosion inhibition. Besides, it does not require sophisticated equipment for determination. The effectiveness of the compounds as corrosion inhibitors for carbon steel in 1M HCl solutions has been investigated at different inhibitor concentrations and at various temperatures.

The weight loss of carbon steel sheets after immersion in 1M HCl without or with different concentrations of the prepared surfactants (inhibitors) were determined using equation (10) in experimental section.

Effect of Chemical Structure

Depending on weight loss data, the corrosion rate (C.R.) in mils per year (mpy) was calculated using equation (12) in the experimental section.

Figs. 37 to 41 illustrate the relation between the rates of corrosion against the inhibitor concentrations. The data obtained for corrosion rate (in mpy) for the esterified polymers. ethoxylated polymers and esters of ethoxylated polymers samples are shown in **Tables 10 to 14**. The data show that the rate of corrosion for the blank sample is the highest one. Also, there is a general trend of a decrease in the rate of corrosion (in mpy) with increasing inhibitor concentration from 50-500 ppm. On the other hand. the surface coverage area (θ) for the

obeikandl.com

different concentrations of the investigated inhibitors in 1 M HCl was calculated by the following equation:

$$\theta = 1 - (\Delta W_i / W_0) \qquad (17)$$

The data obtained for θ are summarized in **Table 10-14**. It was recognized that there is an inverse relation between the rate of corrosion and the surface area covered. In other words, the inhibitors having the higher surface area coverage are those having higher inhibition rate. Their values are in the range of ≈ 0.5 for the lowest inhibitor at low concentrations and ≈ 0.95 for the highest one at high concentrations. The highest value of θ near unity indicates almost full coverage of the metal surface with the adsorbed surfactant. Conclusively, the surfactant inhibitor having near unity θ is considered a good physical barrier that shields the corroding surface from the corrosive medium and reducing the corrosion rate of carbon steel significantly.

The inhibition efficiency of the inhibitors depends on many factors such as the number of adsorption active centers in the molecule and their charge density, molecular size, mode of adsorption, heat of hydrogenation and formation of the metallic complex [98].

The inhibition efficiency (I %) of all the prepared inhibitors was calculated according to the equation (11) given in the experimental section:

$$I\,\% = \frac{\Delta W - \Delta Wi}{\Delta W} x100$$

The I% data obtained at different concentrations namely, 25, 50, 100, 200, 300, 400, 500 and 600 ppm are listed in **Table 15.** From the data in **Table 15** and **Fig. 42,** it is obvious that the inhibition efficiency of the polymers increases until a certain concentration (50 ppm) is reached after which it was decreases. The polymer molecules have internal hydrogen bonds between the hydrogen of –OH groups and nitrogen atoms (H.b.P). The solubility of these polymers at low concentration may depend on the hydrogen bonds between the polymer molecules and water [external hydrogen bonds (H.b.W)] where the molecules prefer to adsorb on the interface and exhibit the maximum efficiency at 50 ppm. At high concentration the polymer molecules tend to

form hydrogen bonds between them that are stronger than the hydrogen bonds between water and polymer molecules. Further the molecules coagulate and desorption from the interface occurrs then the inhibition efficiency decreases. On the other hand the inhibition efficiency for esters of polymers, ethoxylated polymers, and esters of ethoxylated polymers increases with increasing the inhibitor concentration as shown in **Figs. 43 to 46** .

From **Table 15** and **Fig. 47** it can be noted that the inhibition efficiency increases with increasing the degree of polymerization. Increasing the polymerization increases the number of function groups such as oxygen of the ethereal bonds, terminal OH groups, and nitrogen atoms which causes adsorption at the metal surface. The nitrogen atoms are the major adsorption centers for interaction with the metal surface [99]. There is another factor affecting the inhibition efficiency which is the ethylene oxide content. The increase of ethoxylation from 40 to 100 to 120 causes a general elevation of the corrosion inhibition efficiency values. From **Table 15** the I values for $E(40)P_8$, $E(100)P_8$ and $E(120)P_8$ were 89, 90, and 91.7 respectively at 500 ppm . This may be attributed to the increase in the number of ethereal bonds in the molecule. This latter bond incorporation increases the electron density of the molecules which are considered as active centers for the adsorption process. This can be observed clearly from **Fig. 48**.

The data in **Table 15** also show that the inhibition efficiency decreases with increasing the degree of esterfication of the ethoxylated compounds. The ethoxylated polymers have terminal OH groups which enhance the adsorption process on the metal surface. When these compounds are esterified with oleic acid, the OH groups are blocked by the ester groups. Thus it is clear from **Table 15** that the $E(40)P_8O_1$ (low ester degree) exhibited the highest efficiency (95.1 %) than the other compounds.

Table 9: Corrosion Rate and the Degree of Surface Coverage (θ) at Different Concentrations of P_4, P_6, and P_8 in 1M HCl Solution at 298 K.

Inhibitors Code	Concentration (ppm)	Rate of Corrosion (mpy)	(θ)
P_4	Blank	107.56	-
	25	67.65	0.37
	50	23.60	0.78
	100	47.21	0.56
	200	50.38	0.53
	300	52.68	0.51
	400	64.49	0.40
	500	67.65	0.37
P_6	25	59.02	0.450
	50	21.30	0.800
	100	21.88	0.794
	200	23.89	0.777
	300	25.62	0.760
	400	28.21	0.736
	500	30.80	0.713
P_8	25	47.21	0.560
	50	17.27	0.830
	100	19.57	0.817
	200	20.96	0.805
	300	22.45	0.790
	400	23.89	0.777
	500	33.68	0.685

obeikandi.com

Table 10: Corrosion Rate, the Degree of Surface Coverage (θ) at Different Concentrations of P_4O_1, P_6O_1, and P_8O_1 in 1M HCl Solution at 298 K.

Inhibitors Code	Concentration (ppm)	Rate of Corrosion (mpy)	(θ)
P_4O_1	25	53.78	0.50
	50	47.33	0.56
	100	43.01	0.60
	200	35.47	0.67
	300	30.11	0.72
	400	25.79	0.76
	500	25.79	0.76
P_6O_1	25	51.62	0.52
	50	39.78	0.63
	100	32.24	0.70
	200	25.79	0.76
	300	21.50	0.80
	400	16.12	0.85
	500	16.12	0.85
P_8O_1	25	47.30	0.56
	50	41.94	0.61
	100	26.89	0.75
	200	21.50	0.80
	300	19.34	0.82
	400	12.89	0.88
	500	12.89	0.88

obeikandl.com

Table 11: Corrosion Rate and the Degree of Surface Coverage (θ) at Different Concentrations of E(40) P_8, E(100) P_8, and E(120) P_8 in 1M HCl Solution at 298 K.

Inhibitors Code	Concentration (ppm)	Rate of Corrosion (mpy)	(θ)
E(40)P_8	25	19.29	0.820
	50	15.54	0.855
	100	14.97	0.860
	200	12.95	0.879
	300	12.66	0.882
	400	11.80	0.890
	500	11.22	0.895
E(100) P_8	25	17.27	0.839
	50	14.97	0.860
	100	13.81	0.871
	200	12.95	0.879
	300	12.38	0.884
	400	11.80	0.890
	500	10.65	0.900
E(120) P_8	25	11.80	0.890
	50	10.65	0.900
	100	10.07	0.906
	200	10.07	0.906
	300	9.50	0.911
	400	8.92	0.917
	500	8.92	0.917

obeikandl.com

Table 12: Corrosion Rate and the Degree of Surface Coverage (θ) at Different Concentrations of $E(40)P_8O_1$, $E(40)P_8O_4$, and $E(40)P_8O_8$ in 1M HCl Solution at 298 K.

Inhibitors Code	Concentration (ppm)	Rate of Corrosion (mpy)	(θ)
$E(40)P_8O_1$	100	19.29	0.820
	200	18.13	0.831
	300	16.12	0.850
	400	10.07	0.906
	500	8.06	0.925
	600	5.18	0.951
$E(40)P_8O_4$	100	21.30	0.801
	200	19.86	0.815
	300	17.85	0.834
	400	15.83	0.852
	500	14.97	0.860
	600	14.97	0.860
$E(40)P_8O_8$	100	33.97	0.684
	200	31.67	0.705
	300	32.24	0.700
	400	31.38	0.708
	500	31.38	0.708
	600	31.38	0.708

obeikandl.com

Table 13: Corrosion Rate and the Degree of Surface Coverage (θ) at Different Concentrations of $E(100)P_8O_1$, $E(100)P_8O_4$, and $E(100)P_8O_8$ in 1M HCl Solution at 298 K.

Inhibitors Code	Concentration (ppm)	Rate of Corrosion (mpy)	(θ)
$E(100)P_8O_1$	100	21.30	0.801
	200	20.15	0.812
	300	19.29	0.820
	400	18.13	0.831
	500	16.12	0.850
	600	12.66	0.882
$E(100)P_8O_4$	100	24.76	0.769
	200	22.45	0.791
	300	21.88	0.796
	400	20.15	0.812
	500	20.15	0.812
	600	20.15	0.812
$E(100)P_8O_8$	100	41.74	0.611
	200	37.42	0.652
	300	36.56	0.660
	400	35.41	0.670
	500	35.41	0.670
	600	35.41	0.670

obeikandl.com

Table 14: Corrosion Rate and the Degree of Surface Coverage (θ) at Different Concentrations of $E(100)P_8O_1$, $E(100)P_8O_4$, and $E(100)P_8O_8$ in 1M HCl Solution at 298 K.

Inhibitors Code	Concentration (ppm)	Rate of Corrosion (mpy)	(θ)
$E(120)P_8O_1$	100	31.38	0.708
	200	24.47	0.772
	300	22.45	0.791
	400	19.57	0.817
	500	18.42	0.828
	600	18.13	0.831
$E(120)P_8O_4$	100	35.98	0.665
	200	30.23	0.718
	300	29.02	0.730
	400	26.20	0.756
	500	18.13	0.831
	600	18.13	0.831
$E(120)P_8O_8$	100	48.36	0.550
	200	44.05	0.590
	300	41.74	0.611
	400	37.42	0.652
	500	37.42	0.652
	600	37.42	0.652

obeikandi.com

Table 15: Inhibition Efficiency (I %) of the polytriethanolamines, their ethoxylates, and their Esters at Different Concentrations by Weight Loss Measurements at 298K.

Inhibitor code	Inhibition efficiency at different concentrations (ppm).							
	25	**50**	**100**	**200**	**300**	**400**	**500**	**600**
P_4	37.0	78.0	56.0	53.0	51.0	40.0	37.0	-
P_6	45.0	80.0	79.4	77.7	76.0	73.6	71.3	-
P_8	56.0	83.0	81.7	80.5	79.0	77.7	68.5	-
E(40)P_8	82.0	85.5	86.0	87.9	88.2	89.0	89.5	-
E(100)P_8	83.9	86.0	87.1	87.9	88.4	89.0	90.0	-
E(120)P_8	89.0	90	90.6	90.6	91.7	91.7	91.7	-
P_4O_1	50	56	60	67	72	76	76	-
P_6O_1	52	63	70	76	80	85	85	-
P_8O_1	56	61	75	80	82	88	88	-
E(40)P_8O_1	-	-	82.0	83.1	85.0	90.6	92.5	95.1
E(40)P_8O_4	-	-	80.1	81.5	83.4	85.2	86.0	86.0
E(40)P_8O_8	-	-	68.3	70.1	70.3	70.6	70.6	70.6
E(100)P_8O_1	-	-	80.1	81.2	82.0	83.1	85.0	88.2
E(100)P_8O_4	-	-	76.9	79.1	79.6	81.1	81.2	81.2
E(100)P_8O_8	-	-	61.1	65.2	66.0	67.0	67.0	67.0
E(120)P_8O_1	-	-	70.8	77.2	79.1	81.7	82.2	83.1
E(120)P_8O_4	-	-	66.5	71.8	73.0	75.6	83.1	83.1
E(120)P_8O_8	-	-	55.0	59.0	61.1	65.2	65.1	65.2

Open Knowledge.com

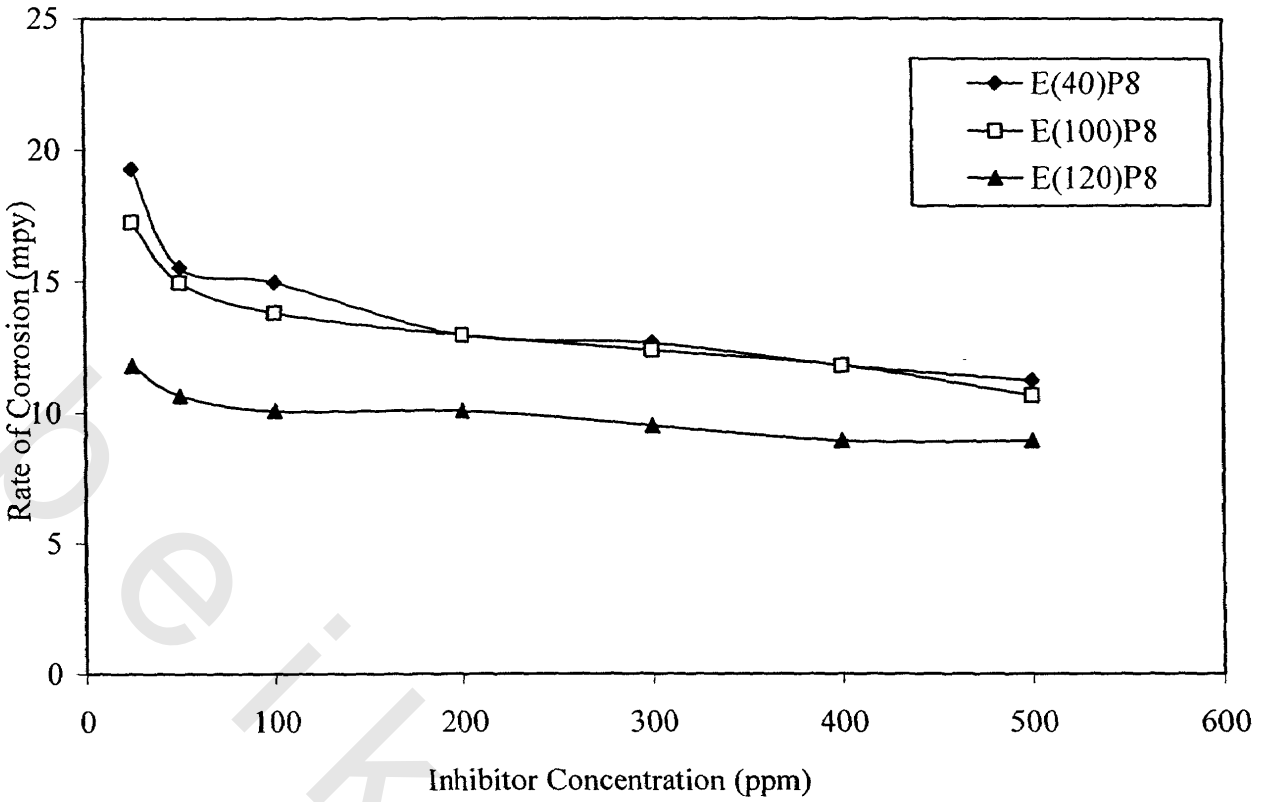

Fig. 37 : Rate of Corrosion For Carbon Steel Dissolution in 1M HCl at Different Concentrations of the Inhibitors $E(40)P_8$, $E(100)P_8$, $E(120)P_8$.

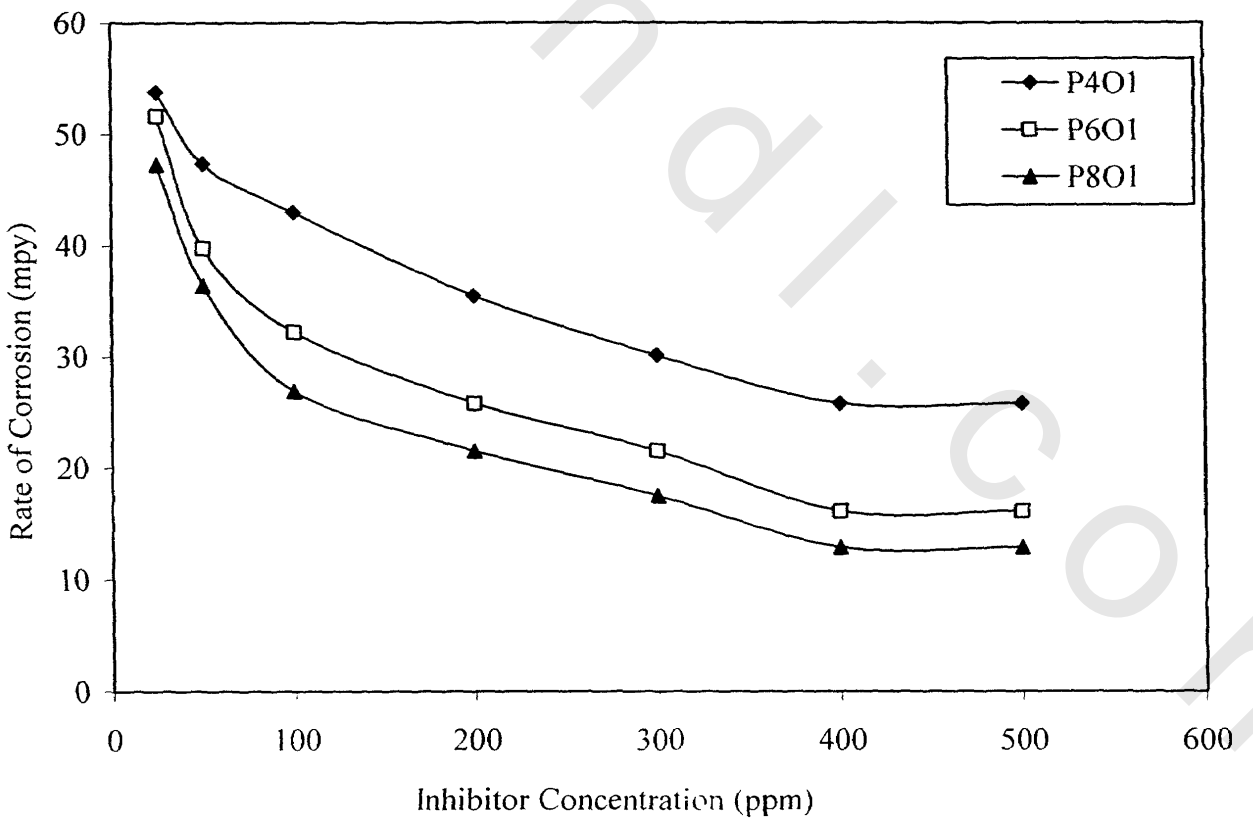

Fig. 38 : Rate of Corrosion for Carbon Steel Dissolution in 1M HCl at Different Concentrations of the Inhibitors P_4O_1, P_6O_1,and P_8O_1.

obeikandl.com

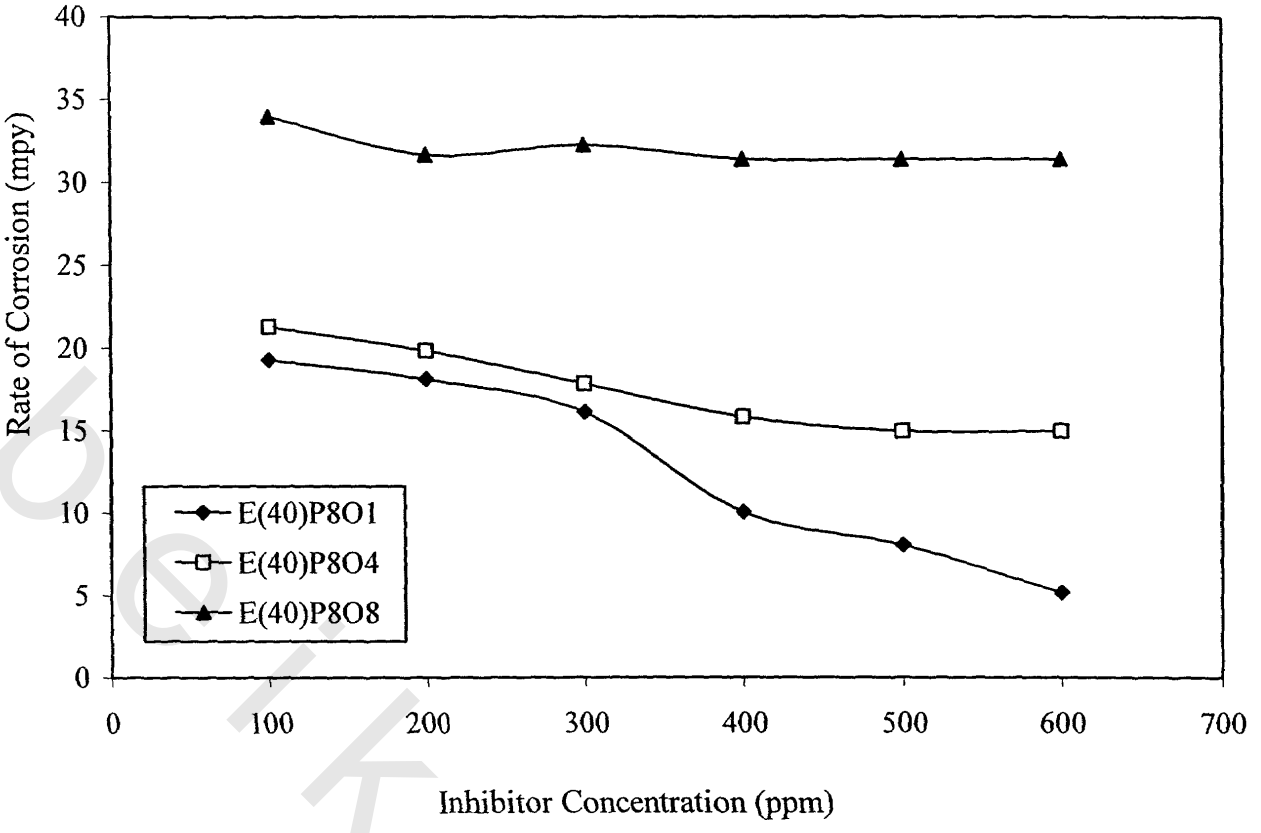

Fig. 39: Rate of Corrosion for Carbon Steel Dissolution in 1M HCl at Different Concentrations of the Inhibitors E(40)P_8O_1, E(40)P_8O_4, E(40)P_8O_8

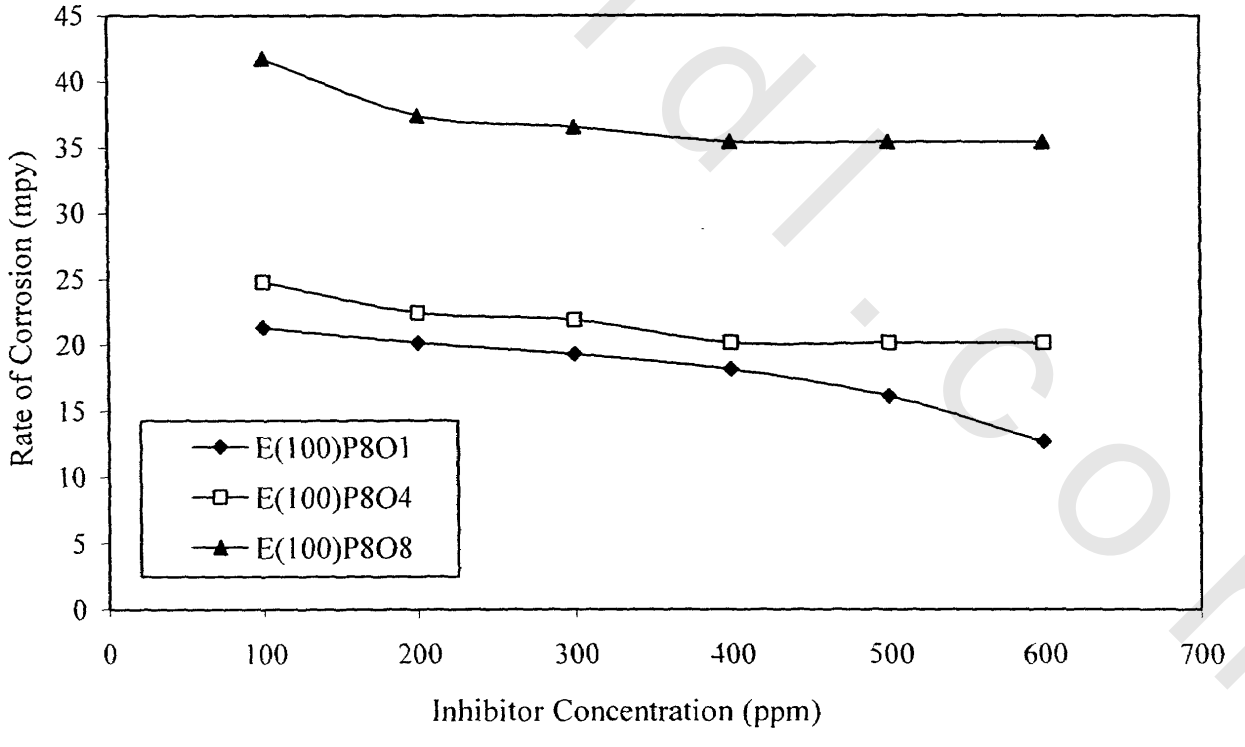

Fig. 40: Rate of Corrosion for Carbon Steel Dissolution in 1M HCl at Different Concentrations of the Inhibitors E(100)P_8O_1, E(100)P_8O_4, E(100)P_8O_8.

obeikandl.com

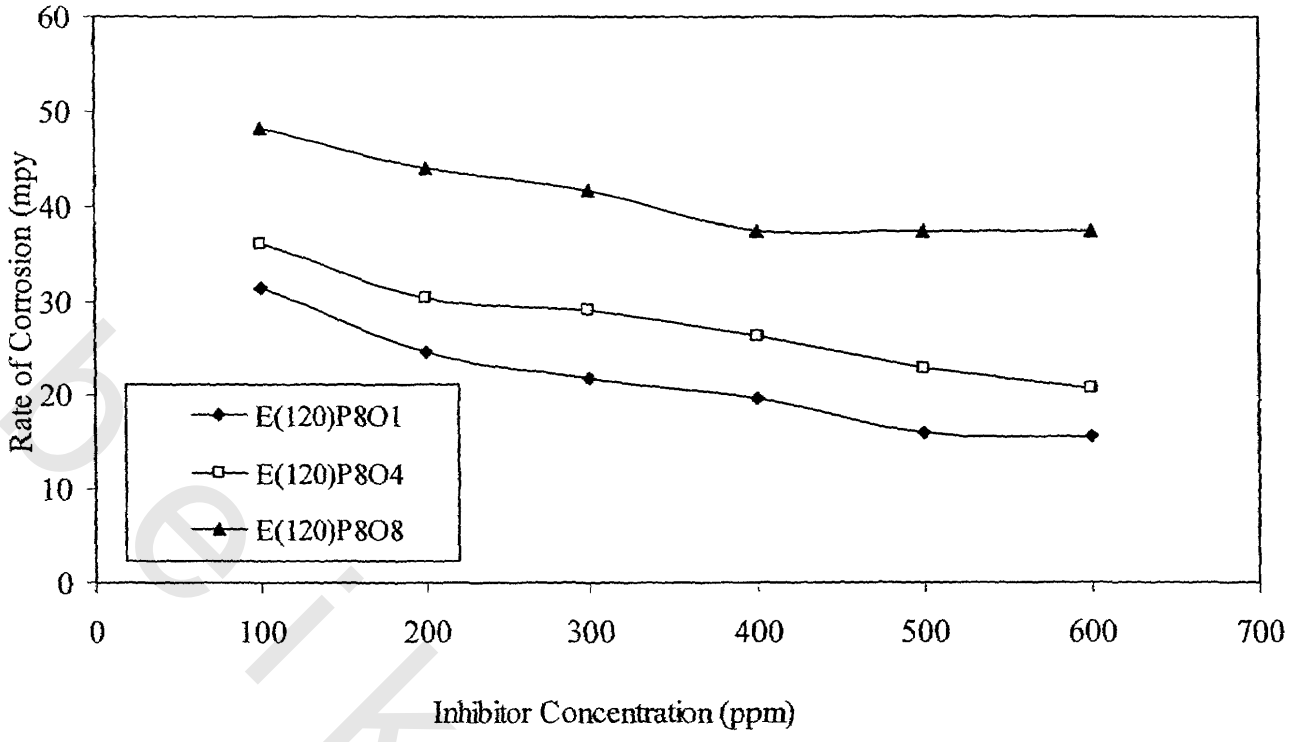

Fig. 41 : Rate of Corrosion for Carbon Steel Dissolution in 1M HCl at Different Concentrations of the Inhibitors $E(120)P_8O_1$, $E(120)P_8O_4$, $E(120)P_8O_8$.

Obeikandl.com

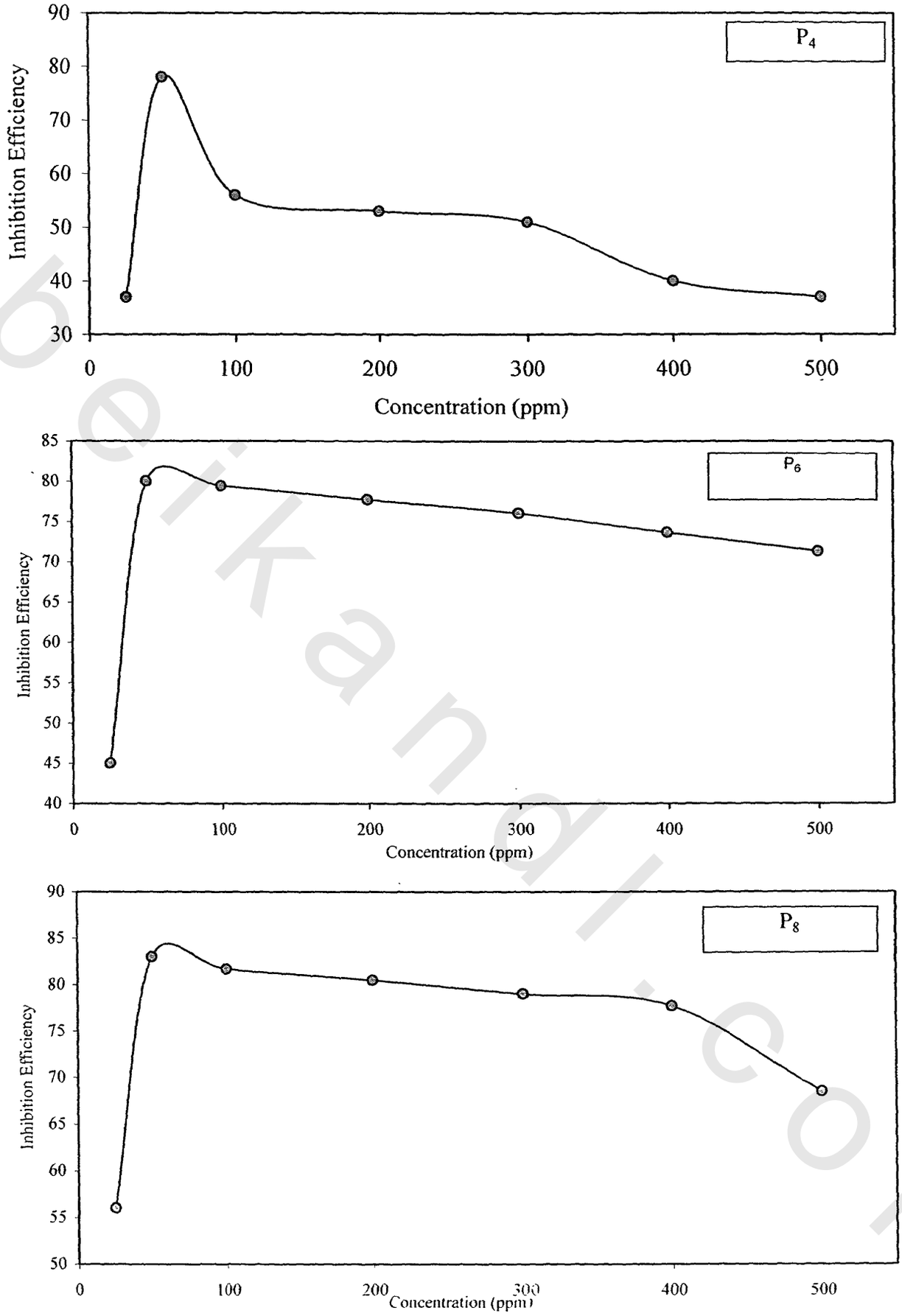

Fig. 42 : Inhibition Efficiency against the Concentration of P_4, P_6, and P_8 for Carbon Steel Dissolution in 1M HCl .

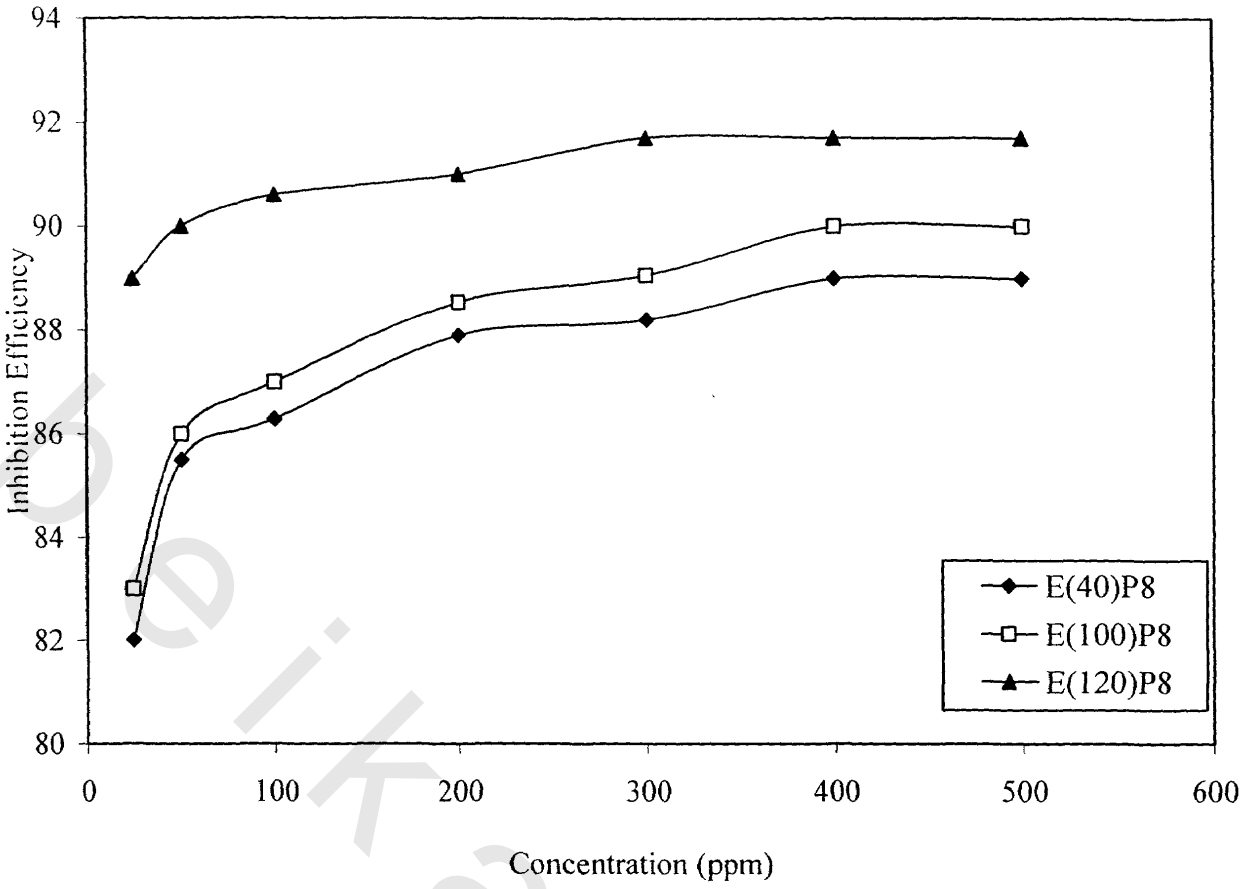

Fig. 43: Inhibition Efficiency against the Concentration of $E(40)P_8$, $E(100)P_8$, and $E(120)P_8$ for Carbon Steel Dissolution in 1M HCl.

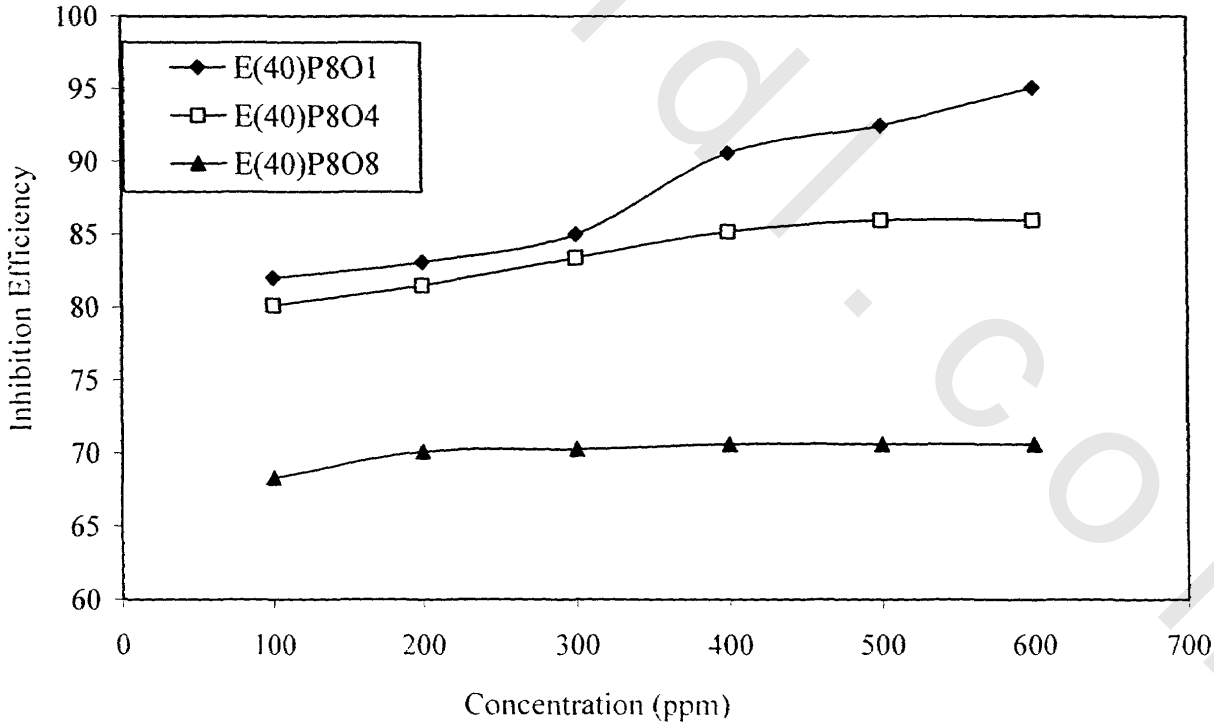

Fig. 44 : Inhibition Efficiency against the Concentration of $E(40)P_8O_1$, $E(40)P_8O_4$, and $E(40)P_8O_8$ for Carbon Steel Dissolution in 1M HCl.

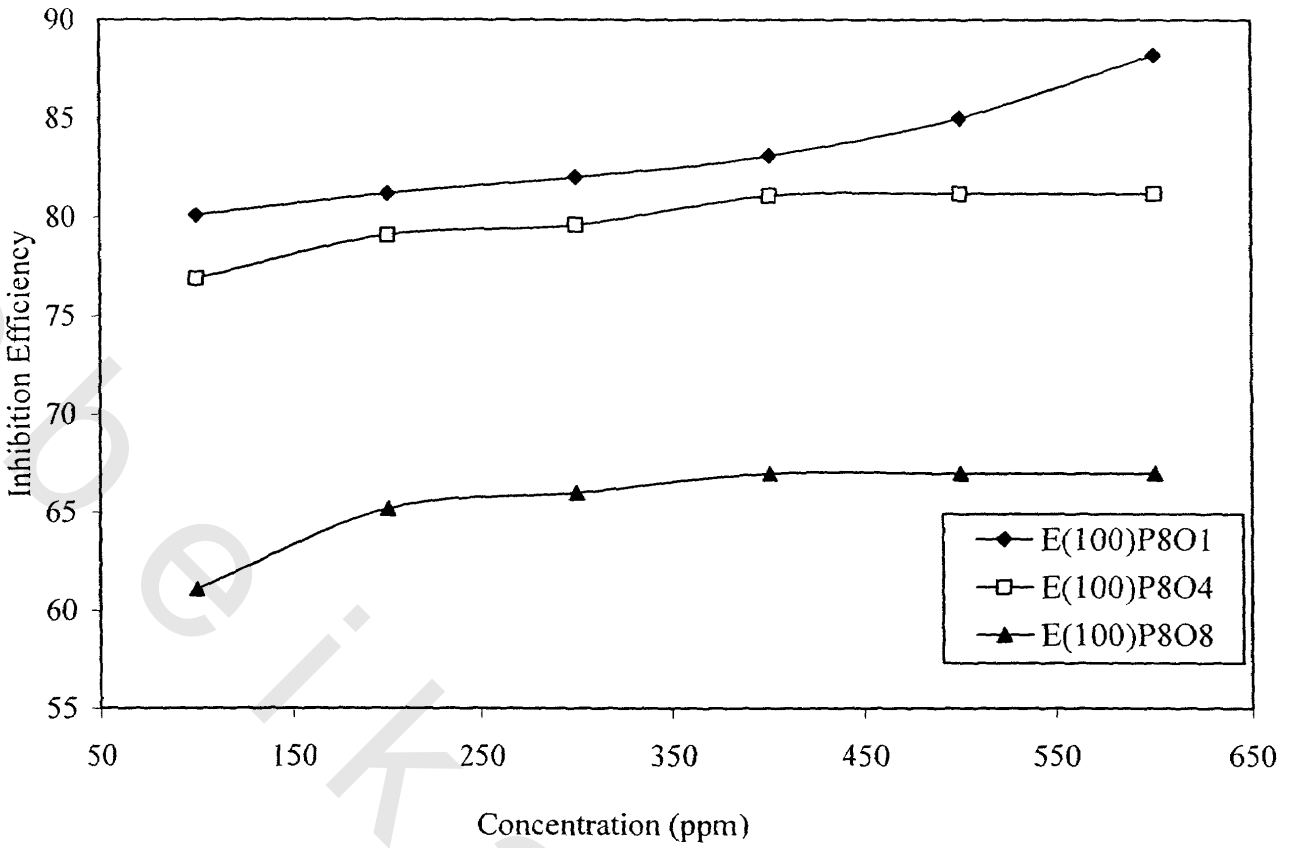

Fig. 45 : Inhibition Efficiency against the Concentration of $E(100)P_8O_1$, $E(100)P_8O_4$, and $E(100)P_8O_8$ for Carbon Steel Dissolution in 1M HCl.

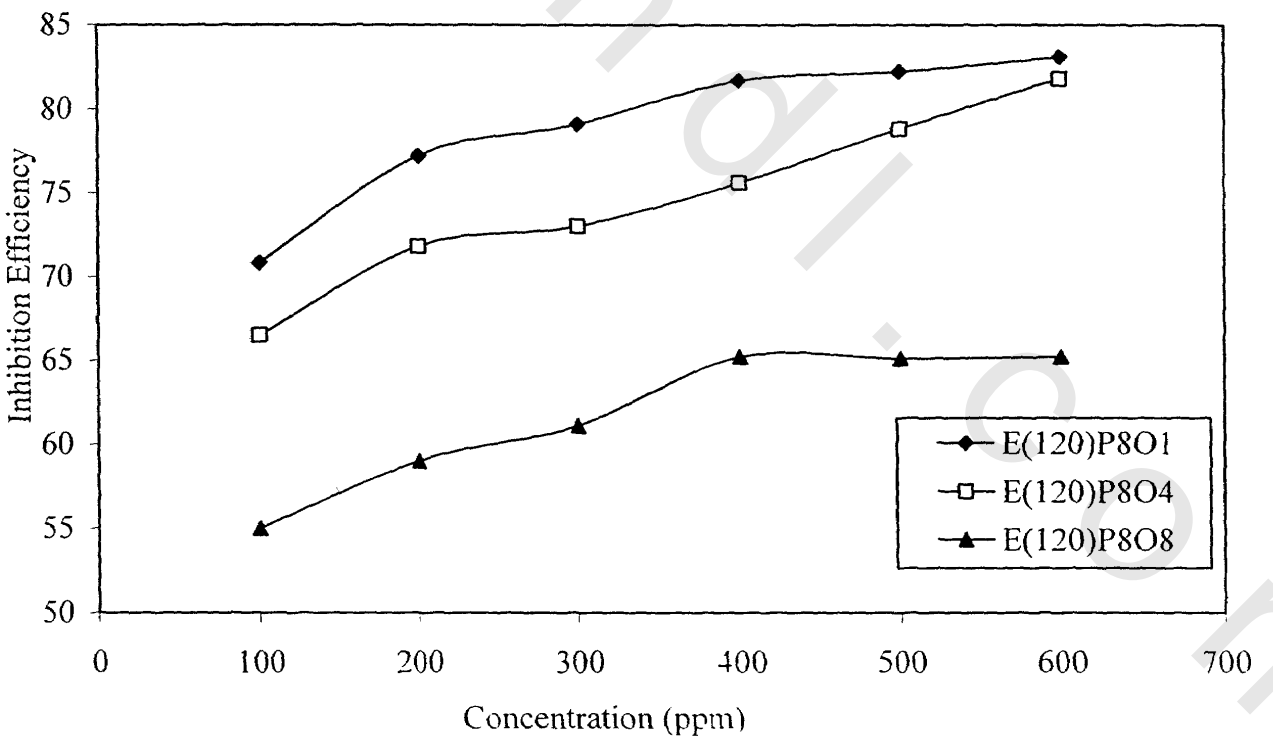

Fig. 46: Inhibition Efficiency against the Concentration of $E(120)P_8O_1$, $E(120)P_8O_4$, and $E(120)P_8O_8$ for Carbon Steel Dissolution in 1M HCl.

Obeikandi.com

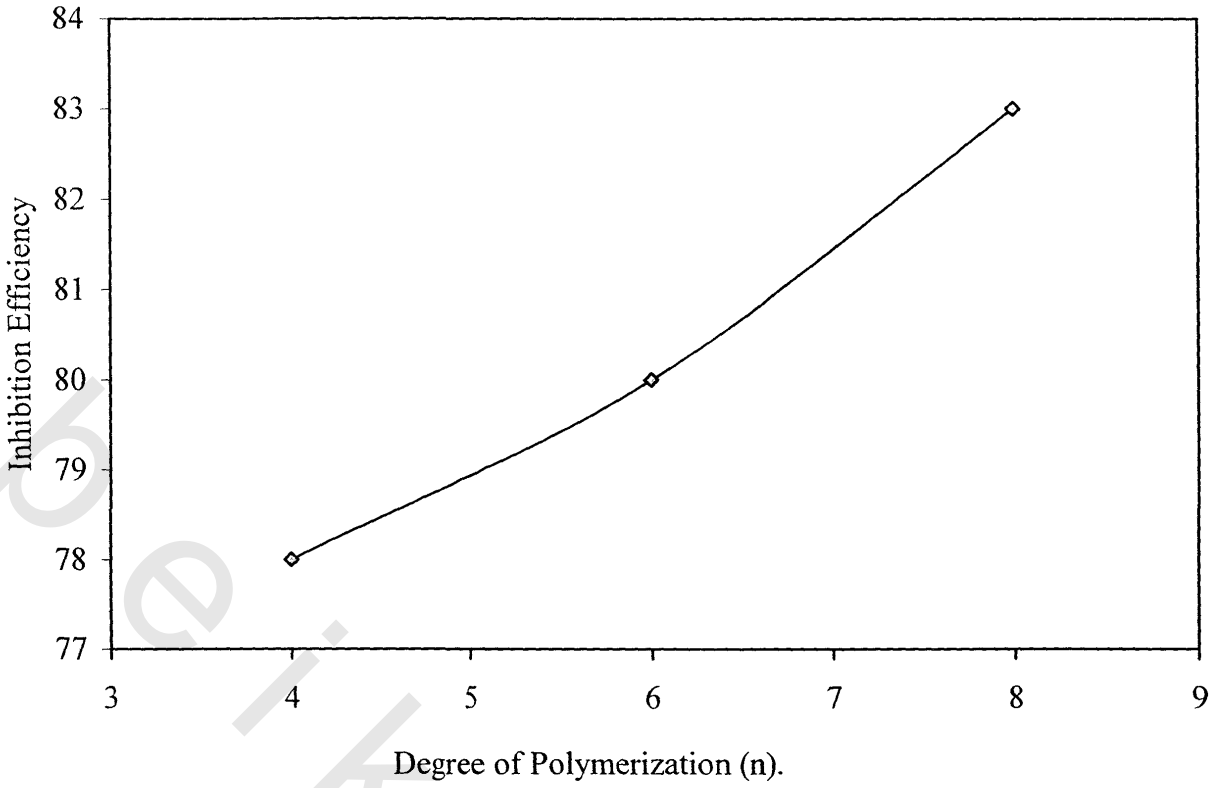

Fig. 47: Inhibition Efficiency against the Degree of Polymerizatinon of P_4, P_6, and P_8 for Carbon Steel Dissolution in 1M HCl at 50 ppm.

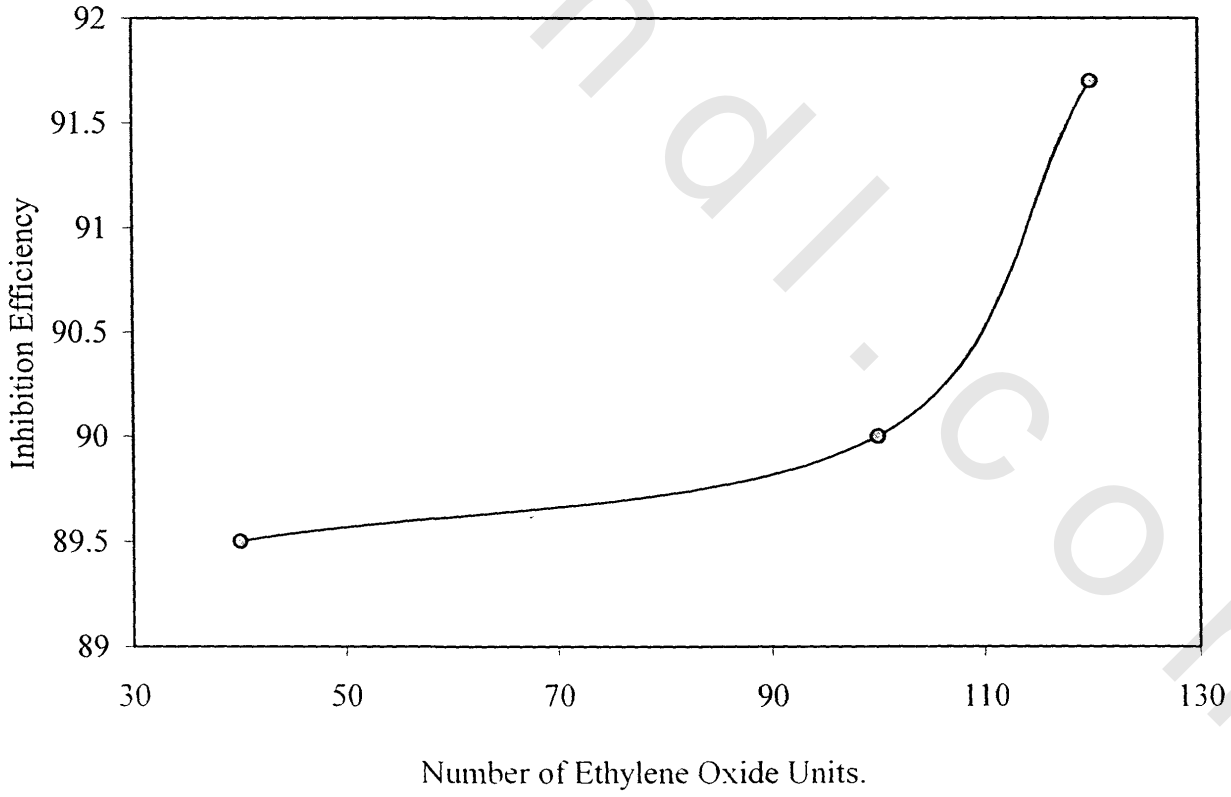

Fig. 48: Inhibition efficiency against the Number of Ethylene Oxide Units of $E(40)P_8$, $E(100)P_8$, and $E(120)P_8$.

obeikandl.com

The values for surface area coverage of the metal surface with the adsorbed species together with the inhibitor concentration in the solution can be utilized to get the adsorption isotherms. Langmuir was the first one who put forward the quantitative theory for adsorption of species on the surfaces [100].

Applying Langmuir adsorption equation (18) for some selected inhibitors. plots of C_i / θ versus Ci are shown in **Figs. 49 to 52** .

$$C_i / \theta = 1/ K_{ad} + C_i \qquad (18)$$

Where: C_i is the inhibitor concentration (in mol/L).

K_{ad} is the adsorption equilibrium constant.

From inspection of the Langmuir plots for esters and ethoxylated polymers **Figs. 49 to 52,** it is found that all the inhibitors investigated showed linear plots and obey the Langmuir adsorption. These isotherms slopes deviated from unity as expected. This deviation may be explained on the basis of the assumption given by Langmuir. He assumed that there is no interaction between the adsorbed molecules. But in practice, there is a mutual repulsion or attraction between the adsorbed species on the metal surface [101-103].

Study of the effect of concentration on corrosion rate

The effect of concentration on the corrosion rate and surface coverage area was investigated. It can be inferred from the data shown in **Tables 10 to 14** that the rate of corrosion becomes nearly constant from 400 ppm. The concentration used was the upper limit throughout this study. Thus, at low concentrations (**Sketch 1**) a mono layer may be formed while at high concentrations an incomplete packing layer of the inhibitor molecules should be formed as shown in **Sketch 2**. At the overdose concentration (at which maximum inhibition efficiency is obtained), the inter space area between the adsorbed inhibitor molecules on the surface may be lower than the area of the inhibitor molecules. Thus, the inhibitor molecules turn out to form the double layer adsorption as shown in **Sketch 3**.

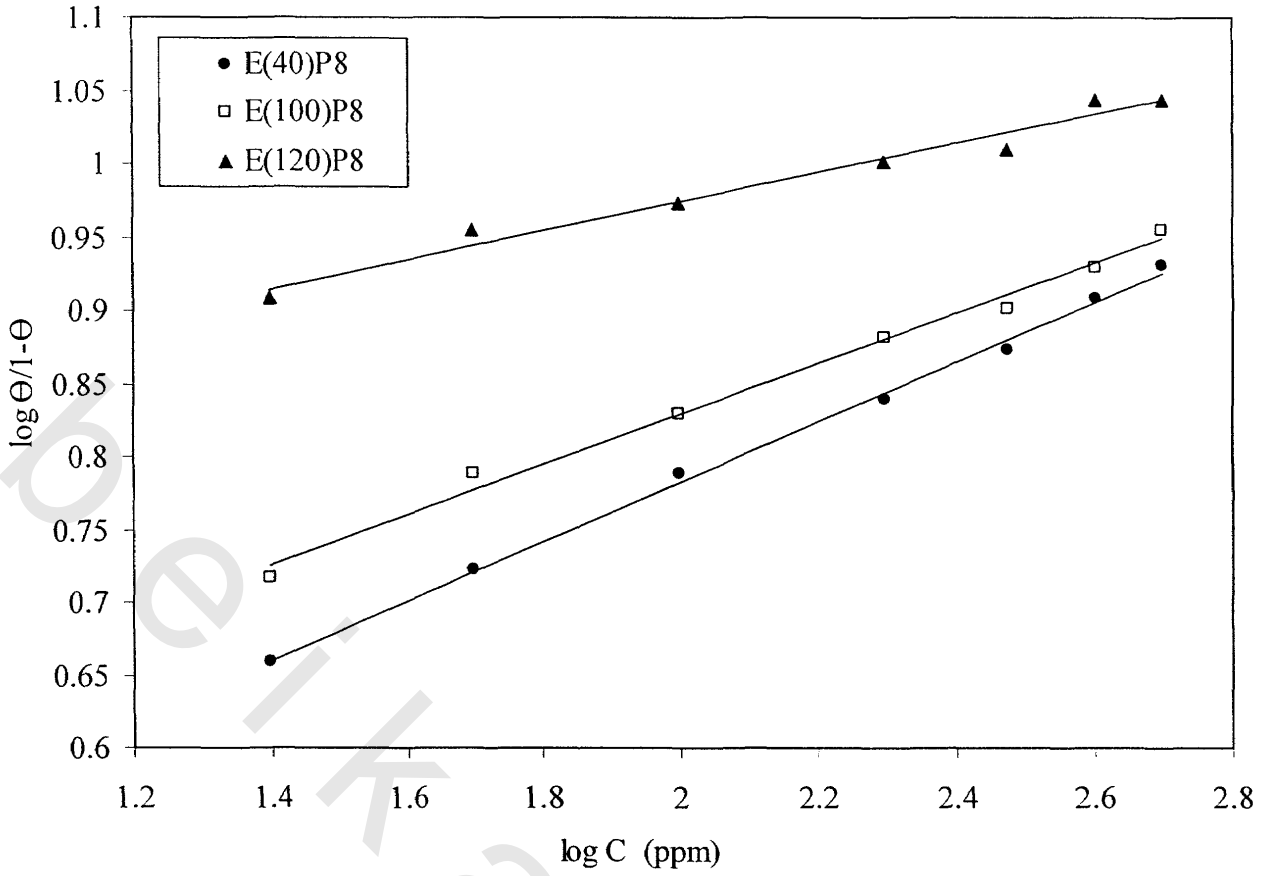

Fig. 49 : Langmuir Adsorption Isotherm of $E(40)P_8$, $E(100)P_8$, and $E(120)P_8$ for Carbon Steel in 1M HCl Solution.

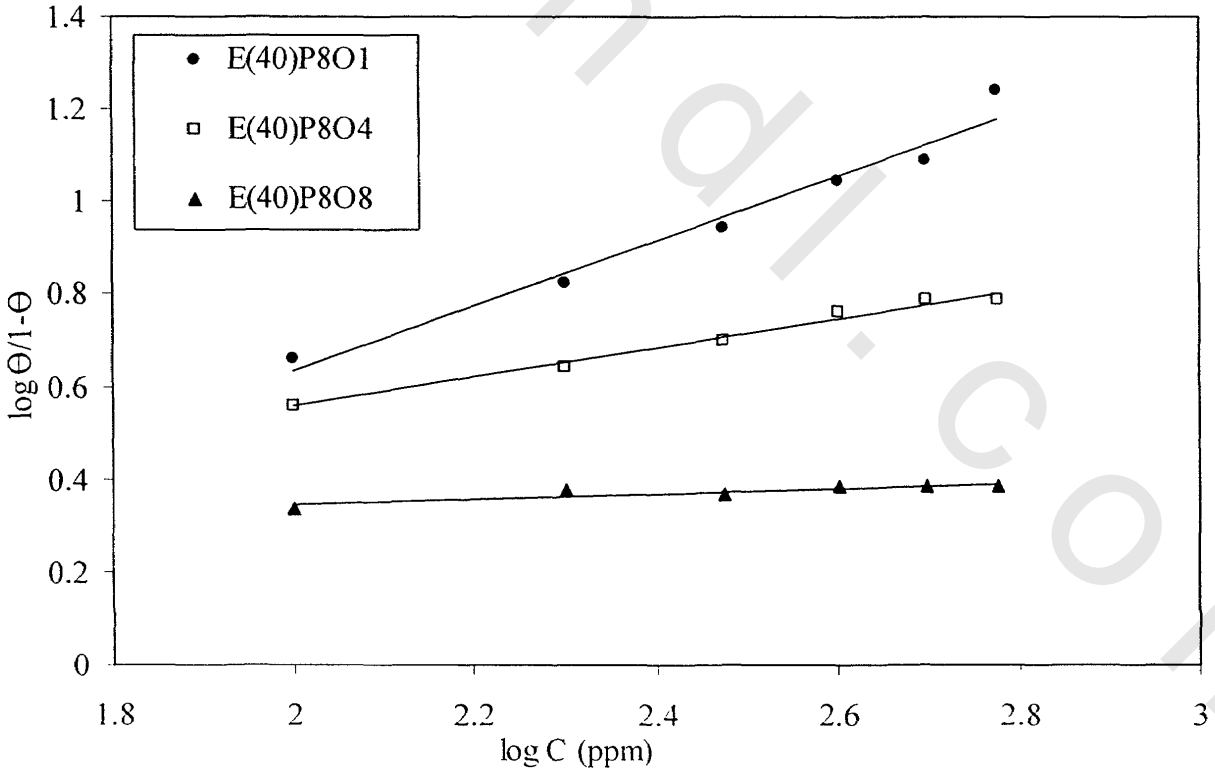

Fig. 50 : Langmuir Adsorption Isotherm of $E(40)P_8O_1$, $E(40)P_8O_4$, and $E(40)P_8O_8$ for Carbon Steel in 1M HCl Solution.

obeikandi.com

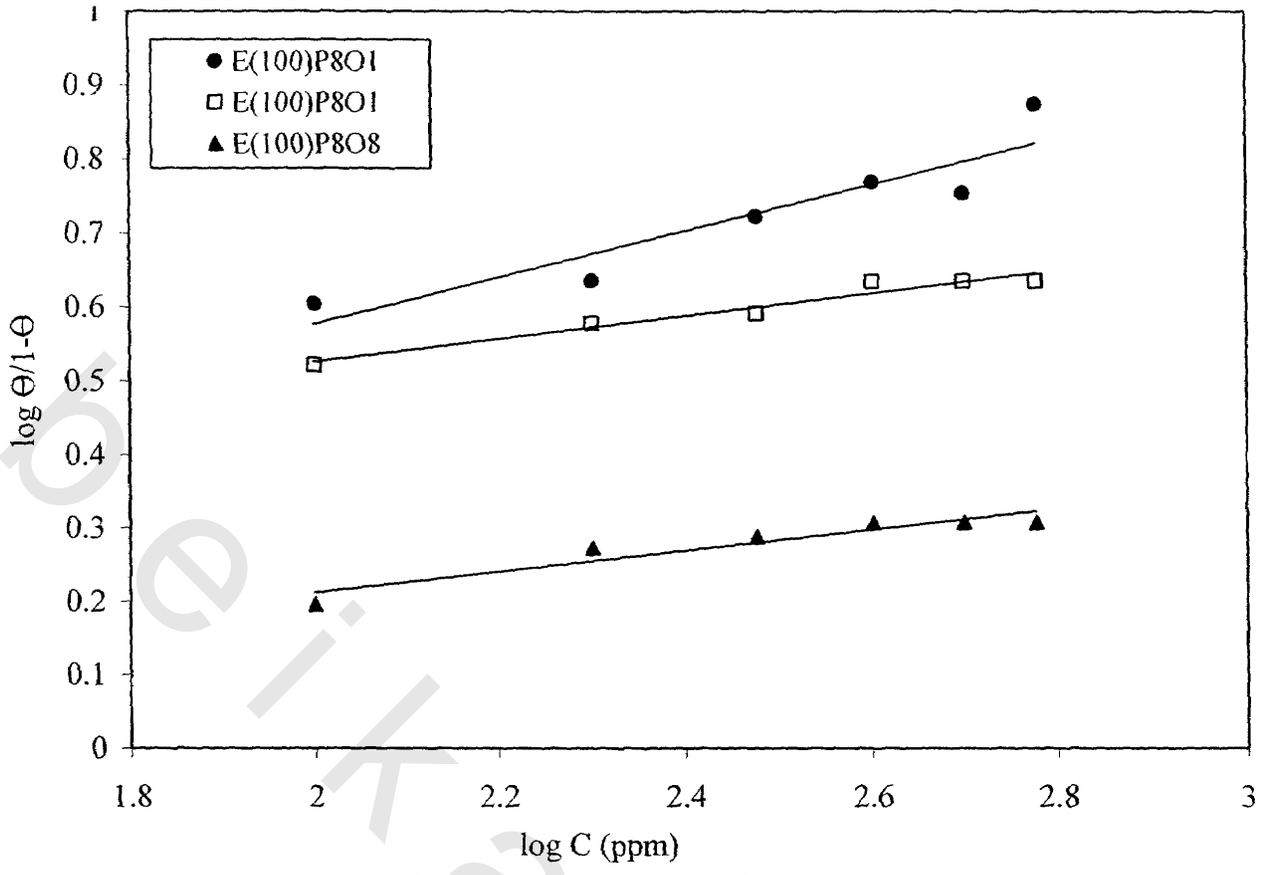

Fig. 51: Langmuir Adsorption Isotherm of $E(100)P_8O_1$, $E(100)P_8O_4$, and $E(100)P_8O_8$ for Carbon Steel in 1M HCl Solution.

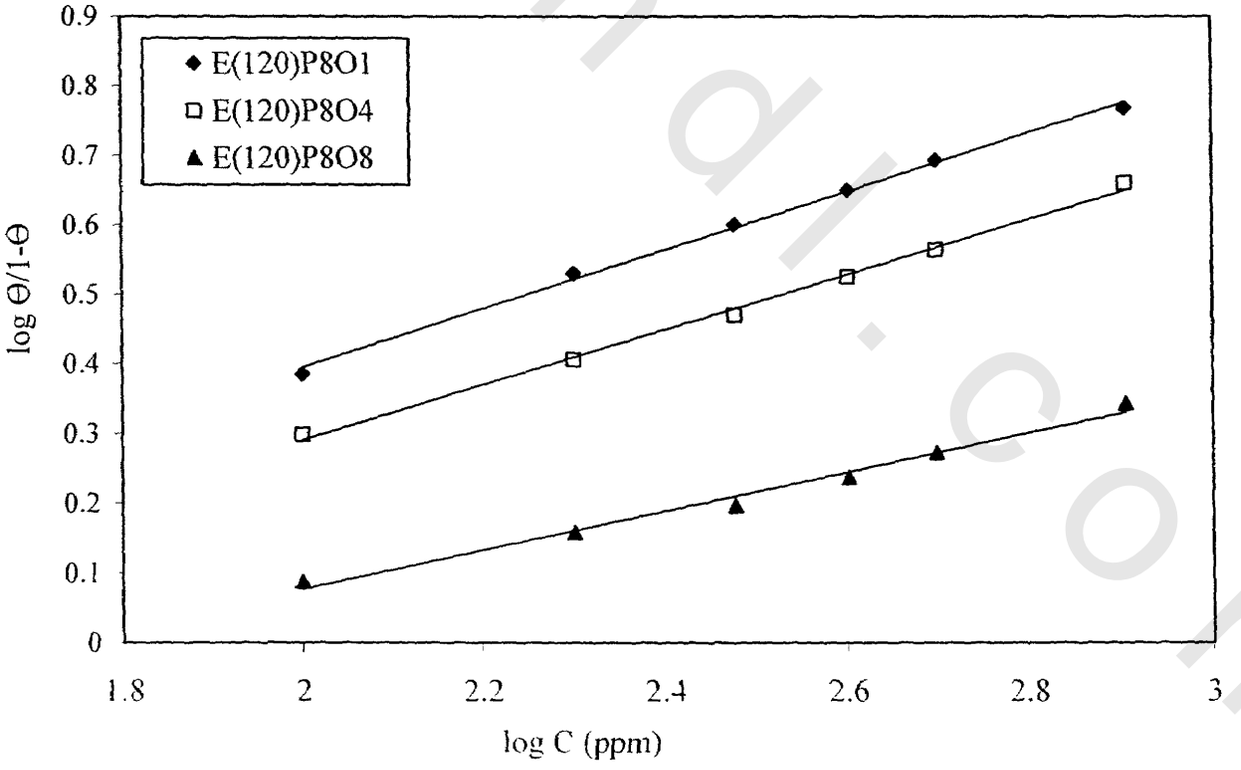

Fig. 52: Langmuir Adsorption Isotherm of $E(120)P_8O_1$, $E(120)P_8O_4$, and $E(120)P_8O_8$ for Carbon Steel in 1M HCl Solution.

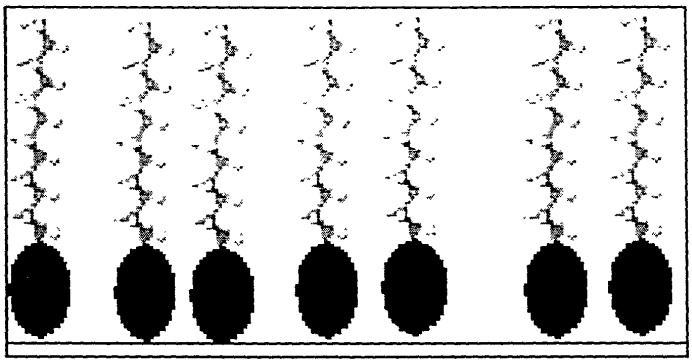

Sketch 1: The Adsorption of Inhibitor on the Surface at Low Concentration.

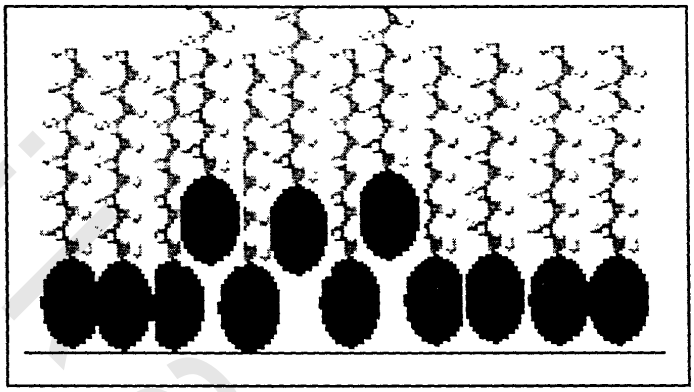

Sketch 2: The Adsorption of Inhibitor on the Surface at High Concentration.

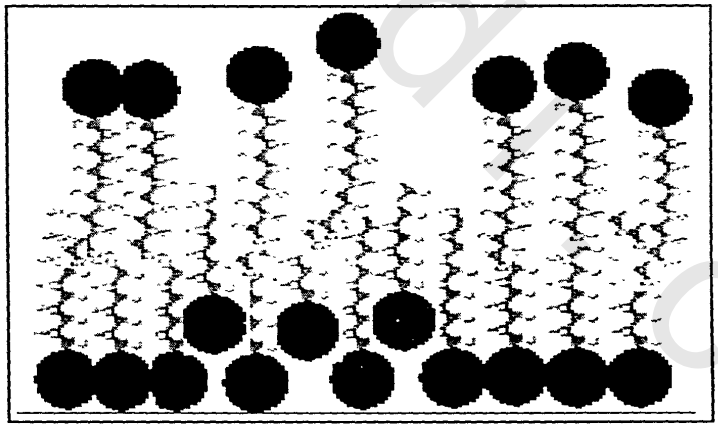

Sketch 3: The Adsorption of Inhibitor on the Surface at the Maximum Inhibition Efficiency Obtained (Overdose Concentration).

obeikandl.com

The Effect of Temperature on the Inhibition Efficiency

The study of the effect of temperature on the inhibition efficiency for corrosion inhibitors is an important factor. This factor helps to elucidate the mechanism and the kinetics of inhibitors and ultimately the proper selection of inhibitors for the specific practical situation. Accordingly, the effect of temperature on the reaction proceeding in pure acids was reported by many researchers [104,105]. The effect of temperature on corrosion using some of the compounds were tested. The effect of increasing temperature from 298 to 338 K on the corrosion inhibition of the inhibitors was studied at concentration 500 ppm in 1 M HCl solution. The apparent activation energies for the steel dissolution process can be evaluated from the following equation:

$$\text{Log } K = (Ea^*/ 2.303R) .1/T + \text{constant} \qquad (19)$$

Plots of the logarithm of the corrosion rate against reciprocal of the absolute temperature (1/T) are shown graphically in **Figs. 53 to 56**. The (Ea*) was obtained from the slopes of these plots.

Table 16, represents the obtained corrosion rate at 298 to 338 K and the corresponding Ea* for 1M HCl solution in absence of any inhibitor. Upon adding 500 ppm of surfactants to the previous system, it was observed that the rate of corrosion decreases significantly compared with the blank as is clear from **Tables 17 to 20.** It is also recognized that the rate of corrosion increases with increasing the temperature from 298 to 338 K. This may be a result of the decreased ion- or dipole–dipole interaction involved between the metal and π- electrons of the inhibitor and/or highly electronegative N and O atoms by increasing the temperature [106].

This decrease in polarization increases the desorption process and hence increases the corrosion rate. This behavior confirms that the inhibition of carbon steel dissolution occurs through physical adsorption of the inhibitor on the metal surface. The Arrhenius equation shows that the smaller the activation energy of the reaction (the lower the energy barrier for dissolution or corrosion), the more rapid the reaction at a given temperature. **Figs. 57 to 60** illustrate the relation between the inhibition efficiency against temperature of some selected inhibitors. From

obeikandi.com

these Figures. it is clear that the inhibition efficiency decreases with increasing temperature for all the inhibitors.

The **Tables 16 to 20**, indicted that the addition of the inhibitor increases the value of activation energy above that of the blank. This phenomenon is often interpreted as physical adsorption leading to the formation of an adsorptive film of electrostatic character [107]. Also, the effects of incorporating oleate groups to ethoxylated polymers were investigated. From the data it is clear that when degree of esterfication increases the activation energy decreases.

Thermodynamic Parameters for the Corrosion Process

Thermodynamic parameters for the corrosion process play an important role in defining the spontaneity of the conversion of the metal to corrosion products that can form in the corrosion environments which the metal is exposed [108-109].

Based on the Ea* values for the corrosion process, the thermodynamic parameters of activation for the corrosion process were calculated. Thermodynamic parameters including enthalpy of activation (ΔH*), free energy of activation (ΔG*) and entropy of activation (ΔS*) were calculated using the following equations:

$$\Delta H^* = Ea^* + RT \quad (20)$$

$$\Delta G^* = RT\,((\ln kt / h) - \ln K) \quad (21)$$

$$\Delta S^* = (\Delta H^* - \Delta G^*)/T \quad (22)$$

Where: **R:** universal constant (=3.814J/mole.K) **h:** Plank's constant

k: Boltzmann constant **K:** corrosion rate

The obtained values are listed in **Tables 21-24**. The negative values of **ΔH*** reflect the endothermic behavior of the inhibitors used on the steel surface for the conversion of the metal to the corrosion products. With respect to the influence of the inhibitor efficiency, the data reveal that **ΔH*** increases generally with increasing the inhibitor efficiency. This increase may be due to the power of the inhibitor and the stronger adsorption on the metal surface. The values of **ΔG***

are all negative. On the other hand, **ΔG*** values in presence of the inhibitors are higher than that obtained from 1M HCl (blank), and hence the process is activation controlled.

A new relation is introduced to shed light on the relation between the inhibitor efficiency and the change of temperature along both series. The increment of decreased efficiency per unit temperature (ΔI /Δ°C) was calculated. The inhibition efficiency at both the lowest (298K) and the highest studied temperatures (338 K) and (ΔI /Δ°C) are listed in **Table 25**.

From the data obtained, it can be seen that the value of (ΔI /Δ°C) increases with increasing ethylene oxide content as shown in **Fig. 61**. The ethoxylated compounds are incomplete surfactants so physical adsorption by the terminal –OH groups on the surface is greater than the chemical adsorption for these molecules. At the same time the ethylene oxide chains shield the nitrogen atom, consequently the chances for chemical adsorption decrease. But after they have been converted to the complete surfactant form by esterification, the values of (ΔI /Δ°C) decreased. This can be attributed to the sterochemical structures of the ethoxylated form. The increase of the number of ester groups from 1 to 4 to 8 reduces the chance of the physical adsorption which may be due to the -OH groups. This may be due to the compound becoming more strongly directed by the eight oleate groups to adsorb on the surface. However this behavior was not observed in the case of the high ethoxylated groups (100 and 120). From **Table 25** the values of (Δη /Δ°C) for $E(100)P_8O_1$, $E(100)P_8O_4$, $E(100)P_8O_8$, $E(120)P_8O_1$, $E(120)P_8O_4$, and $E(120)P_8O_8$ are (0.69, 0.72 , 0.86, 0.47, 0.55, and 0.62 respectively) increase with increasing degree of esterfication. These results may be due to the increase of ethylene oxide units leading to coiling and shielding in the molecule. This further decreases the chances of the chemical adsorption so that the (Δη /Δ°C) values increase. These results are illustrated in **Fig. 62.**

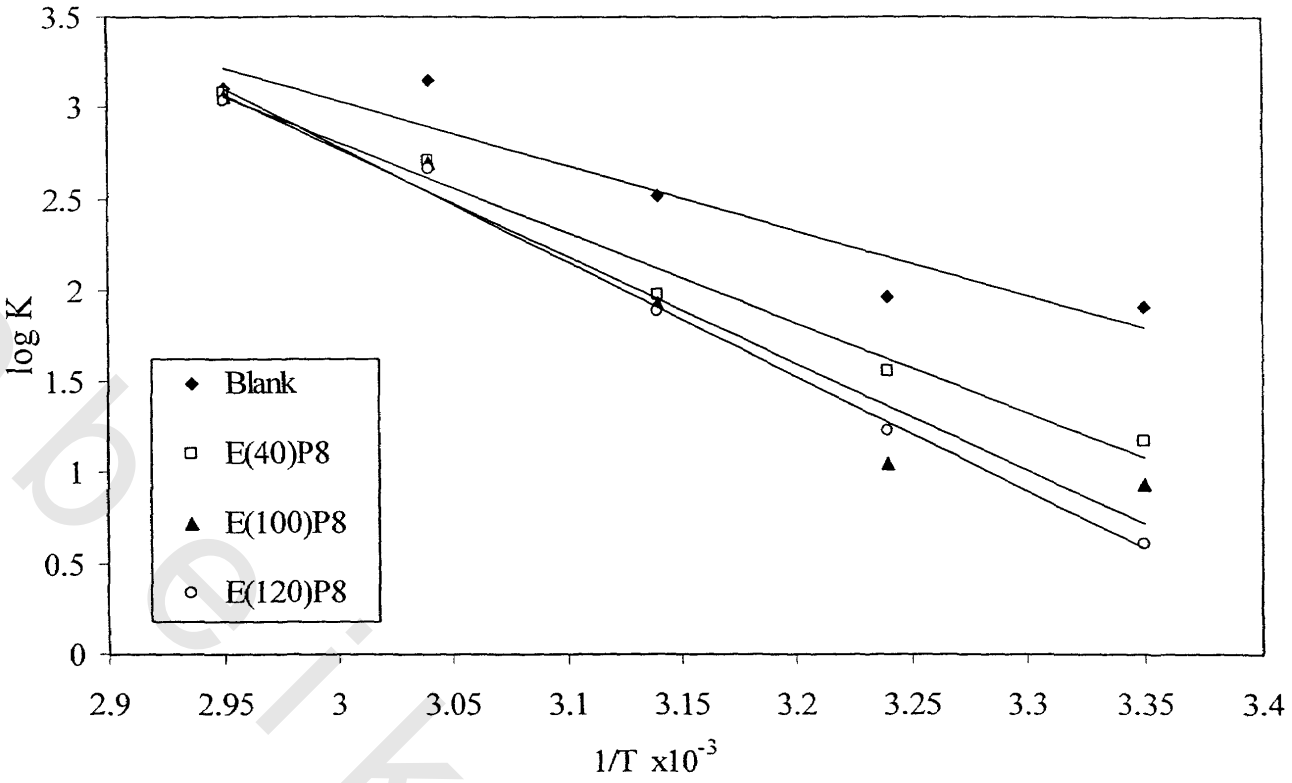

Fig. 53: log K-1/T Curves for Carbon Steel Dissolution in 1M HCl in Absence and Presence of the Inhibitors $E(40)P_8$,$E(100)P_8$,$E(120)P_8$ at Different Temperatures.

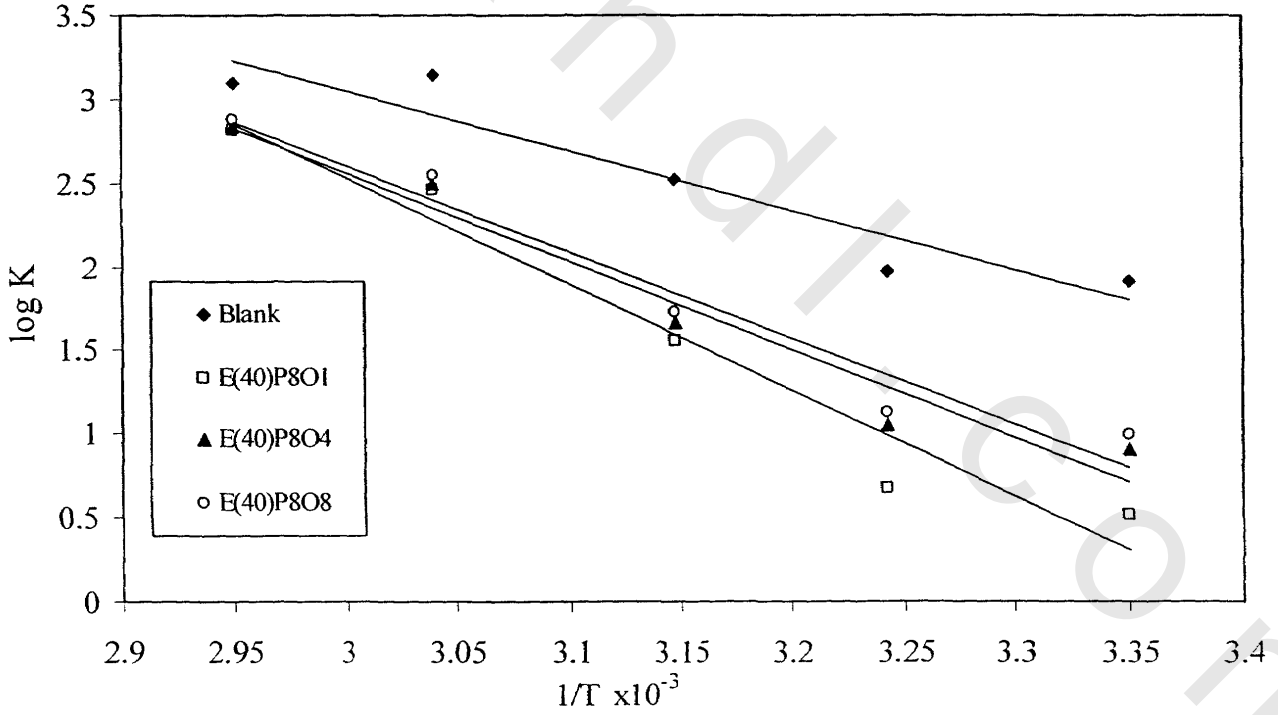

Fig . 54 : log K-1/T Curves for Carbon Steel Dissolution in 1M HCl in Absence and Presence of the Inhibitors $E(40)P_8O_1$.$E(40)P_8O_4$,$E(40)P_8O_8$ at Different Temperatures.

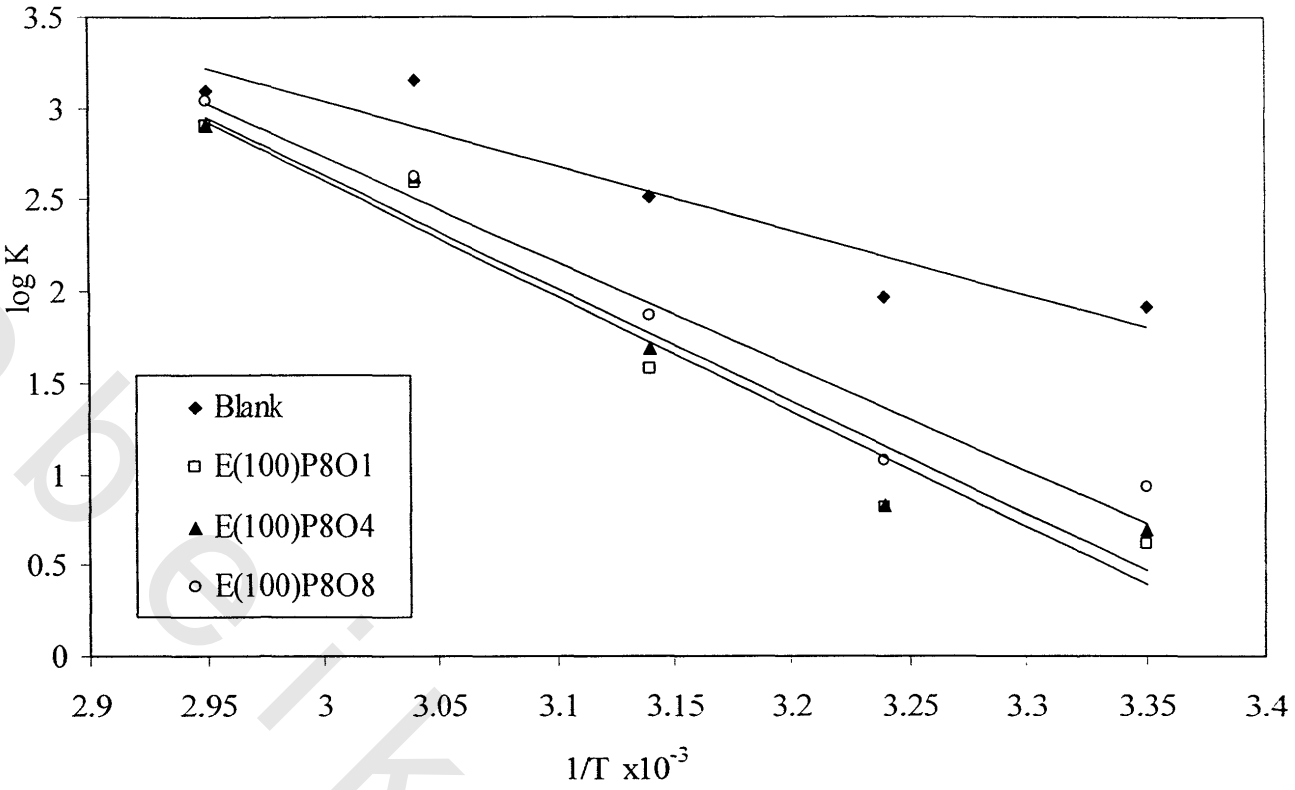

Fig. 55 : log K-1/T Curves for Carbon Steel Dissolution in 1M HCl in Absence and Presence of the Inhibitors $E(100)P_8O_1$, $E(100)P_8O_4$, $E(100)P_8O_8$ at Different Temperatures.

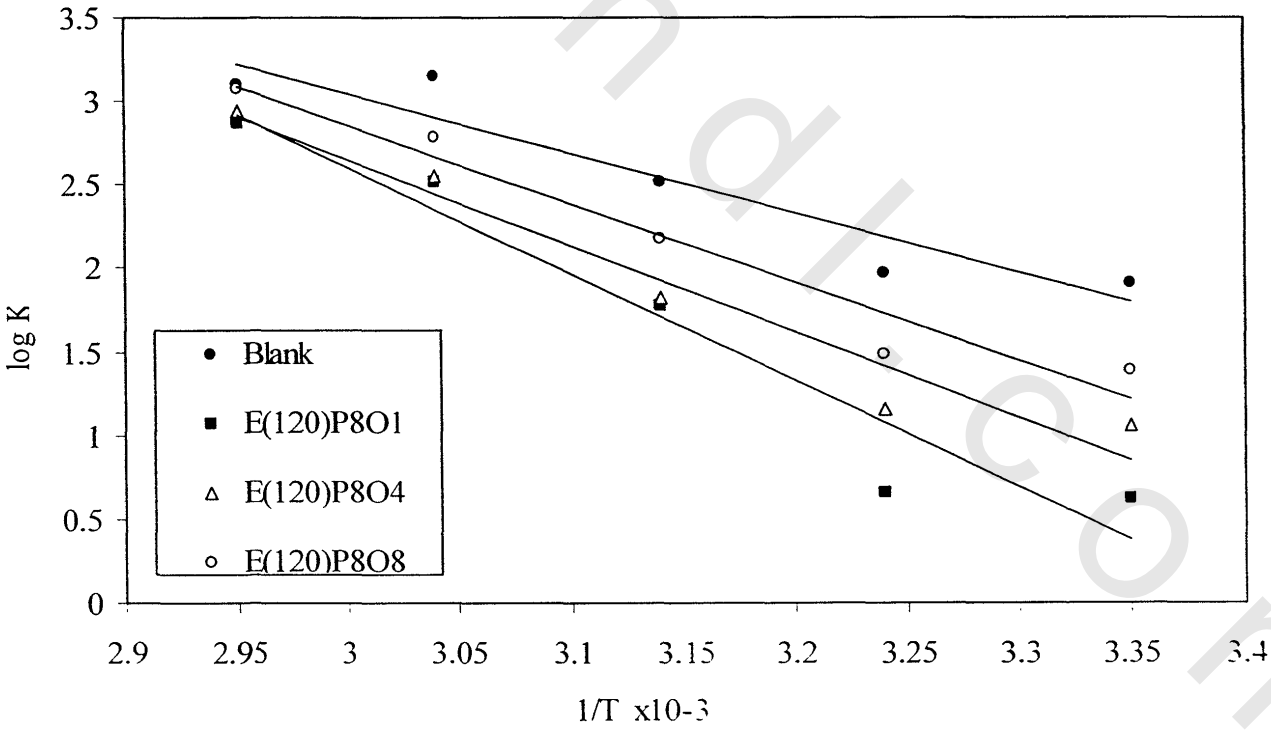

Fig. 56 : log K-1/T Curves for Carbon Steel Dissolution in 1M HCl in Absence and Presence of the Inhibitors $E(120)P_8O_1$, $E(120)P_8O_4$, $E(120)P_8O_8$ At Different Temperatures.

Obeikandl.com

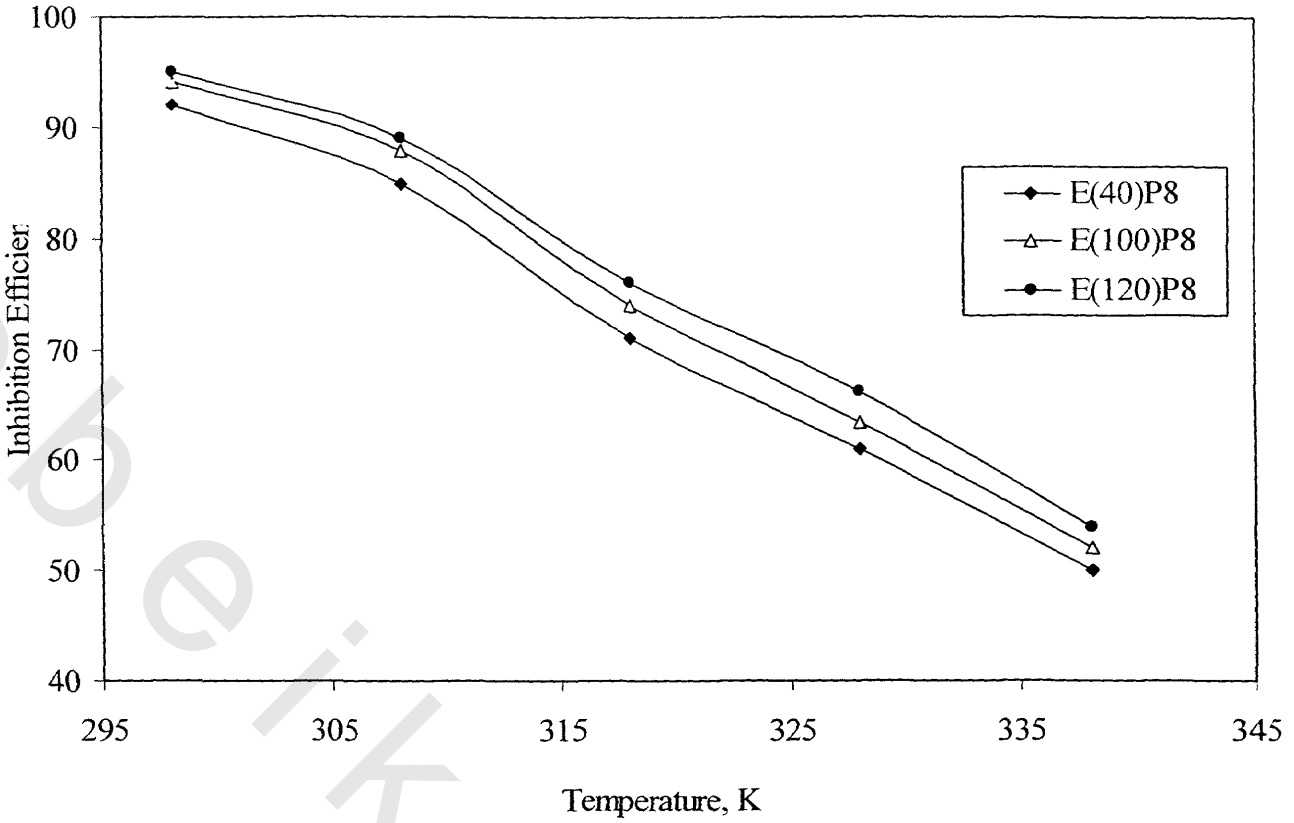

Fig. 57 : Inhibition Efficiency for Carbon Steel Dissolution in 1M HCl in Presence of the Inhibitors, $E(40)P_8$, $E(100)P_8$, $E(120)P_8$ at Different Temperatures.

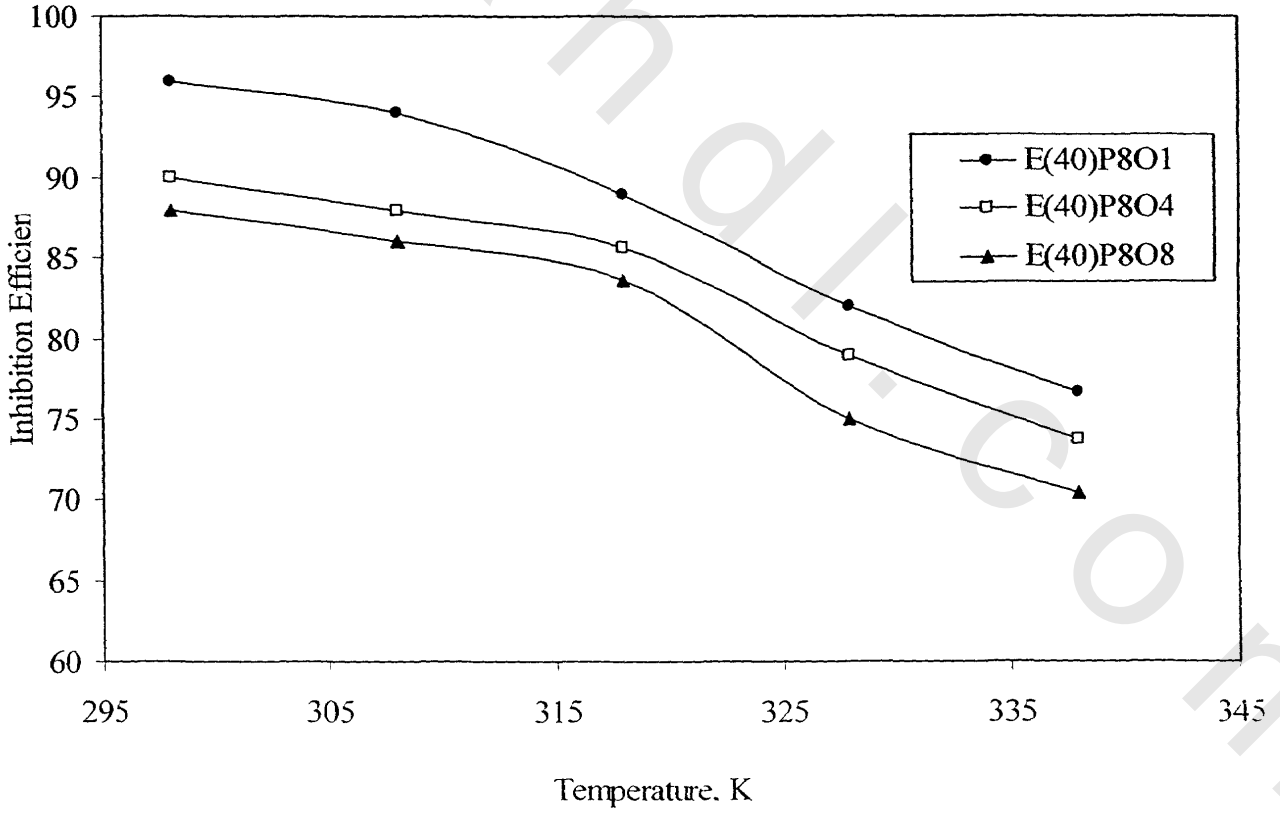

Fig. 58 : Inhibition Efficiency for Carbon Steel Dissolution in 1M HCl in Presence of the Inhibitors $E(40)P_8O_1$, $E(40)P_8O_4$, $E(40)P_8O_8$ at Different Temperatures.

Open Knowledge

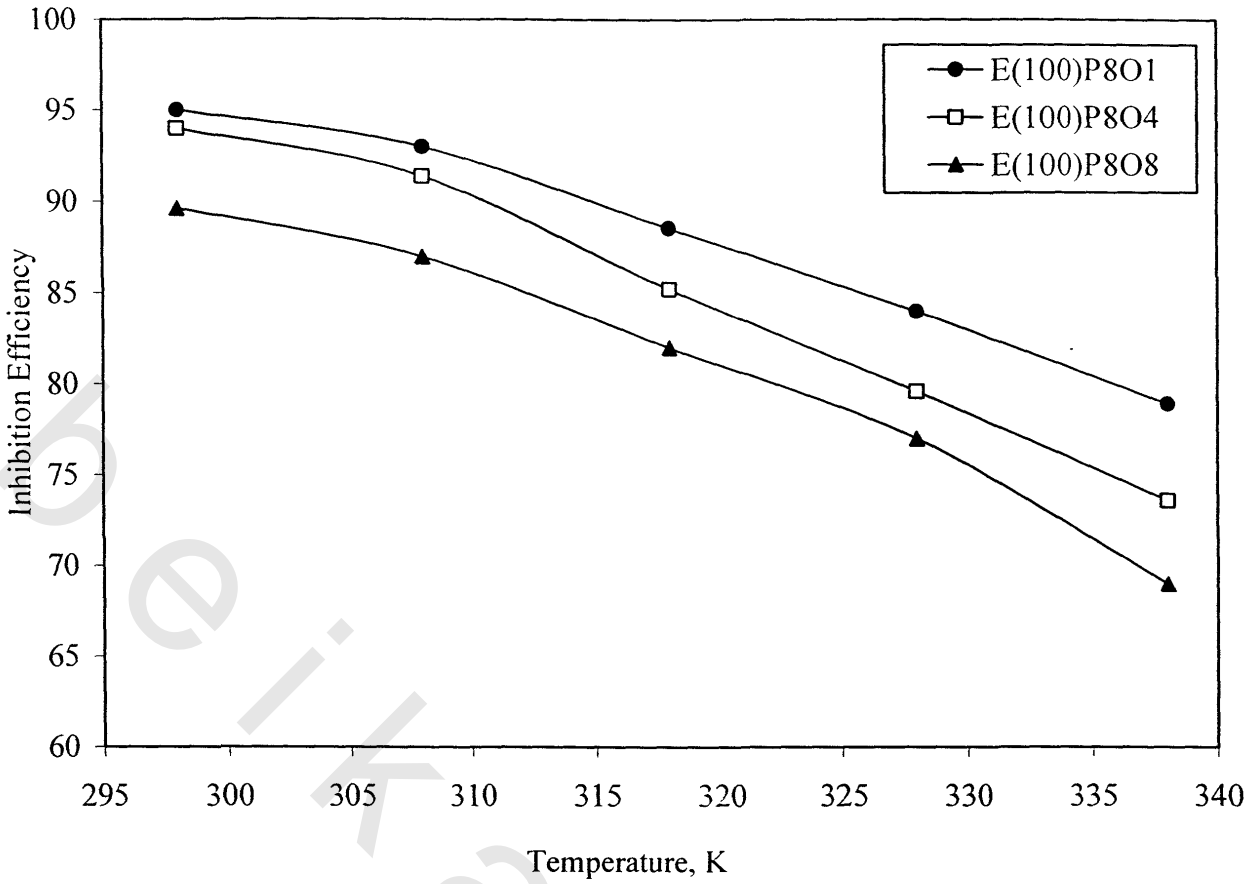

Fig. 59: Inhibition Efficiency for Carbon Steel Dissolution in 1M HCl in Presence of The Inhibitors $E(100)P_8O_1$, $E(100)P_8O_4$, $E(100)P_8O_8$ at Different Temperatures.

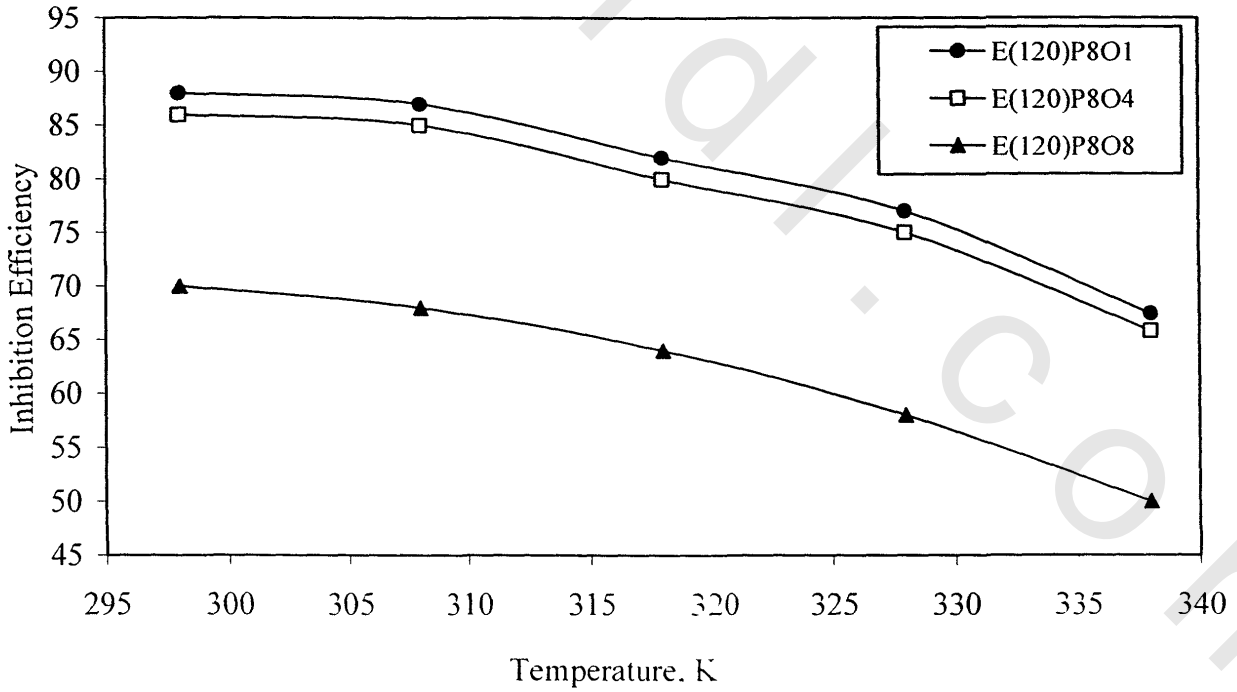

Fig. 60: Inhibition Efficiency for Carbon Steel Dissolution in 1M HCl in Presence of the Inhibitors $E(120)P_8O_1$, $E(120)P_8O_4$, $E(120)P_8O_8$ at Different Temperatures.

Table 16: Corrosion Rate and Activation Energy for the Blank Carbon Steel in 1M HCl Solution at Different Temperatures.

Temperature (K)	Corrosion Rate (mpy)	Ea* K.j. mol^{-1}
298	82.80	31.26
308	95.12	
318	331.73	
328	1445.33	
338	2439.04	

obeikandl.com

Table 17: Corrosion Rate Dependence of Carbon Steel, the Degree of Surface Coverage (θ), the Percentage Inhibition (I%) and Activation Energy at Different Temperatures in 1M HCl Solution in Presence of 500 ppm of the Inhibitor $E(40)P_8$, $E(100)P_8$, $E(120)P_8$.

Inhibitors Code	Temperature (K)	Corrosion Rate (mpy)	(θ)	(I %)	Ea* K.j. mol^{-1}
$E(40)P_8$	298	14.26	0.8277	82.77	43.47
	308	14.79	0.8445	84.45	
	318	96.53	0.7090	70.90	
	328	520.31	0.6400	64.00	
	338	1219.52	0.5000	50.00	
$E(100)P_8$	298	8.70	0.8949	89.49	51.55
	308	16.98	0.8214	82.14	
	318	86.58	0.7390	73.90	
	328	505.86	0.6500	65.00	
	338	1170.73	0.5200	52.00	
$E(120)P_8$	298	4.14	0.95	95.00	55.25
	308	10.46	0.8900	89.00	
	318	76.63	0.7689	76.89	
	328	462.50	0.6800	68.00	
	338	1121.95	0.5400	54.00	

obeikandi.com

Table 18: Corrosion Rate Dependence of Carbon Steel, the Degree of Surface Coverage (θ), the Percentage Inhibition (I%) and Activation Energy at Different Temperatures in 1M HCl Solution in Presence of 500 ppm of the Inhibitor E (40)P_8O_1, E(40)P_8O_4, E(40)P_8O_8.

Inhibitors Code	Temperature (K)	Corrosion Rate (mpy)	(θ)	(I %)	Ea* K.j. mol^{-1}
E(40)P_8O_1	298	3.31	0.9600	96.00	55.68
	308	4.75	0.9500	95.00	
	318	36.82	0.8890	88.90	
	328	289.06	0.8000	80.00	
	338	653.66	0.7320	73.20	
E(40)P_8O_4	298	8.28	0.90	90.00	46.46
	308	11.41	0.8800	88.00	
	318	47.76	0.8560	85.60	
	328	317.97	0.7800	78.00	
	338	695.12	0.7150	71.15	
E(40)P_8O_8	298	9.93	0.8800	88.00	45.41
	308	13.31	0.8600	86.00	
	318	54.40	0.8360	83.60	
	328	361.33	0.7500	75.00	
	338	758.54	0.6890	68.90	

obeikandl.com

Table 19: Corrosion Rate Dependence of Carbon Steel, the Degree of Surface Coverage (θ), the Percentage Inhibition (I%) and Activation Energy at Different Temperatures in 1M HCl Solution in Presence of 500 ppm of the Inhibitor E (100)P_8O_1, E (100)P_8O_4, E (100)P_8O_8.

Inhibitors Code	Temperature (K)	Corrosion Rate (mpy)	(θ)	(I %)	Ea* K.j. mol^{-1}
E(100)P_8O_1	298	4.14	0.9500	95.00	55.68
	308	6.65	0.9300	93.00	
	318	38.14	0.8850	88.50	
	328	390.23	0.7300	73.00	
	338	802.44	0.6710	67.10	
E(100)P_8O_4	298	4.96	0.9400	94.01	54.63
	308	6.84	0.9280	92.80	
	318	49.09	0.8520	85.20	
	328	433.59	0.7000	70.00	
	338	824.39	0.6620	66.20	
E(100)P_8O_8	298	8.5	0.8973	89.73	50.50
	308	11.79	0.8760	87.60	
	318	75.64	0.7719	77.19	
	328	433.59	0.7000	70.00	
	338	1097.56	0.5500	55.00	

obeikandl.com

Table 20: Corrosion Rate Dependence of Carbon Steel, the Degree of Surface Coverage (θ), the Percentage Inhibition (I%) and Activation Energy at Different Temperatures in 1M HCl Solution in Presence of 500 ppm of the Inhibitor E (120)P_8O_1, E (120)P_8O_4, E (120)P_8O_8.

Inhibitors Code	Temperature (K)	Corrosion Rate (mpy)	(θ)	(I %)	Ea* K.j. mol^{-1}
E(120)P_8O_1	298	9.93	0.8800	88.00	55.68
	308	12.36	0.8700	87.01	
	318	59.71	0.8200	82.00	
	328	332.42	0.7700	77.00	
	338	756.10	0.6900	69.00	
E(120)P_8O_4	298	11.59	0.8600	86.00	45.06
	308	14.26	0.8500	85.01	
	318	66.34	0.8000	80.00	
	328	361.33	0.7500	75.00	
	338	878.05	0.6400	64.00	
E(120)P_8O_8	298	24.75	0.7010	70.10	40.84
	308	30.44	0.6799	67.99	
	318	119.42	0.6400	64.00	
	328	607.03	0.5800	58.00	
	338	1219.52	0.5000	50.00	

obeikandi.com

Table 21: Thermodynamic Functions of Activation of the Surfactants.

Inhibitor code	Temp., (K)	Ea* K.j.mol^{-1}	- Δ G* K.j.mol^{-1}	Δ H* K.j.mol^{-1}	ΔS* K.j.mol-1.K^{-1}
Blank	298	31.26	50.19	31.57	0.27
	308		53.51	31.58	0.28
	318		70.39	31.59	0.34
	328		91.02	31.60	0.41
	338		100.54	31.61	0.44
E(40)P_8	298	43.47	30.61	44.61	0.25
	308		31.22	44.65	0.25
	318		55.42	44.69	0.31
	328		78.24	44.73	0.37
	338		91.60	44.77	0.40
E(100)P_8	298	51.55	24.59	52.69	0.25
	308		33.26	52.73	0.28
	318		54.11	52.77	0.34
	328		77.89	5281	0.40
	338		91.08	52.91	0.42
E(120)P_8	298	55.24	16	56.38	0.24
	308		27.58	56.42	0.27
	318		52.62	56.46	0.34
	328		76.76	56.50	0.40
	338		90.53	56.53	0.43

obeikandi.com

Table 22: Thermodynamic Functions of Activation of the Surfactants.

Inhibitor code	Temp., (K)	Ea* K.j.mol^{-1}	- Δ G* K.j.mol^{-1}	Δ H* K.j.mol^{-1}	ΔS* K.j.mol^{-1}.K^{-1}
E(40)P_8O_1	298	55.68	13.61	56.82	0.23
	308		18.31	56.86	0.24
	318		43.73	56.90	0.31
	328		70.88	56.94	0.38
	338		83.56	56.98	0.41
E(40)P_8O_4	298	46.46	24.02	47.60	0.24
	308		28.60	47.64	0.25
	318		46.89	47.68	0.29
	328		72.08	47.72	0.36
	338		84.36	47.75	0.39
E(40)P_8O_8	298	45.41	26.09	46.55	0.24
	308		30.41	46.56	0.25
	318		48.47	46.62	0.29
	328		73.68	46.66	0.38
	338		85.48	46.70	0.39

openkanal.com

Table 23: Thermodynamic Functions of Activation of the Surfactants

Inhibitor code	Temp., (K)	Ea* K.j.mol^{-1}	- Δ G* K.j.mol^{-1}	Δ H* K.j.mol^{-1}	ΔS* K.j.mol^{-1}.K^{-1}
E(100)P_8O_1	298	55.68	16.14	56.82	0.24
	308		22.27	56.86	0.25
	318		44.16	56.90	0.31
	328		74.64	56.94	0.40
	338		86.21	56.98	0.42
E(100)P_8O_4	298	54.63	18.22	55.77	0.24
	308		22.60	55.80	0.25
	318		47.22	55.84	0.32
	328		75.96	55.89	0.40
	338		86.56	55.92	0.42
E(100)P_8O_8	298	50.50	24.43	51.64	0.25
	308		28.98	51.68	0.26
	318		52.30	51.72	0.32
	328		75.96	51.76	0.38
	338		90.25	51.79	0.42

openkanal.com

Table 24: Thermodynamic Functions of Activation of the Surfactants

Inhibitor code	Temp., (K)	Ea* K.j.mol^{-1}	- Δ G* K.j.mol^{-1}	Δ H* K.j.mol^{-1}	ΔS* K.j.mol^{-1}.K^{-1}
E(120)P_8O_1	298	55.68	26.09	56.82	0.27
	308		29.54	56.86	0.28
	318		49.60	56.90	0.33
	328		72.63	56.94	0.39
	338		85.44	56.98	0.42
E(120)P_8O_4	298	45.06	27.85	46.19	0.24
	308		31.22	46.23	0.25
	318		50.87	46.27	0.30
	328		73.68	46.31	0.36
	338		87.37	46.35	0.39
E(120)P_8O_8	298	40.84	36.47	41.98	0.26
	308		40.12	42.02	0.27
	318		58.00	42.06	0.31
	328		80.17	42.09	0.37
	338		91.60	42.13	0.39

obeikandl.com

Table 25: Inhibition Efficiency Depression against the Temperatures Program

Inhibitor Code	Inhibition efficiency		ΔI	Δη/Δ°C
	25°C	65 °C		
E(40)P_8	82.77	50.00	32.77	0.81
E(100)P_8	89.49	52.00	37.49	0.93
E(120)P_8	95.00	54.00	41	1.02
E(40)P_8O_1	96.00	73.20	22.8	0.57
E(40)P_8O_4	90.00	71.15	18.85	0.47
E(40)P_8O_8	87.00	68.90	18.1	0.45
E(100)P_8O_1	95.00	67.10	27.9	0.69
E(100)P_8O_4	94.01	65.00	29.01	0.72
E(100)P_8O_8	89.3	55.00	34.3	0.86
E(120)P_8O_1	88.00	69.00	19	0.47
E(120)P_8O_4	86.00	64.00	22	0.55
E(120)P_8O_8	75.10	50.00	25.1	0.62

obeikandl.com

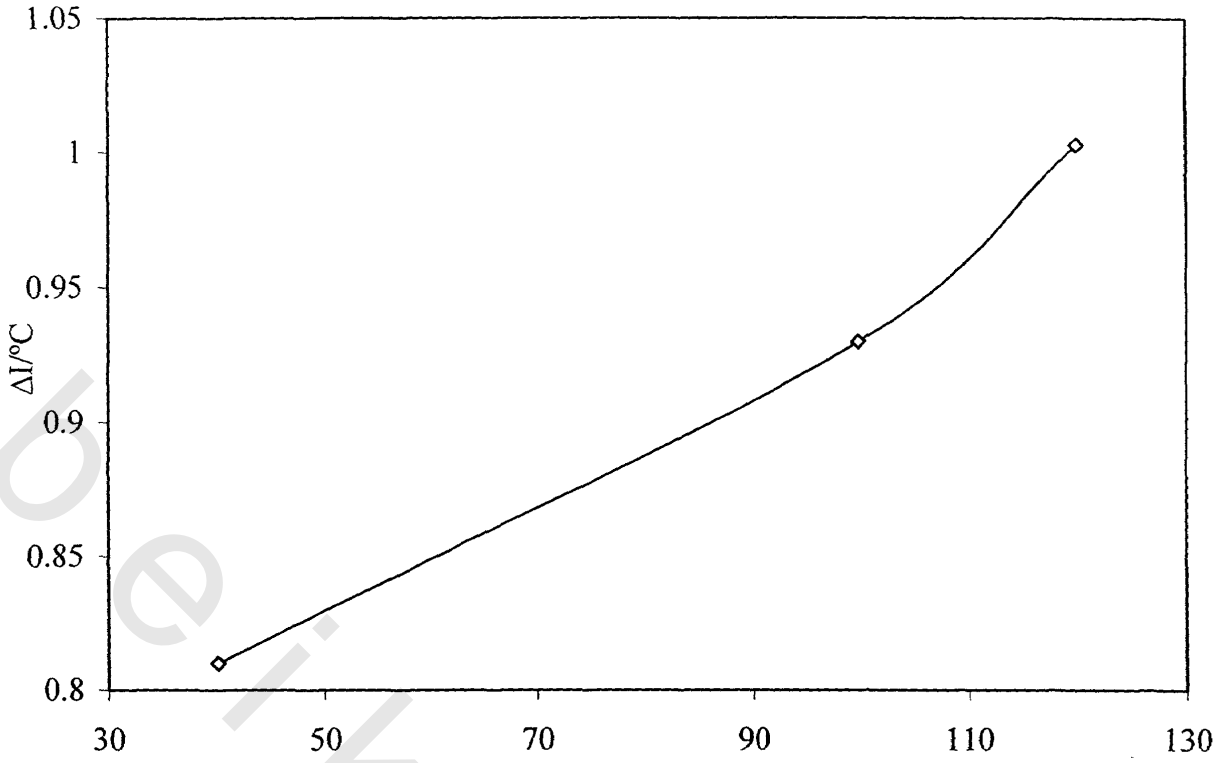

Fig. 61: Relationship between the Number of Ethylene Oxide Units and ΔI/°C.

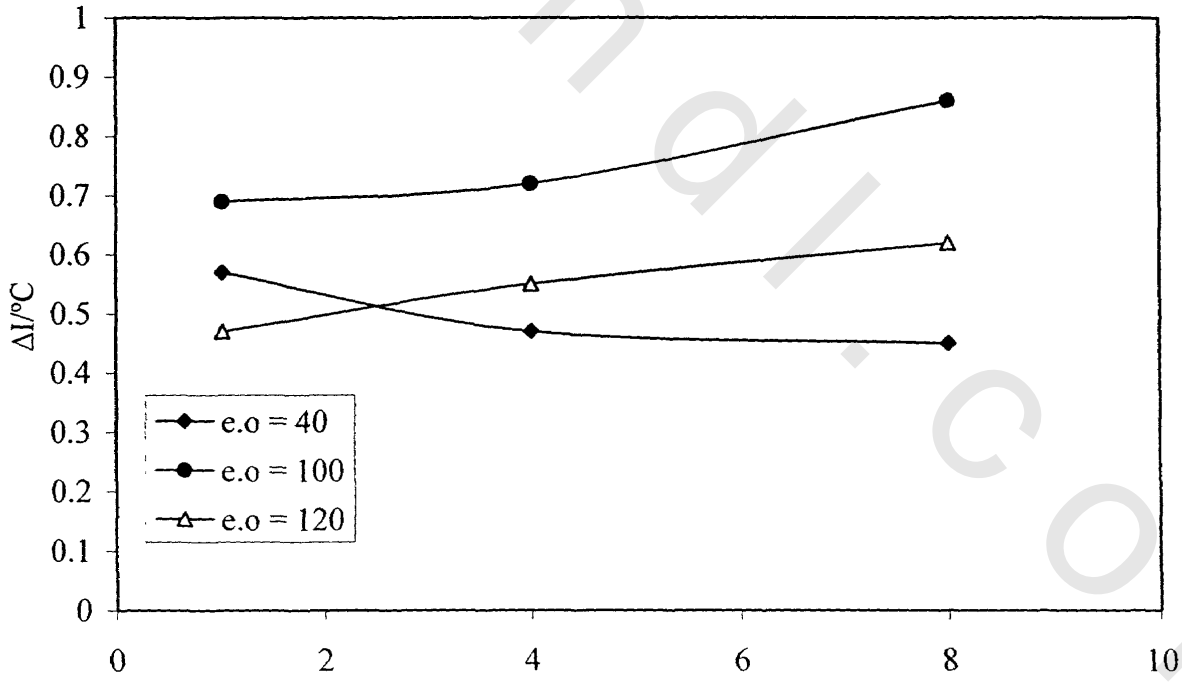

Fig. 62: Relationship Between Different Molar Ratio of Esterification and ΔI/°C

Surfactants as Emulsion Breakers.

During the production of crude oil, water mixes with it and forms a stable water-in-oil emulsion (w/o). The emulsion must be separated into two distinct phases before the crude oil is transported for further processing. The cost of the transportation either by pipelines or by tankers is then reduced. The damage of distillation equipment and catalyst poising is avoided by removing water and other poisonous material at the source itself. One of the readily used methods for breaking the emulsion is chemical demulsification by demulsifiers. The main objective of this study is to synthesize some demulsifiers from local and available raw materials and investigate their efficiency in breaking the w/o emulsions.

In oil field w/o emulsions, a stabilizing interfacial film can be formed from the asphaltene and resin fraction of the crude oil. This causes special problems because the films are viscoelastic then a mechanical barrier to coalescence exists. This may yield a high degree of emulsion stability. The demulsifiers are surfactants designed to reduce emulsion stability by displacing or destroying the effectiveness of the original stabilizing agents at the interface. The formulations of demulsifiers are selected to provide specific properties including molecular weight, hydrophile-lipophile balance (HLB), stability, rate of diffusion into the interface, and effectiveness of destabilizing the interface. However, the correct selection of the demulsifier can be confirmed only by application by treating a sample with bench top or simulator tests. It is well known that when a surfactant is brought into contact with a water-oil system, individual surfactant molecules have an opportunity to pass into both phases. For a system at equilibrium, a state of lower energy for the surfactant molecule would be one in which it straddles the interface, with the polar group remaining in the water and the hydrophobic tail in the oil. As the concentration of surfactant at the interface would be very high, the adjacent molecules would tend to orient themselves to be substantially parallel to each other [110].

When surfactant molecules pack together at the interface forming a monolayer, they do not act independently and intermolecular interactions are often great between neighboring

molecules. The hydrophobic interactions between the adjacent alkyl groups provide a force tending to pack the molecules closer together. The hydrophilic groups on the other hand, have a strong affinity for water so that there is a tendency for them to be spaced out to allow as much water as possible to solvate each head group and then a separation should occur.

Effect of Molecular Structure on the Demulsification Process.

The data in **Tables 26, 27** show HLB, the amount of separated water and the demulsification efficiency for a control sample and the prepared esters of polytriethanolamine and esters of ethoxylated polytriethanolamine at different concentration using crude oil emulsion (50 % water) at 60 °C.

The control sample is an emulsion without adding demulsifier. The control sample shows only 10 % separation after 43 days. Upon adding the demulsifiers mentioned latter, it was found that generally the percentage of separated water increases while the time required for separation decreases with increasing the demulsifier concentration.

The effect of structural modification of the compounds prepared show a demulsification efficiency as seen in **Table 28.** In this table the polymer P_8 and their ethoxylate (e.o = 40 units) do not look like surfactants because the chemical structure is a hydrophilic moiety and they does not exhibit any demulsification efficiency. The same polymer was esterfied by 4 mole oleic acid (P_8O_4) which then exhibited 100 % demulsification efficiency at 300 ppm and 60 °C (50 % w/o emulsion) after 240 min. On the other hand, the ester of the ethoxylated polymer ($E(40)P_8O_4$) gave a demulsification efficiency 100 % under the same conditions after 90 min. The products P_8O_4 and $E(40)P_8O_4$ were modified to give a surfactant like structure (hydrophil-lipophil moiety), hence they were solubilized in the emulsion phase and partitioned between the oil and water via their good surface active properties to produce rupture of the interface and further the demulsification.

Regarding to the data in **Table 27** for $E(40)P_8O_4$ and $E(100)P_8O_4$, the increase in (e.o) content is accompanied by an increase in the demulsification efficiency. This behavior may be

obeikandi.com

due to the demulsifier molecule will have more suitable amphiphilic structure that permits a better partitioning at w/o interface and hence more effective adsorption. As a result of adsorption enhancement a better demulsification performance was obtained. On the other hand, the demulsification efficiency for E (120)P_8O_4 decreases, this may be due to the coiling of ethylene oxide chains. It was also found that the demulsification efficiency increases with increasing the degree of esterfication which enhances the solubility of demulsifier molecules in the oil phase. The solubility of demulsifier in oil may help to produce partitioning between the emulsion phases, so that the demulsification process performance increases.

Effect of Dose on Demulsification Efficiency

The efficiency of demulsifier depends on many factors related to its structure. Such factors include the mode of demulsifier injection, the amount of water and the age of the emulsion [111]. One of the most important parameters governing adsorption of demulsifier at the interface is the demulsifier concentration [112]. This meaning is shown in **Tables 26, 27** and illustrated in **Figs 63 and 64**. By following up the illustration, it can be concluded that, the increasing of demulsifier concentration increases the demulsification efficiency. Generally the demulsification efficiency increases by increasing concentration of the demulsifier. These data, indicate that increasing the demulsifier concentration leads to an increase of the adsorption of the demulsifier molecules per unit area on the W/O interface replacing thus the native emulsifiers (asphaltene), which causes the mechanical stability of the interfacial film. The stability of this film continues to decrease and it gets thinner until it collapses totally with further adsorption of the demulsifier agent [113].

Table 26: Water Separated and Demulsification Efficiency of Crude-Oil Emulsion Treated by Esters of Polytriethanolamine at Water Content 50%, 240 min. and 60 °C.

Demulsifier	ppm	HLB	Water Separated, ml	Demulsifier Efficiency
Control	0	-	0	0
P_8O_2	200	13.57	23	46
	300		25	50
	400		25	50
	500		26	52
P_8O_3	200	11.75	50	100
	300		50	100
	400		50	100
	500		50	100
P_8O_4	200	10.38	16	32
	300		50	100
	400		50	100
	500		50	100
P_8O_5	200	9.31	35	70
	300		44	88
	400		48	96
	500		50	100
P_8O_6	200	8.46	20	40
	300		25	50
	400		32	64
	500		50	100
P_8O_7	200	7.76	17	34
	300		19	38
	400		30	60
	500		38	76

oberkanol.com

Table 27: Water Separated and Demulsification Efficiency of Crude-Oil Emulsion Treated by Esters of Ethoxylated Polytriethanolamine at Water Content 50%, 90 min. and 60 °C.

Demulsifier	ppm	HLB	Water Separated, ml	Demulsifier Efficiency
Control	0	-	0	0
$E(40)P_8O_4$	200	14.76	35	70
	300		40	80
	400		43	100
	500		50	100
$E(40)P_8O_8$	200	11.77	50	100
	300		50	100
	400		50	100
	500		50	100
$E(100)P_8O_4$	200	16.88	46	92
	300		50	100
	400		50	100
	500		50	100
$E(100)P_8O_8$	200	14.64	50	100
	300		50	100
	400		50	100
	500		50	100
$E(120)P_8O_4$	200	17.25	10	20
	300		15	30
	400		15	30
	500		18	36
$E(120)P_8O_8$	200	15.20	20	40
	300		20	40
	400		20	40
	500		40	80

openkanal.com

Effect of Hydrophilic-Lipophilic Balance (HLB) on the Demulsifier performance

The HLB concept, firstly proposed by Graifin [114] is considered as an important parameter in predicating the action of a surfactant on the w/o emulsions. The HLB of a system is an important parameter for effective demulsification [115,116]. Non-ionic surfactants offer certain advantages over conventional ionic one. The most important one is the ability to make control changes in the hydrophilicity of the surfactant. This is particularly true or polyoxyethylene compounds in which there is a possibility of changing the length of the polyoxyethylene chain and consequently modifying the HLB.

When the demulsifier is initially introduced to the w/o emulsion, it will be thermodynamically stable at the interface of the water droplets. In this respect, the surfactants that possess a high HLB migrate faster to the interface than those have a low HLB. As a result of such enhanced migration towards the interface, the surfactant forms a continuous hydrophilic pathway between the dispersed water droplets. This leads to a rupture of the surrounded interfacial oil film of the water droplets.

Through this study, the HLB values of the different prepared demulsifiers belonging to the three groups are calculated using Griffin equation proposed by Griffin and listed in **Table 26.** A graph representing HLB values against the time required to achieve 100% demulsification efficiency (complete water separation) is shown in **Figs. 65 to 68**. It is found that P_8O_3 with a HLB = 11.5 achieved very good demulsifier performance. This may be explained on the basis of the partitioning of the demulsifier molecules between the oil phase and water droplets. The maximum demulsification efficiency achieved is a partition coefficient equal to unity. Thus the P_8O_3 may exhibit a partition coefficient close to the unity.

Table 28: Effect of Structure Modification on the Demulsification Process.

Surfactants Code	Amount of Separated Water (ml)	Demulsification Efficiency (η %)	Surfactants Like Form
P_8	0	0	-Ve
$E(40)P_8$	0	0	-Ve
P_8O_4	50	100	+Ve
$E(40)P_8O_4$	50	100	+Ve

obeikandl.com

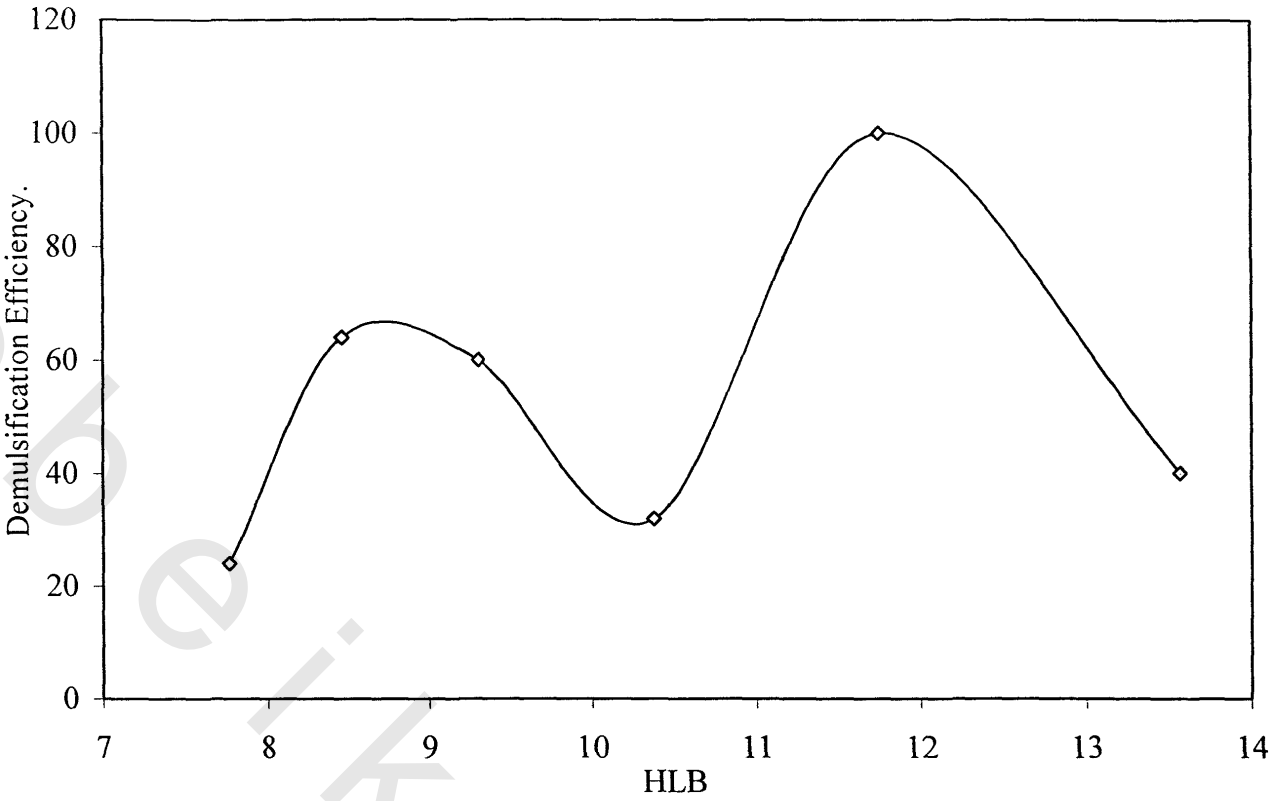

Fig. 65: Relationship Between Demulsification Efficiency and HLB of Crude Oil Treated by Esters of Polytriehanolamine at 50% Water, 200 ppm, 240 min, and 60 ^{0}C.

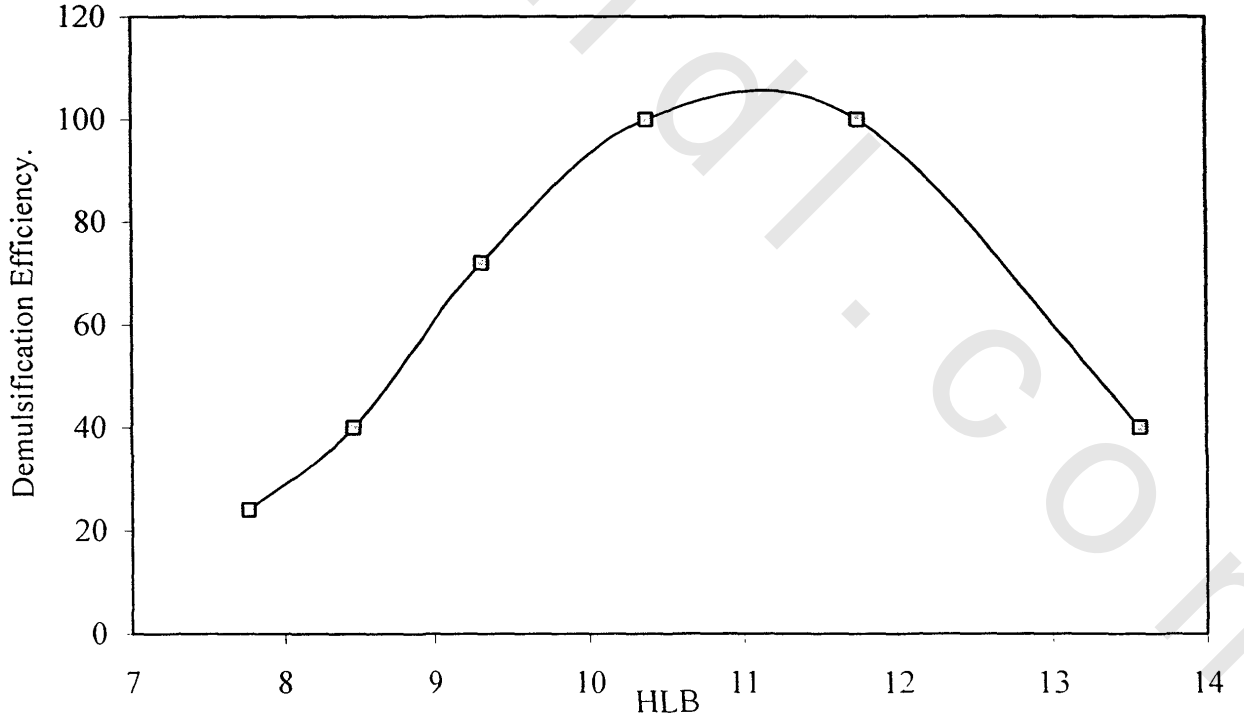

Fig. 66 : Relationship Between Demulsification Efficiencyand HLB of Crude Oil Treated with Estesrs of Polytriehanolamine at 50% Water, 300 ppm, 240 min, and 60^{0}C.

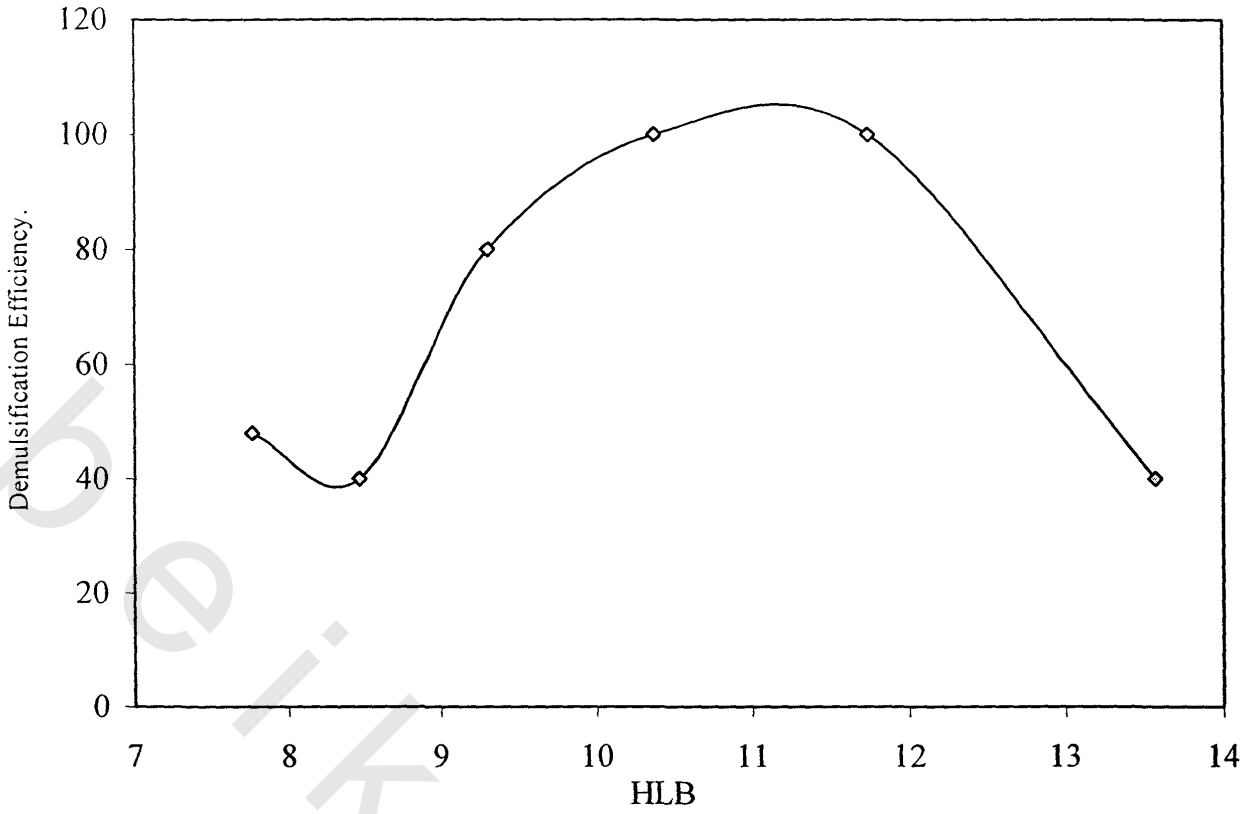

Fig. 67: Relationship Between Demulsification Efficiencyand HLB of Crude Oil Treated With Esters of Polytriehanolamine at 50% Water, 400 ppm, 210 min, and 60^{0}C

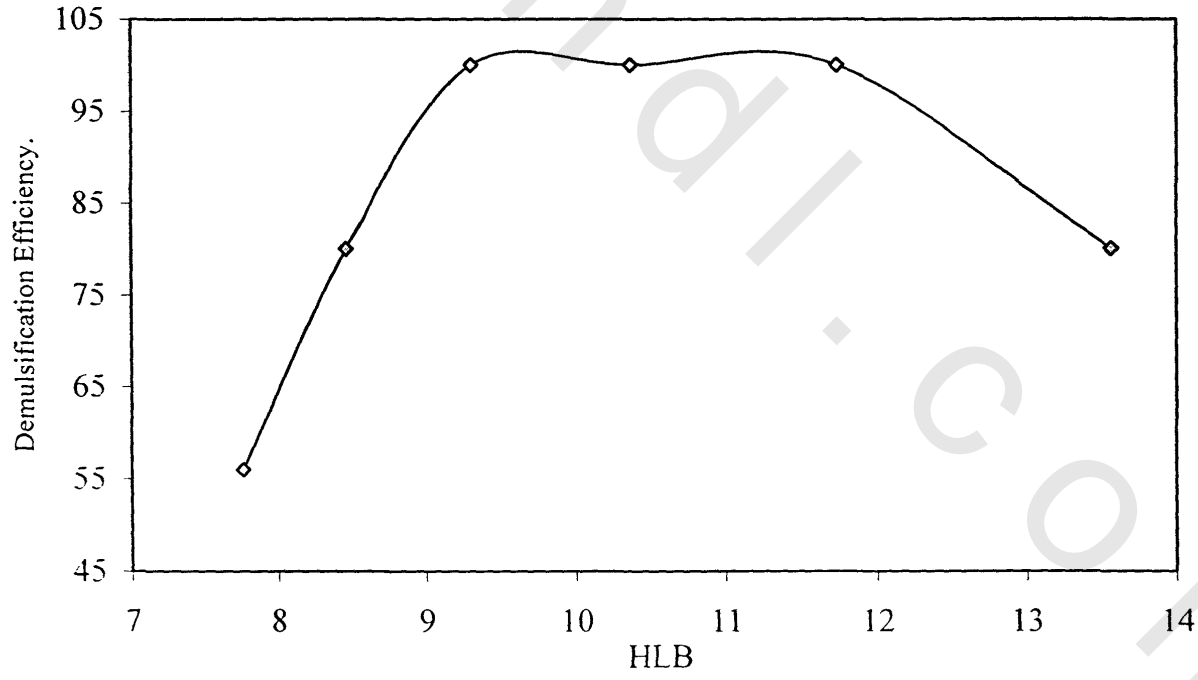

Fig. 68: Relation Between Demulsification Efficiencyand HLB of Crude Oil Treated With Esters of Polytriehanolamine at 50% Water, 500 ppm, 240 min, and 60 ^{0}C.

obeikandl.com

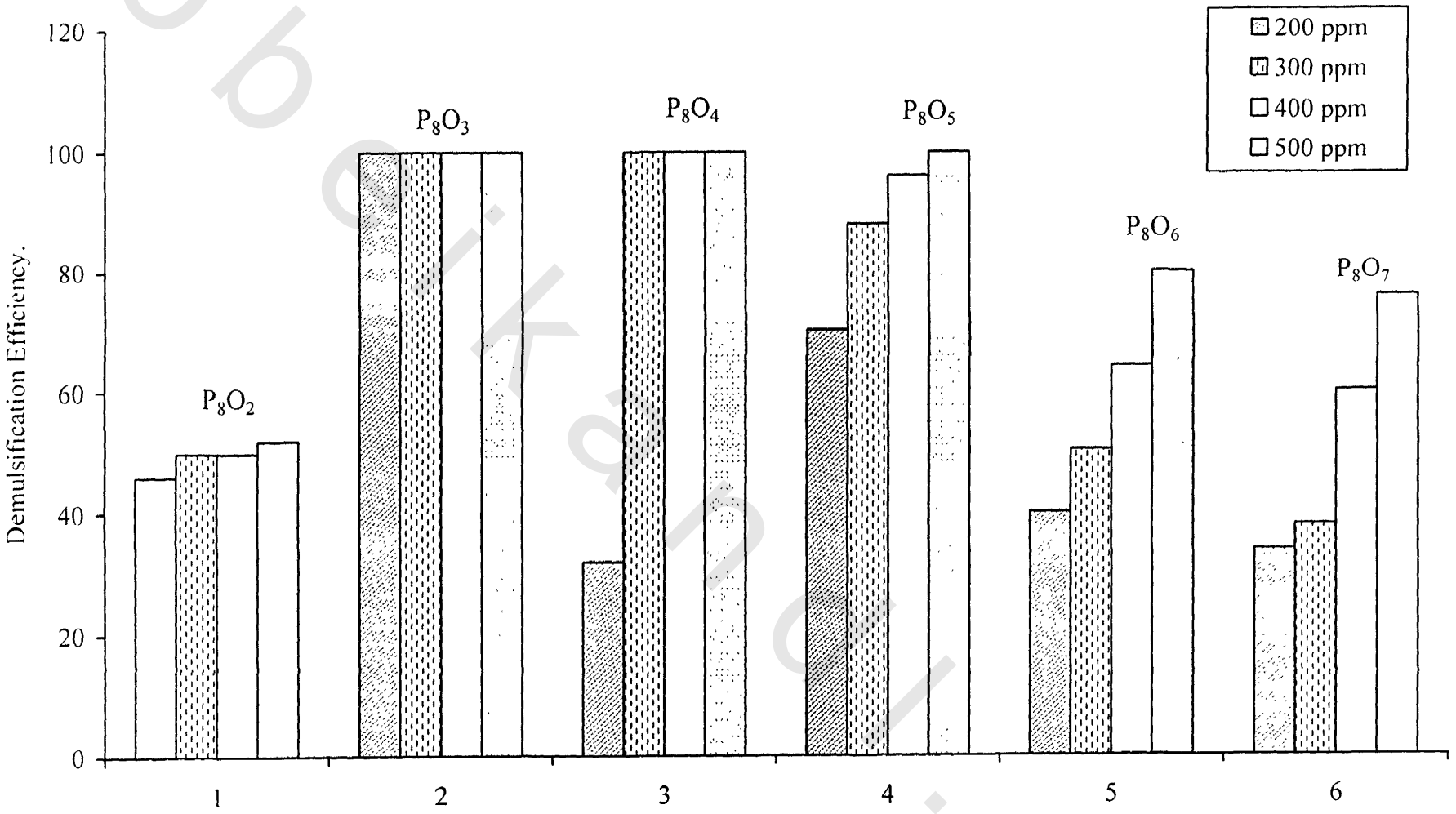

Fig. 63 : The Demulsification Efficiency of Crude-Oil Treated by Esters of Polytriethanolamine at Water Content 50%, 240 min, and 60 °C at Different Concentrations.

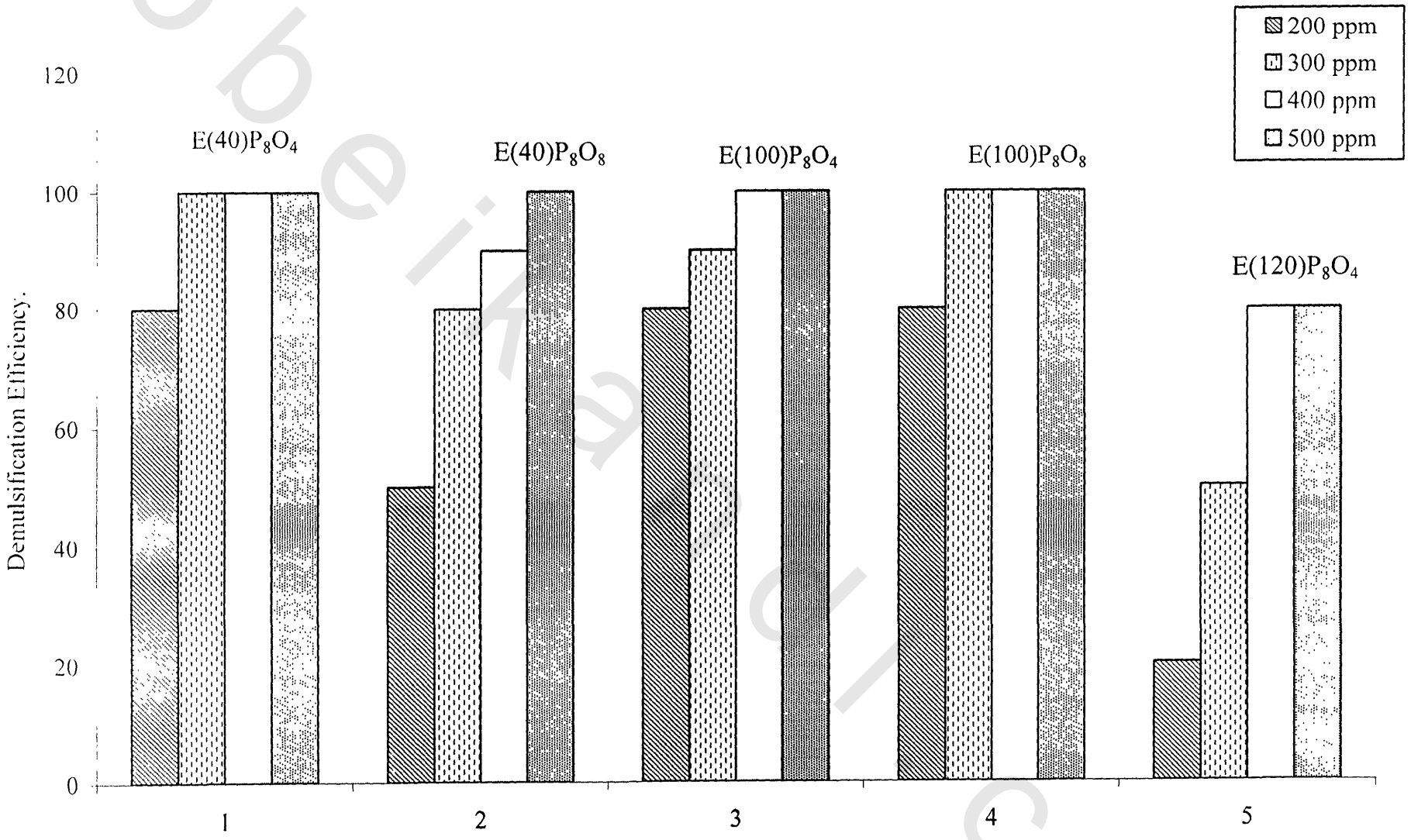

Fig 64 : The Demulsification Efficiency of Crude-Oil Treated by Esters of Ethoxylated Polytriethanolamine at Water Content 50%, 90 min, and 60 oC at Different Concentrations.